UNIVERSITY
OF GÄVLE

FACULTY OF ENGINEERING AND SUSTAINABLE DEVELOPMENT

Department of Building, Energy and Environmental Engineering

Preliminary design of an off-grid photovoltaic system for smallholder water pumping in Sub-Saharan Africa

Asier Jauregui Prada

2018

Student thesis, Master degree (one year), 15 HE

Energy Systems

Master Programme in Energy Systems

Supervisor: Björn Karlsson

Examiner: Taghi Karimipanah

Abstract

Sub-Saharan Africa is the region in the world that suffers the most from poverty and its worst effects: hunger, lack of water and diseases. This problem is far from decreasing: in the past years there has been a peak in undernourishment in the continent. Furthermore, according to ongoing research, the area is expected to be one of the most affected by climate change.

A solution that tackles at the same time water scarcity, diseases, hunger and greenhouse gas emissions is therefore urgent. Luckily, with the development in the past years of the solar photovoltaic and battery technologies, these solutions can now compete head-to-head with fossil-fuelled pumps. Indeed, the photovoltaic water pump (PVWP) is becoming the preferred solution by locals and NGOs, enabling a cheaper, less pollutant and more self-sustainable growth vector.

In this thesis, a PVWP system is pre-designed. This means that the effect of the different variables over the system are studied, without aiming to design any specific system. However, the calculations are done with the specific climatic conditions of Fada N'gourma (Burkina Faso) as an example.

To start, the importance of water for basic supply, sanitation and agriculture is researched through reviewing existing literature. The specific advantages of an advanced method of irrigation such as drip irrigation are also investigated.

To continue, the analysis of the influence of each parameter intervening in the system is undertaken. First, a method to calculate the watering needs of the plants (through the concept of evapotranspiration), and simultaneously the passive self-regulation of PVWP systems for irrigation purposes is analysed. Second, the possibility to calculate faithfully the optimal angle with only climatic values and the size of the orchard is demonstrated. Third, a model to obtain the optimal diameter of the pipes through the optimisation of the cost is elaborated. The specific influence of the pump efficiency in this process is also explored. Fourth, an analysis on the effect in the system resilience to weather changes depending on the different starting dates for planting the crops is done.

To finish, some considerations and a preliminary design are made. The option of implementing a storage system is discussed, analysing the advantages of batteries and the water tanks as options. A quick economical evaluation is also done, leading to the conclusion that a PVWP system of the characteristics studied is viable under most of the circumstances.

Table of contents

List of tables

List of figures

1 INTRODUCTION

This thesis is done in cooperation with an NGO based in Bilbao, called TADEH. The aim of TADEH is to improve people's life in countries in development in a sustainable way, according to the principles of self-supply.

This project aims to explore the different factors that must be taken into account in order to design a photovoltaic water pump system. Hence, it can be considered as a pre-study to set the ground floor for further research that will develop commercial implementations or PVWP systems specific designs

1.1 Problem

Poverty in sub-Saharan Africa is still one of the biggest problems of the century, and it risks increasing as climate change menaces to hit already weakened economies. Thus, a solution that tries to cope with this poverty problem, while at the same time reducing the increase in climate change, urges.

With the recent advancements in technology, solar photovoltaic systems and batteries are becoming cheaper, managing even to overtake traditional sources of energy even in the economic front. And Africa is especially fit for this technology due to hard access to fuels, lack of electric grids and a high solar intensity. However, the impoverished situation of the area has prevented the rapid growth in the business seen in other regions, regions having indeed fewer physical advantages for it. But with the rise of new types of business models, low income families are more likely to accede to these technologies nowadays, if a proper ecosystem is implemented and proper external help is obtained.

This opens the perspective not only to enable electricity access in the most obvious sense (lighting, electricity for mobile phones or computers, etc.), but also, and most important, it enables the access to a reliable source of water. Indeed, electrical pumps lead to an increase in the use of water, allowing to improve the sanitation, hygiene and agricultural output of a household, while reducing the time consumed.

These uses are cornerstones for the empowerment and improvement of the conditions in sub-Saharan Africa. All of them are indeed vital for improving health conditions, helping to reduce many of the diseases and deaths of the region caused by lack of sanitation or hunger. The reduction in the time employed to obtain the water is also key for the development, empowering especially the most vulnerable groups: women and children. Indeed, the time saved would allow to develop remunerated jobs or to further in the education, helping to trigger a locally grown development.

This vision of an empowerment of the society will remain the most important perspective of this work. Undeniably, one of the problems international cooperation has faced over the past is that help was not sustainable without further external help. Thus, instead of contributing to empowerment, it tended to increase the dependency of the "helped" society, exacerbating the neo-colonialist power dynamics in place. It is therefore important to acknowledge this, to be able to avoid major problems that bad cooperation can trigger.

1.2 Aims and goals

The aims this study are:

1. To analyse the needs of water of an average low-income household for water supply, sanitation and irrigation of an orchard.
2. To study the influence of the different design parameters of a photovoltaic water pump system for irrigation and WSS:
    a. Tilt of the solar panel.
    b. Efficiency of the pump.
    c. Size of the orchard.
    d. Depth of the groundwater.
    e. Diameter of the pipes.
3. To dimension a PVWP after selecting the optimal or the typical values of the parameters studied.
4. To do a basic economic analysis of such systems.

1.3 Literature review

1.3.1 Importance of Water Supply and Sanitation (WSS)

Access to water of quality and proximity is one of the biggest problems that society faces today. Indeed, having a reliable and safe source of water at home not only combats malnutrition, but strongly prevents the contraction of serious diseases (Bartram and Cairncross, 2010). According to WHO's data from 2002, 4.2% of all the deaths worldwide (2.41 million, from which 2,24 are children) could have been avoided with measures that improve overall access to water, sanitation and hygiene (Prüss-Üstün *et al.*, 2008).

Although avoiding the deaths and illnesses should be enough reason to act, water scarcity is a limitation for economic development and imposes high costs on the poorest and most vulnerable (UN-Water, 2015). In developing countries, the loss is estimated at 1.5% of GDP due to the lack of Water Supply and Sanitation (WSS), with notable regional differences (WHO, 2012), the consequences being higher among the poor (Bartram and Cairncross, 2010).

Despite all this, WSS do not receive as much attention compared to its importance, especially in the face of Malaria, HIV and tuberculosis (Bartram and Cairncross, 2010). This is especially dramatic, knowing that improving hygiene, sanitation and access to water are one of the most cost-effective measures to improve public health (Leimbach *et al.*, 2018). Indeed, the Benefit-cost ratio of intervening to obtain universal access to drinking water is 2 to 1 in the world, according to conservative estimates (WHO, 2012). According to other studies, the return is between USD 1.5 and USD 12 per dollar invested in basic water access, and it would mainly help women and children (Hutton, Haller and Bartram, 2007).

1.3.2 People without access to WSS

Currently the number of people who need to improve their access to drinking water is still high. According to data from the Joint Monitoring Program for water supply (JMP), 748 million people (11% population) use unimproved water sources in 2012, of which 90% belong to the rural world (Who and Unicef, 2014). Moreover, the International Journal of Environmental Research and Public Health estimates that 1.8 billion people (28%) use unsafe water in the world (Onda, Lobuglio and Bartram, 2012).

Largely thanks to the awareness of countries and associations, these numbers are being reduced. In 1990, 76% of the population had access to an improved water source, in 2012 it was 89%, or 2.3 billion more people (Who and Unicef, 2014). Indeed, the world has reached the Millenium Development Goals (MDG) 7c in water access (Who and Unicef, 2014).

1.3.3 Sub-Saharan Africa: a non-solved problem

But this good trend has been mainly boosted by the rapid rise of China and India. In the case of sub-Saharan Africa (SSA), the increase has not been enough to achieve the MDG 7c, and this is especially noticeable in rural areas (Who and Unicef, 2014). Thus, in SSA, access to improved water sources has increased only 11% from 1990 to 2008, although for example in Sierra Leone it has fallen by 23% (Salami *et al.*, 2011).

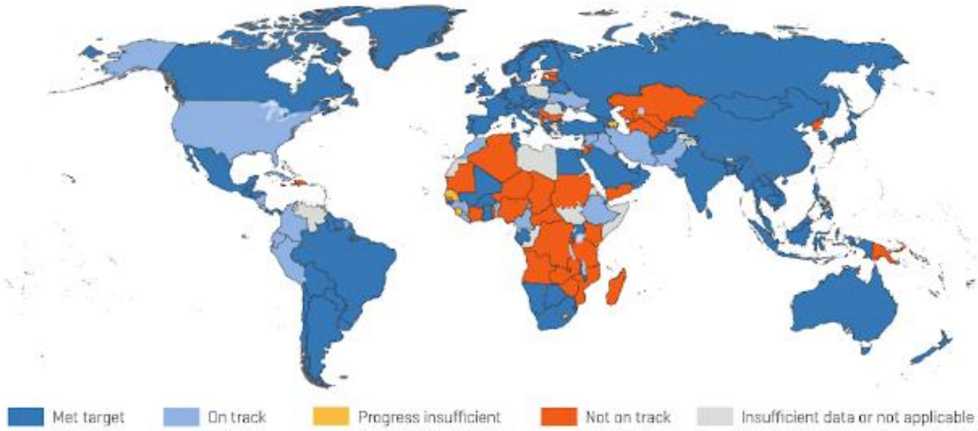

Figure 1. Progress with the MDG targets (Who and Unicef, 2014)

In SSA, 36% still do not have access to an improved water source, which is 325 million (Who and Unicef, 2014). In addition, 160 million people in Africa, especially women, spend substantially more than 30 minutes per barrel to fill it (Bartram and Cairncross, 2010). This is one of the greatest economic impacts of poor access (Hutton, Haller and Bartram, 2007), along with deaths and diseases. Therefore, in addition to affecting countries unequally, it also affects women and children, the main ones usually in charge to fill the barrels.

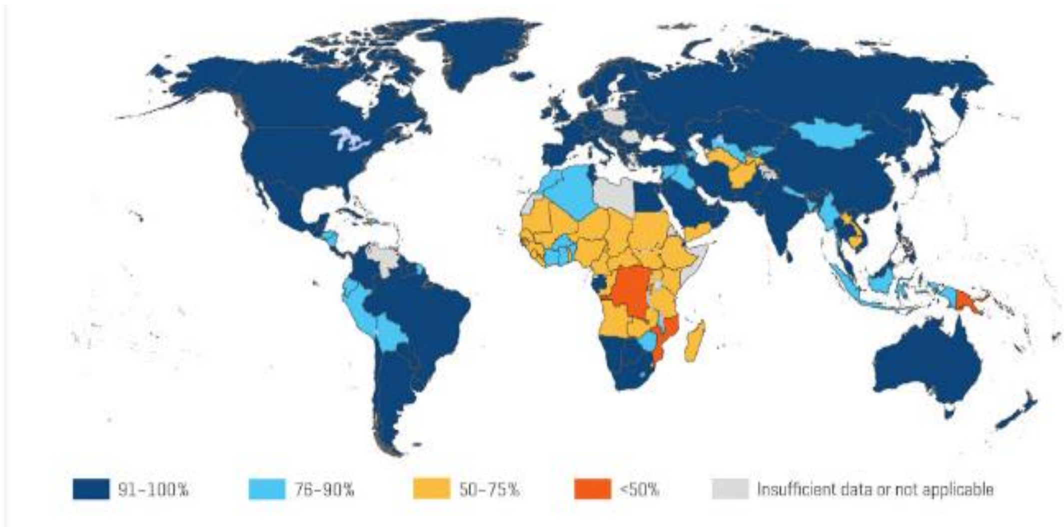

Figure 2. % of population with improved drinking water source (Who and Unicef, 2014)

Economically Africa is the region most affected by poor WSS coverage, with studies estimating that it creates losses of 5 (UN-Water, 2015) or 4.3%. (WHO, 2012) of its GDP. And these values could even increse to almost 10% due to climate change (Leimbach *et al.*, 2018) además puede aumentar un 5% más a causa del cambio climático (UN-Water, 2015). For all the above, SSA is the region of the world where more money will cost to reach the MDG target for WWS, half of the cost being for rural (WHO, 2012). But this does not avoid SSA to be one of the regions with the highest benefits obtained by dollar invested: the Benefit-cost ratio of intervening to obtain universal access to drinking water is 2.5 to 1 in SSA according to conservative figures (WHO, 2012), 4.4 to 1 (Hutton, Haller and Bartram, 2007).

1.3.4 Sanitation and hygiene

Although it has been mentioned so far, sanitation and hygiene deserve a differentiated section, because it is usually considered that access to water for drinking is enough. Indeed, in 2015 2,4 billion in the world still do not have access to improved sanitation, 695 million of which in SSA (Who and Unicef, 2014).

There is strong empirical evidence that sanitation and hygiene are paramount for health, as for example the case of England and Wales between 1840 and 1910 shows (Bell and Millward, 2018). It is therefore vital that access to water is not limited to 2-5 liters per day and person to drink, but that special attention be paid to sanitation and hygiene.

In this regard, SSA continues to be one of the areas with the worst conditions, with ¾ of the rural population without sanitation coverage in 2008. Moreover, due to the lower interest in this type of intervention, it has only increased by 3% since 1990 (Salami *et al.*, 2011). This is despite being very cost effective, since according to (WHO, 2012), the benefit-cost ratio of intervening to obtain universal access to improved sanitation is 2.8 to 1 in SSA and 5.5 to 1 in the world.

1.3.5 The importance of water for agriculture

1.3.5.1 Hunger in Sub-Saharan Africa

The relevance of water is not reduced to sanitation and drinking: in developing regions, despite economic growth, this number has continued to rise. There are 815 million people in the world who suffer from hunger in 2016, 204 of which in SSA. Even more people suffer from severe food insecurity: 31% of the SSA population (306.7 million). Indeed, SSA is the only large region in the world where the MDG for hunger has not been met (Bain *et al.*, 2013; FAO *et al.*, 2017). These problems would besides worsen due to climate change increasing the droughts and causing migration (Bain *et al.*, 2013).

1.3.5.2 Macroeconomic benefits

A significant fraction of people suffering food insecurity in SSA are from the agricultural sector, even if they spend on average 50-80% of their income on food. This is the paradox of the continent: many farming families are net consumers of food (Banerjee and Duflo, 2007). In fact, one of the basic problems of poverty and malnutrition is the lack of productivity in the rural world, mainly due to lack of water and adequate methods of crop management (irrigation, fertilizers, fertilizer, etc.). Projects trying to improve the management of crops tackle this problem increasing food availability, access and use (Burney *et al.*, 2010). 115 billion dollars could be saved annually with a more productive use of water in the world (UN-Water, 2015). Other studies suggest that a comprehensive strategy for water management could increase production by 41% (Leimbach *et al.*, 2018).

It is thus necessary to increase the productivity of the fields in developing countries if the serious problem of poverty and malnutrition is to be addressed, by increasing water access and management.

1.3.6 Possible solutions

1.3.6.1 Type of system

There are nevertheless multiple ways to extract groundwater, being currently the main ones in SSA the manual systems, the wind power water pump (WPWP), the PVWP and the Diesel Water Pump (DWP). Manual systems, although effective to cover basic water consumption needs, are not a reasonable solution for agriculture because they require large quantities of water. PVWPs are already cheaper than DWPs, as well as more ecological and sustainable (they last between 15 and 25 years with minimal maintenance). If we compare them with the WPWP, the PVWP is much more reliable, and is cheaper in most of the climatic conditions of the continent. (Prüss-Üstün *et al.*, 2008; Burney *et al.*, 2010; Campana, Li and Yan, 2015).

Moreover, there is an interesting phenomenon to point out that makes solar panels especially suitable for this type of solutions. Indeed, the water demand is given by the evapotranspiration values of the plants to be irrigated, to which the amount of water absorbed by the rainfall is subtracted. But the evapotranspiration is directly related to the insolation (Allen, Pereira, Raes, Smith, *et al.*, 1998; Zhang *et al.*, 2014); thus, in a cloudy day, the production of electricity is reduced but also is the need for water. This effect would be especially dramatic if the clouds bring rain.

Therefore, the PVWP system does not require big storage systems if it is correctly designed, since it self-regulates passively, as most of the water is for agriculture. The small fluctuations could be supplied by a reduced water tank (Burney *et al.*, 2010). In conclusion, PVWP systems seem to be the optimal ones for this type of projects.

1.3.6.2 Advantages of drip irrigation systems

The drip irrigation technique is the second biggest opportunity to reduce water consumption after improving crops (Dobbs *et al.*, 2011). Besides saving water, the drip allows to save energy, chemigation and labour (Marsh *et al.*, 2007), as well as the nitrogen to apply (Singandhupe *et al.*, 2003), reducing the nutrient leaching (Woltering, Pasternak and Ndjeunga, 2011).

According to Dobbs *et al.* (2011), the average harvest improves by 45%, and it can also reduce the use of fertilizer (for example in India, 40% reduction), or of water between 20 and 60%. 2.2.12 estimates in commercial cash-crops 31-37% less water use and up to 12.5% more fruits (Singandhupe *et al.*, 2003). An empirical example of success might be Israel, which has multiplied by 12 its agricultural production, maintaining constant the water consumption for 50 years. This is partly due to drip and fertigation (drip + fertigation in water) (Dobbs *et al.*, 2011).

Drip irrigation can work with low pressure (LPS) at 70 g / cm2 (or 0.7 mCA) in small fields, ideal for the use in small farms where this pressure could be obtained through a high tank (Marsh *et al.*, 2007; Woltering, Pasternak and Ndjeunga, 2011). This technology has easy and cheap operation and maintenance, although it requires training and periodic technical assistance for at least 2 years (Woltering, Pasternak and Ndjeunga, 2011).

This technique is preferable for fruits and vegetables (Dobbs *et al.*, 2011), and potatoes, so, in the first instance, its use would be better limited to this type of crops (Woltering, Pasternak and Ndjeunga, 2011). This type of crop can easily be sold, and if needed cereals could be bought since they are cheaper to produce in large fields, cheap and simple to transport.

Finally, according to Burney *et al.* (2010) a PVWP with drip improves up to 80% the living standard in economic and nutritional terms. Therefore, drip irrigation systems with PVWP for a medium-sized orchard for fruits and vegetables seems to be a proper option for the problems considered in this work.

1.3.7 Values of water needed

1.3.7.1 Water for WSS

The importance of WSS has already been stated in previous sections, but a value to be used needs to be obtained. According to Howard and Bartram (2003), optimal access to water is when the consumption it is greater than or equal to 100 litres per person and day, and with water supplied by multiple faucets at home. This will be the number that will be assumed in this work for WSS, although the creation of a piping system for the installation of multiple faucets will not be considered.

1.3.7.2 Size of the fields to irrigate

On the other hand, water for irrigation is not so easy to study. It has already been estimated that the water to be used will be for an orchard independent of the land in which the staple foods are grown. Therefore, this field will be small, and used to produce vegetables, fruits, vegetables or potatoes.

In Balana *et al.* (2017) they talk of an orchard of 250 m^2; and in Woltering, Pasternak and Ndjeunga (2011) three possible sizes are mentioned to install a drip system in SSA: 80, 500 and 5000 m2. Moreover, the average field size in Burkina Faso is 0.12 ha (Houessionon *et al.*, 2017). This same study considered that farmers with less than 250 m2 had a small field, and with more of 500 one large. Last, in a study in 2009 orchards of 120 m2 per woman were installed that gave good results (Burney *et al.*, 2010).

1.3.7.3 Water to use for irrigation

Woltering, Pasternak and Ndjeunga (2011) estimates the maximum required to irrigate with drip would be 8 mm/day in the conditions of the Sahel and in a crop like the one proposed in this work. On the other hand, Campana (2015) considers that the maximum value for an alfalfa field in China is 10 mm/day. Finally, Balana *et al.* (2017) estimates that a field of lettuce would need 3.6 mm/day in the Sahel. The same study estimates that in the case of growing tomatoes, the amount would be 4.5 mm/day in the Sahel.

1.3.8 Quantitative benefits of an irrigation system

The economic benefits of improving access to water for irrigation at the macroeconomic level have already been studied, but we must also look at the benefits per household.

In Burney *et al.* (2010) it is argued that a 500 m^2 orchard has a 15-month payback time, while for a 5000 m^2 (subsequently divided between independent farms) it is of 5-6 months. These numbers, although they must be taken with care, are encouraging for this type of intervention. For its part, Woltering, Pasternak and Ndjeunga (2011) estimated that the Benefit-cost of a drip system exceeding 500 m^2 is 2 to 1, which supports the previous statement.

In Balana *et al.* (2017) gross income values are estimated in an orchard of 250 m^2 in the Sudano-Sahel for lettuce, tomatoes and peppers. In the case of lettuce, considering 6 annual cycles (rapid growth), the income is 10,32 USD/m^2 per year. For a tomato orchard with 3 production cycles, the income would be 17,50 USD/m^2 year. Finally, for peppers in two crops, the value is 9,72 USD/m^2.

On the other hand, in Burney *et al.* (2010) it is estimated that in a plot of 5000 m^2 divided into individual gardens of 120 m^2 the benefit is 2 USD/m^2 with a drip irrigation system.

1.3.9 Acceptance of the population

Improving access to water for irrigation is not only recommended by expert studies but is what the farmers themselves prefer. Thus, in a study carried out in Burkina Faso, it was found that farmers preferred interventions that guaranteed above all constant water supply, efficient water use and labour saving, abundant crop nutrients and soil health improvement (Houessionon *et al.*, 2017).

Drip is also a technique already contrasted and known, so its implementation should not have many complications. In fact, drip irrigation was already the most widely used method in Burkina Faso (33% already using drip), as well as 22.3% already using deep well drilling (Houessionon *et al.*, 2017).

Thus, according to this same study (values converted from F CFA) in Burkina Faso, farmers are willing to pay, per hectare and per production, for drip 302 $, for organic matter recovery 191 $, for deep well 33 $, for drilling 62 $. If we segregate the poorest, they would pay $ 285 for drip and $ 163 for Deep well (more than normal). The latter shows that it is the poorest farmers who see the most interest they could get from the aid when drilling to extract water to irrigate.

1.3.10 Aquifers in Africa

Since this work is about a water-pump system, the study of the aquifer conditions is capital. Below is a map of the estimated depth of groundwater in Africa done by the British Geological Survey (MacDonald *et al.*, 2011). It can be observed that in most of the continent water is found at less than 25 m deep, especially when considering SSA.

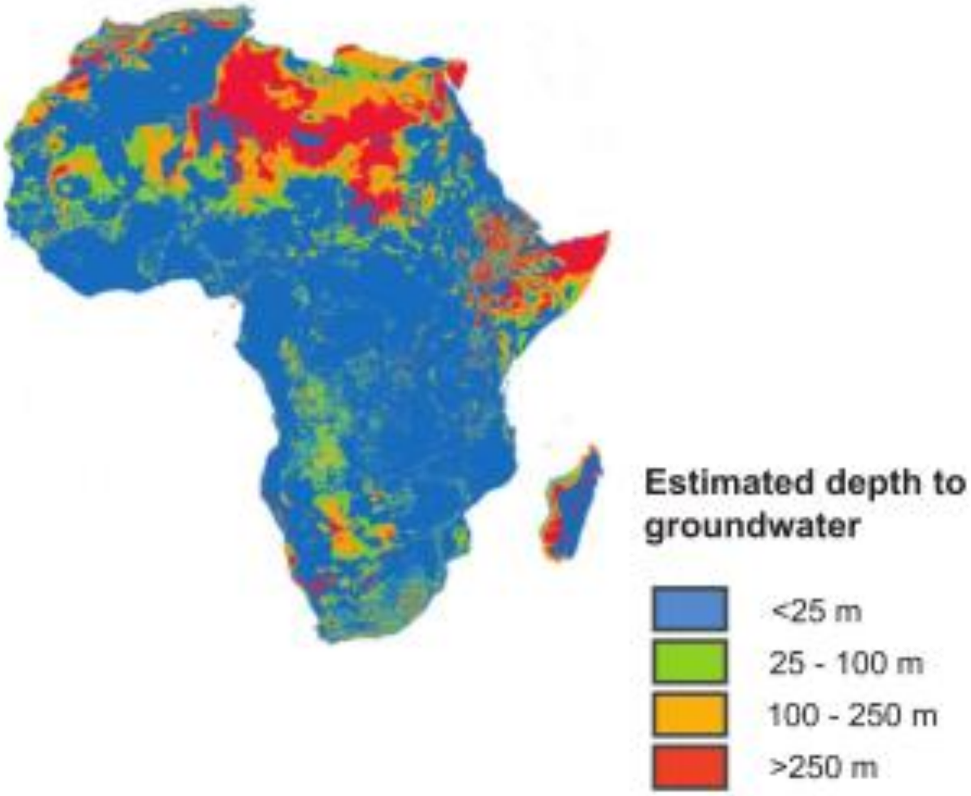

Figure 3. Estimated Depth to groundwater (MacDonald *et al.*, 2011)

Another interesting parameter to take into account is the aquifer productivity, which is the capacity of an aquifer to provide a certain water flow. This can be seen in the Figure 4, also by the British Geological Survey. Note that most of the aquifers of the continent have a higher productivity that 0,5 L/s (green and blue areas), which is 1,8 m^3/h.

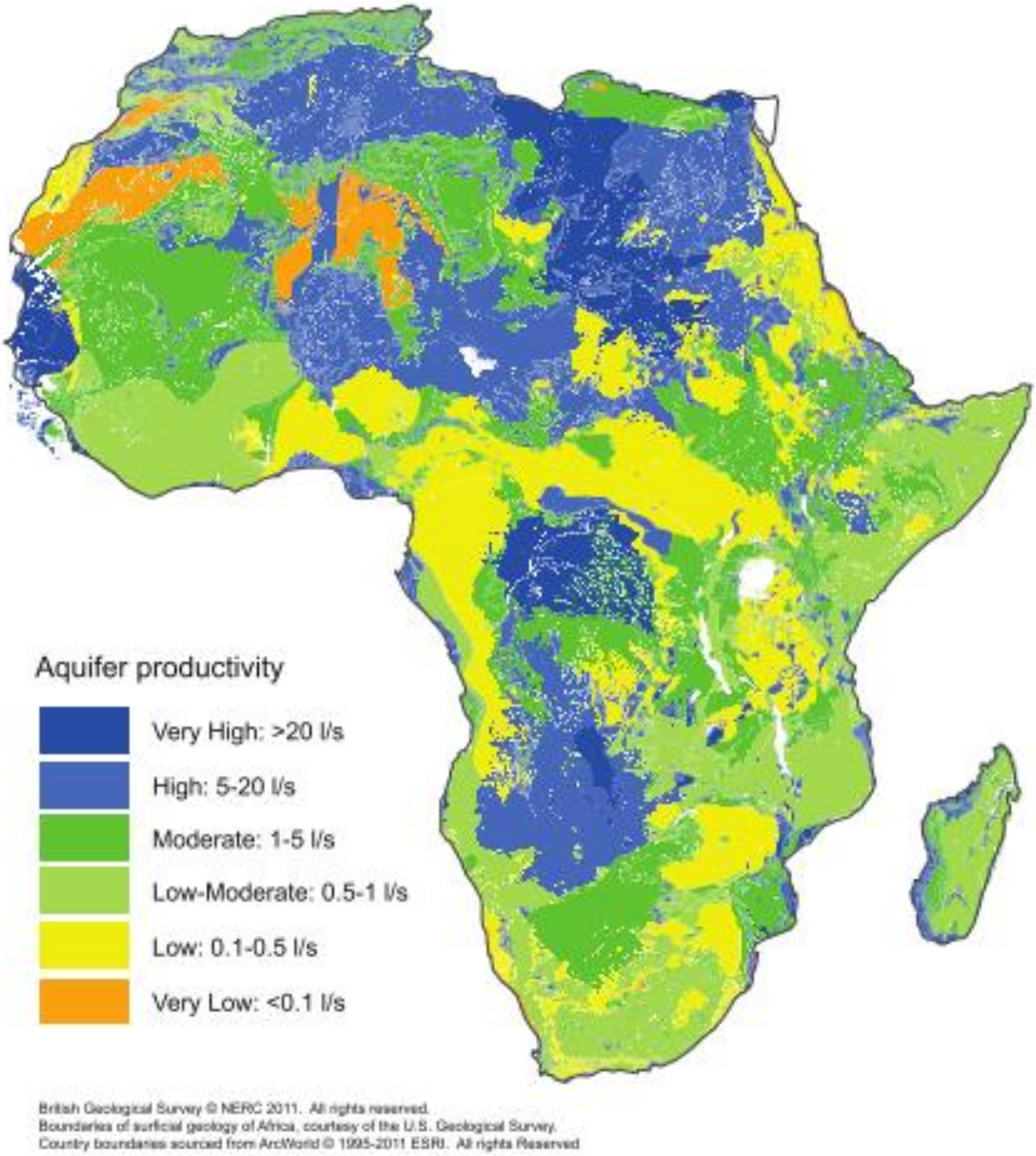

Figure 4. Aquifer productivity in Africa (MacDonald *et al.*, 2011)

1.3.11 Climatic conditions

1.3.11.1 Precipitations

Sub-Saharan has a great variety of climates, from tropical to desertic. The precipitations in the continent can be seen in Figure 5. These values are important to consider, since the precipitation has a direct impact in the amount of water needed for the crops.

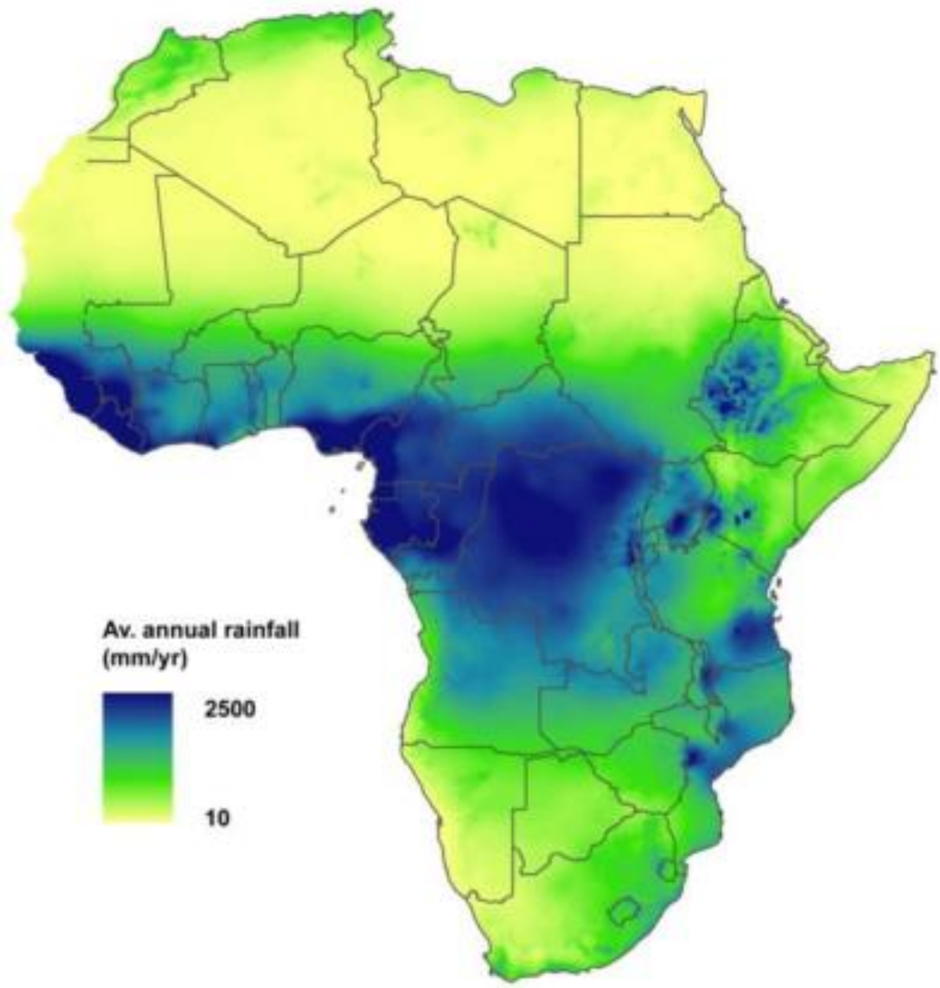

Figure 5. Rainfall data in Africa (MacDonald and Bonsor, 2011)

1.3.11.2 Solar intensity

Last, SSA is centred around the equator, and as so, it receives a lot of sun. In fact, the places were the sun received is the least (even though not small) are the ones where it rains the most. This is intuitive since clouds cover the sun, but it poses no problem for a PVWP as stated in subsection 1.3.6.1. The values of the radiation intensity can be seen below.

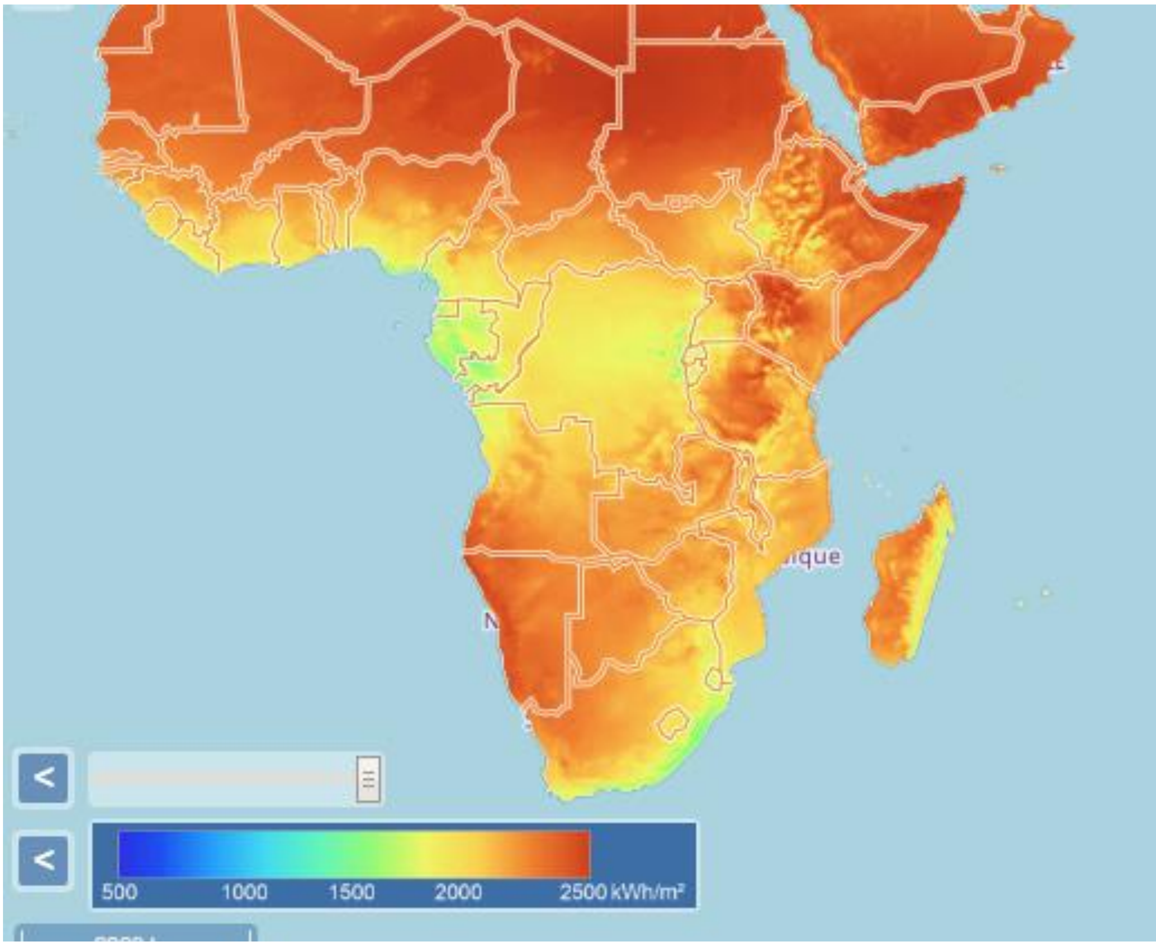

Figure 6. Solar radiation per year [PVGIS]

2 THEORY AND METHODS

2.1 Theory

2.1.1 Evapotranspiration of the crop field

The evapotranspiration is the loss of humidity of a surface by direct evaporation alongside with de loss of water due to plant transpiration. Its value is typically measured in mm/day (or just mm), which is a simplification for mm/(m^2·day), or litres per day per square metre (Zhang *et al.*, 2014).

There is not an exact formula to calculate the value of the evapotranspiration of a field due to its complexity, but several empirical approximations have been proposed along the years. These are usually obtained for a reference evapotranspiration (ET_0, normally alfalfa at a specific state of growth), that is later multiplied by a single crop coefficient K_c (Equation 1). The result of this product is the real evapotranspiration ET_c which now depends on the type of crop and phase of growth.

EQUATION 1

$$ET_c = ET_0 \cdot K_c \;\; [mm \cdot day^{-1}]$$

2.1.1.1 Mean values for reference evapotranspiration

Without any calculations, there are some generalizations on the values that ET_0 should have for different conditions throughout the bibliography. For example, FAO states that in warm zones (+30ºC), if they are arid the value is to be between 6 and 8 mm/day, if it is a tropical or sub-tropical climate between 5 and 7 mm/day, and in temperate regions, between 4 and 9 (Allen, Pereira, Raes and Smith, 1998). Furthermore, according to Serdeczny *et al. (*2017), the maximum value is 8 mm/day for similar conditions. Finally, with a more specific example, the maximum for tomato in Niger is estimated to be 4,5 mm/day (Balana *et al.*, 2017).

Therefore, even though with some variations regarding different climates and sources, it appears that ET_0 is comprised between 4 and 9 mm for all the possible climates in Sub-Saharan Africa.

2.1.1.2 Equations to obtain the reference evapotranspiration ET_0

Once having an idea of the values to obtain, two different empirical formulas are going to be used: the Hargreaves equation (Hargreaves and Zohrab, 1985), and the method of the net radiation (Irmak *et al.*, 2003).

Net radiation method

EQUATION 2

$$ET_0 = 0{,}489 + 0{,}289 \cdot R_n + 0{,}023 \cdot T \;\; [mm \cdot day^{-1}]$$

T is the average temperature of the day, in this case, the monthly average is used.

Rn is the net solar radiation. Since it is a complex data to obtain, we will use the maximum direct solar radiation, because it is easier to obtain, and since it is higher, it will give a more conservative value.

Hargreaves equation

EQUATION 3

$$ET_0 = 0{,}0023 \cdot R_a \cdot \sqrt{T_{max} - T_{min}} \cdot (T + 17{,}8)\ \ [mm \cdot day^{-1}]$$

Ra is the extra-terrestrial radiation

Tmax is the maximum temperature in the day, in this case the monthly average maximum is used.

Tmin is the minimum temperature in the day, in this case the monthly average minimum is used.

T is the average temperature of the day, in this case, the monthly average is used.

2.1.2 Concept of the single crop coefficient, Kc

The single crop coefficient "brings" the information of the type of crop and the phase of the growth it is undergoing in Equation 1. Of these two variables, the phase of the growth is the one that has a biggest influence over Kc, as can be seen in the next graph presenting the values of Kc for one planting cycle of tomato (Allen *et al.*, 1998; where several other crops are also presented). The type of crop will have an effect on the maximum Kc, and on the shape of the cycle.

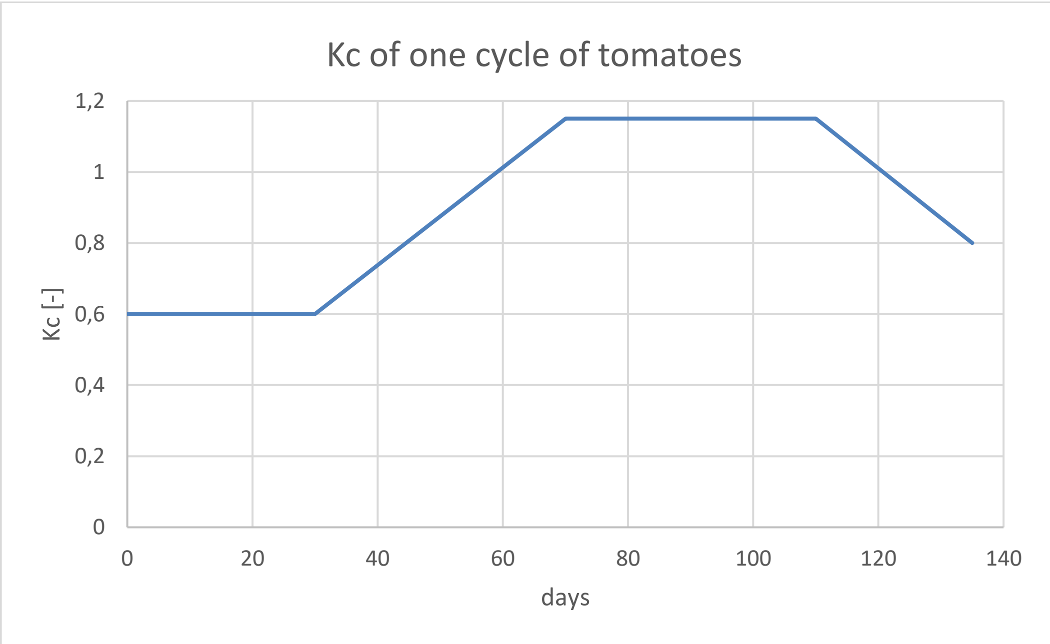

Figure 7. Kc evolution over one planting cycle of tomato (Testa, Gresta and Cosentino, 2011)

The evolution of Kc shows the four phases of growth that most crops endure. These are the initial phase, where Kc is at its minimum, the development phase, where Kc increases, the middle season phase, where Kc remains constant at its maximum, and the final phase, where Kc decreases (Allen G. *et al.*, 2006).

2.1.3 Watering necessities

Even though ETc states the amount of water plants need for their correct growth, it is not the water amount to artificially provide. This is because water is obtained by the plants also through natural rain or soil capillarity. Soil capillarity will be ignored in this work because it is very mild in most conditions, and particularly in the Sahel region (except for oasis). But the rain is to be considered if pursuing a more precise estimation.

These assumptions are summarized in the following equation for the Watering needs (Watering):

EQUATION 4

$$Watering = ET_c - Prec_{ef}$$

Where $Prec_{ef}$ stands for effective precipitation; effective for the watering needs. Quite so, not all the rainfall is absorbed by the plants, and can be subtracted from the irrigation needs. There is indeed a sum of factors, such as deep infiltration or superficial and underground runoff, that must be considered to transform the measured precipitation into effective precipitation. All these factors are extremely complex to obtain in a precise way, but as with ET_0, some empirical models have been developed.

According to FAO (Dastane, 1978), one of the best methods for arid or semi-arid zones (such as the one selected for this work in the Sahel) is the one developed by the US Bureau of Reclamation. According to Ruiz Baena (2017), a simplification of the formula is as follows:

EQUATION 5

$$Prec_{ef} = Prec \cdot \frac{(125 - 0.2 \cdot Prec)}{125} \quad , when\ Prec < 250\ mm/mes$$

EQUATION 6

$$Prec_{ef} = 125 + 0.1 \cdot Prec \quad , when\ Prec > 250\ mm$$

2.1.4 Peak extraction hours

As for the way the water pump works day-to-day, some simplifications are assumed for this thesis. First, the extraction is considered constant during the time of work of the pump. Second, for the time of work of the pump, a concept similar to the sun peak hours (SPH) is used, but applied to the energy generation of a PV panel of 1 kWp. Thus, the peak extraction hours (PEH from now on) would be the number of hours needed to reach the energy production if the panel produced at its peak power on a constant basis. It is easy to note then that if the energy generated by a 1 kWp PV system is measured in kWh per day, the PEH is equivalent in number to the energy generated.

The PEH does therefore not depend on the volume needed to be extracted, but depends on the solar system design, mainly the type of solar PV panel, the energy losses, the azimuth and angle of inclination. The first three are determined already for all the thesis, but the angle of inclination is to be determined for each specific design. Therefore, the monthly water flow evolution will depend work on the angle of inclination chosen, which makes it important to evaluate all the possible options.

2.1.5 Dynamic Head

To calculate the value of the losses generated by the friction of the pipes, the steps of (Milnes, 2000) are going to be followed. First of all, the total head is defined as:

EQUATION 7

$$H_{tot} = H_{stat} + H_{dyn} \ \{m\}$$

Where Hstat is the static head, which is the height difference between the surfaces of the well and the tank. In this case, we will consider it constant to simplify the calculations, but it would vary in a real situation, and obtained after the following formula:

EQUATION 8

$$H_{stat} = Depth\ well + height\ tank = Depth\ well + 2\ m$$

As for Hdyn, it is the dynamic head, resulting of the friction of the water while circulating through the system, being the representation as height of the pressure drop. Hdyn is obtained through the basic equation of Darcy-Weisbach:

EQUATION 9

$$H_{dyn} = \frac{K \cdot \mathrm{v}^2}{2g} \ \{m\}$$

Where g is the accelation of the gravity (9,81 m/s^2) and v is the average velocity of the water through the pipe, obtained dividing the water flow by the area of the pipe:

EQUATION 10

$$\mathrm{v} = \frac{Q}{A} = \frac{Q}{\pi \cdot R^2} = \frac{4 \cdot Q}{\pi \cdot D^2} \ \{m \cdot s^{-1}\}$$

As for K, it is the loss coefficient, which is the sum of two different losses:

EQUATION 11

$$K = K_{fittings} + K_{pipe} \ \{-\}$$

Kfittings represents the losses generated by the discrete elements of the system. In this case we consider that the system pump/pipes have two non-return valves, two pipe inlets, three 90º bends and one Bell outlet. Still following 3.2.01, the result is:

$$K_{fittings} = 4{,}6 \ \{-\}$$

As for Kpipe, it is more complex to calculate, and is the loss generated by the friction of the fluid against the walls of the pipe while flowing through it. It is calculated as:

EQUATION 12

$$K_{pipe} = \frac{f \cdot L}{D} \ \{-\}$$

Where L is the length of the pipe (in m), in this work $L = H_{stat} + 3\ m$; D is the diameter of the pipe (in m) and f is the friction coefficient (dimensionless), obtained with the Colebrook White equation:

EQUATION 13

$$f = \frac{0{,}25}{\left(log\left(\frac{e}{3{,}7 \cdot D} + \frac{5{,}74}{Re^{0{,}9}}\right)\right)^2} \ \{-\}$$

Where e is the roughness factor, dependant on the pipe material (since the pipes used are going to be of PVC, it is $1{,}5 \cdot 10^{-6}$ m) and Re is the Reynold number:

EQUATION 14

$$Re = \frac{\mathrm{v} \cdot D}{\nu} \ \{-\}$$

Where ν is the kinematic viscosity (in m^2/s), and $\nu = 1{,}31 \cdot 10^{-6}$.

Now, if we substitute develop the equations to the limit, we obtain the following formula for Hdyn where it is simply dependent on D (in m) and Q (in m3/s).

EQUATION 15

$$H_{dyn} = \frac{\left(K_{fittings} + \frac{\frac{0{,}25}{log^2\left(\frac{e}{3{,}7 \cdot D} + \frac{5{,}74}{\left(\frac{4 \cdot Q}{\pi \cdot D \cdot \nu}\right)^{0{,}9}}\right)} \cdot L}{D}\right) \cdot \left(\frac{4 \cdot Q}{\pi \cdot D^2}\right)^2}{2g}$$

Substituting the values we already know:

$$H_{dyn} = \frac{\left(4{,}6 + \frac{\frac{0{,}25}{log^2\left(\frac{1{,}5 \cdot 10^{-6}}{3{,}7 \cdot D} + \frac{5{,}74}{\left(\frac{4 \cdot Q}{\pi \cdot D \cdot 1{,}31 \cdot 10^{-6}}\right)^{0{,}9}}\right)^2} \cdot (Depth + 5)}{D}\right) \cdot \left(\frac{4 \cdot Q}{\pi \cdot D^2}\right)^2}{2 \cdot 9{,}81}$$

$$H_{dyn} = \left(0{,}2345 + \frac{0{,}01274}{D \cdot log^2\left(\frac{1{,}5 \cdot 10^{-6}}{3{,}7 \cdot D} + 5{,}74 \cdot \left(\frac{\pi \cdot D \cdot 1{,}31 \cdot 10^{-6}}{4 \cdot Q}\right)^{0{,}9}\right)} \cdot (Depth + 5) \right) \cdot \left(\frac{4 \cdot Q}{\pi \cdot D^2}\right)^2$$

Thanks to this equation, the effect of these two variables over the dynamic head can be calculated.

2.1.6 Estimated power and energy consumption

Once Htot obtained, the power and energy required by the pump is to be obtained. The power needed in each moment to use the pump is with the equation:

EQUATION 16

$$P\ \{W\} = \frac{\rho\{kg \cdot m^{-3}\} \cdot g\{m \cdot s^{-2}\} \cdot H_{tot}\{m\} \cdot Q\{m^3 \cdot s^{-1}\}}{\eta_{pump}}$$

$$Q = f(tilt, month, Area, \eta_{pump})$$

$$H_{tot} = f(Q, D, depth, \eta_{pump})$$

$$P = f(tilt, month, Area, D, depth) = f(Q(t), D); \{Area, depth, \eta_{pump}\}$$

This value varies with Q and H, and therefore varies with the angle of inclination, the diameter of the pipe and the date of the year. It is also different for each depth and size of the field. The last two variables are used as parameters, as they do not vary once the project chosen. The power can then be estimated as a function of the flow rate range and diameter.

On the other hand, the energy needed is calculated with the following formula:

EQUATION 17

$$E\ \{J\} = \frac{\rho\{kg \cdot m^{-3}\} \cdot g\{m \cdot s^{-2}\} \cdot H_{tot}\{m\} \cdot V\{m^3\}}{\eta_{pump}}$$

Is therefore also dependent on the same variables and parameters as P.

$$E = f(Q(t), D); \{Area, depth, \eta_{pump}\}$$

2.2 Methods

2.2.1 Calculations

All the calculations with the exception of the energy generated (obtained by PVGIS) and the optimal angle per month are obtained through excel calculations, with the formulas explained throughout the work.

2.2.2 PVGIS

The data of the energy generated is obtained through PVGIS, a free software from the EU. To do so, we enter in the program and select a point on the map (in our case, close to Fada N'Gourma). We choose it far from the population because the system is going to be mainly rural, and we do not want to have any external factor influencing.

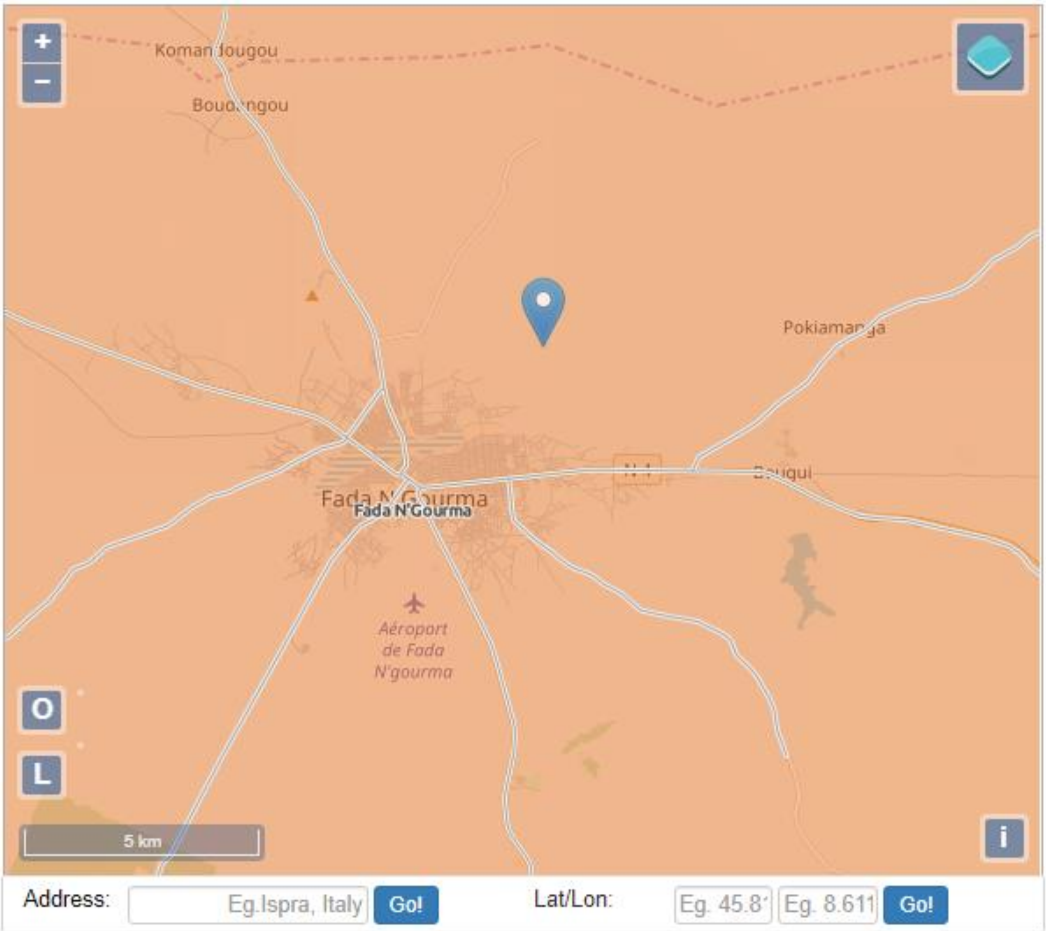

Figure 8. Selection of the location in PVGIS

The, we select the option GRID CONNECTED. This is done because we consider the system as able to run without batteries, and thus we want the energy used when produced

The solar system used is of Cadmium Telluride (CdTe), since they are the ones with best performance in these conditions (Andrić *et al.*, 2018), but it is not part of the thesis to determine it. A 1 kWp system is selected as reference, and the system losses are kept at the default (14%). The system is free-standing and the azimuth is put at 0°: since it is not going over a roof, we have freedom of movement.

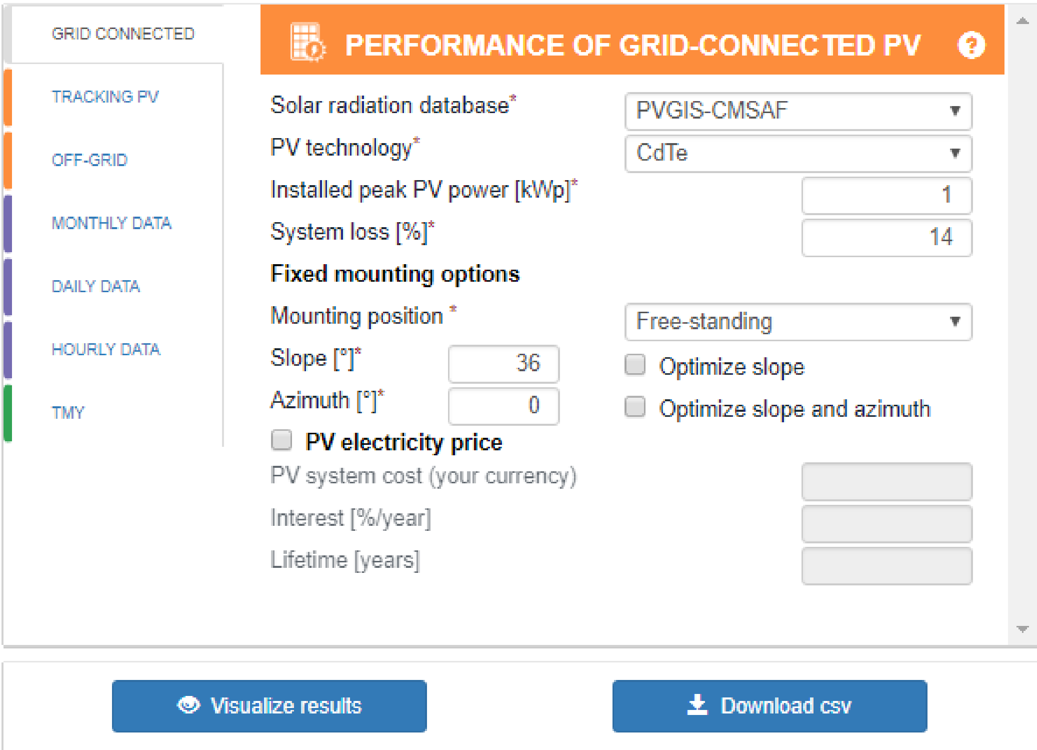

Figure 9. PVGIS window to introduce parameters of the system

The angles Will vary over the study. In this figure, 36° is marked. For negative values of the slope, they have to be written in positive and change the azimuth angle to 180°.

The results are then displayed as shown below.

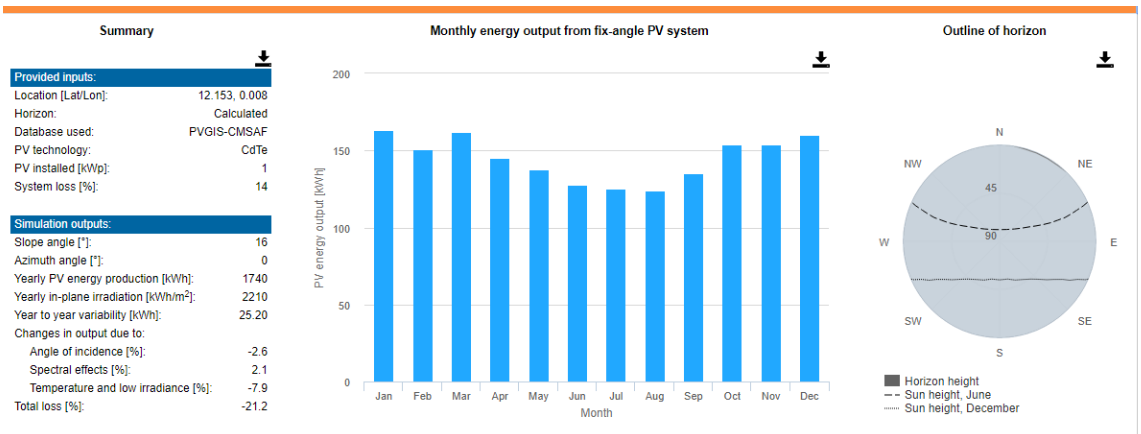

Figure 10. "Visualize results" window in PVGIS

3 RESULTS AND DISCUSSION

Before starting, some parameters and information must be decided. First, the location: Burkina Faso has been chosen as a country because of the great number of data found referred to this country. Moreover, part of Burkina Faso is in the Sahel or next to it, a region with problems for watering crops and chronic hunger. The exact location chosen was Fada N'Gourma, because it is close to the Sahel, and had many data collected. In this region, the rain is not excessive (Figure 5), it has good solar radiation (Figure 6), and the aquifer productivity is above 0,5 L/s (Figure 4).

Second, the size of the orchard must be decided. After what was discussed in 1.3.7.2, we will work with three hypotheses of field size: 120 m2, 250 m2 and 500 m2, depending on the will of the farmer. These are relatively small orchards, that can help with extra incomes and food.

Finally, the depth is to be selected. The water in the region chosen is entirely above 25 m underground (Depth<25 m; Figure 3). Therefore, three different values of depth are going to be studied in this thesis: 7, 15 and 25 m.

3.1 Climatic conditions

3.1.1 Average temperatures

Once the location selected, the temperature is one of the easiest parameters to obtain. In this thesis, the values of different sources are considered to obtain our own results. These sources show the average monthly temperatures (The World Bank Group, 2015; CLIMATE-DATA.ORG, 2018; Weatherbase, 2018), and the average minimum and maximum (CLIMATE-DATA.ORG, 2018; Weatherbase, 2018).

With these data, the average of the three is calculated, and the absolute average maximum and average minimum are obtained. These results are shown in the following figure, where the range of temperatures in Fada N'Gourma are easy to identify.

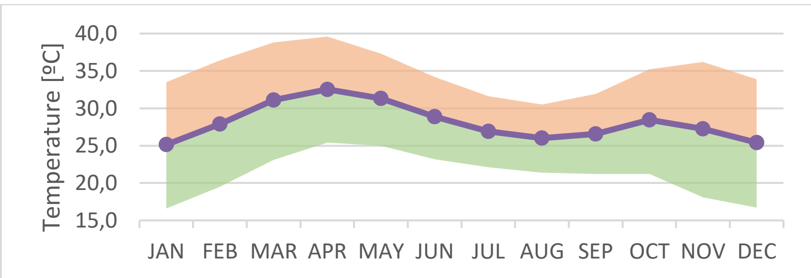

Figure 11. Range of temperatures in Fada N'Gourma

The maximum temperature is in spring, and the lowest around the winter and the summer. However, they remain high temperatures throughout the year, without huge variations, which is to be expected near the Sahel region.

3.1.2 Precipitation

The data bases used prior also present the average precipitation of the years they have measured. To have a more comprehensive estimation of the precipitation, in this study the monthly average of the three, as well as the minimum and maximum, is obtained. These values of precipitation are going to be essential to estimate the water needed for irrigation.

Since the data used are averages, their variability is very small, which can be seen in the next graph.

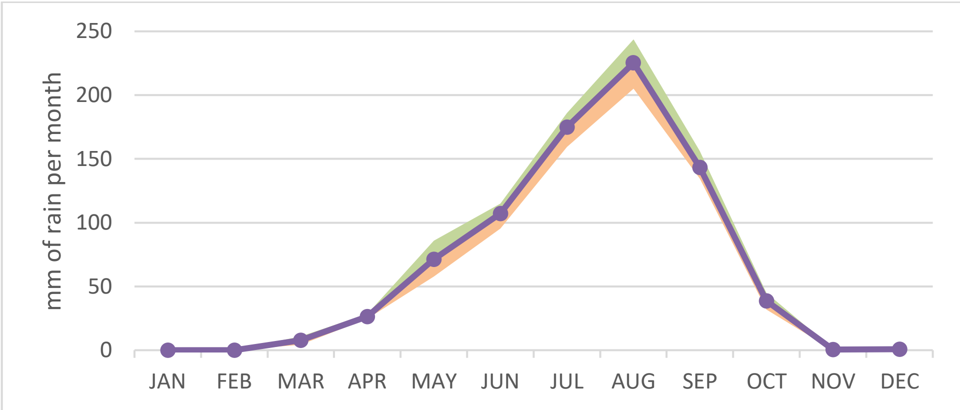

Figure 12. Range of precipitations in Fada N'Gourma

The graph shows how the dry season occurs in winter, with no rain at all between November and January. On the other hand, the rainy season is in summer, with a steep increase in precipitations until August, where the maximum is achieved.

3.1.3 Radiation

The values of the radiation in the location chosen are essential for this work. Indeed, solar radiation influences both most important parameters. On the one hand, it is a key factor in the calculation of the evapotranspiration of the crops alongside with the temperature, and therefore, influences the demand. On the other hand, it the main factor in the solar energy production by the PV system, influencing then also the supply.

But the solar radiation is divided into different categories. In this case we are going to focus on the direct and the extra-terrestrial solar radiation.

The values for the direct solar radiation are obtained on Weatherbase (2018) after 22 years of measurements, and they present the daily average, maximum and minimum. It is relevant to present the range these numbers can be contained in because direct global radiation depends not only on the geographical position but also on variations in the climate. As for the extra-terrestrial solar radiation, it only depends on the position of the system, and therefore can be easily calculated without the need of empirical measurements. In this work, these values were obtained through www.saecanet.com (2010). All these are presented in Figure 13.

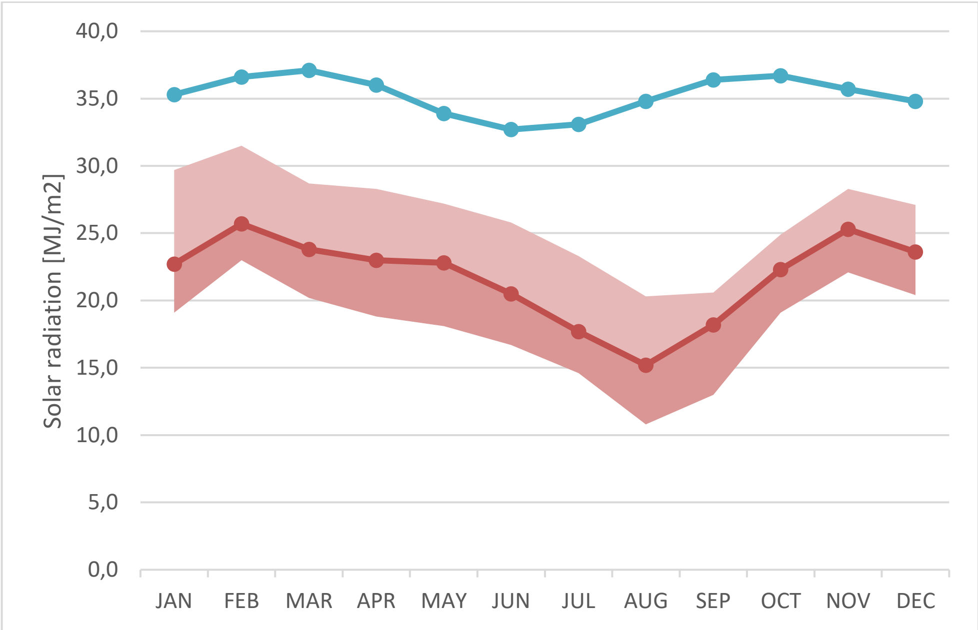

Figure 13. Extra-terrestrial solar radiation (in blue) and range for solar direct radiation (in red), in MJ/m² for Fada N'Gourma

With the help of the figure we can observe how the extra-terrestrial solar radiation has a minimum in June, due to the longest distance to the sun in this month and the latitude. As for the direct solar radiation, it attains its minimum in August. Interestingly, it can be noted that the trend matches the one of the extra-terrestrial radiation from October to March, the months of the dry season. On the other hand, it drops during the wet season in a similar shape as the precipitations trend increases.

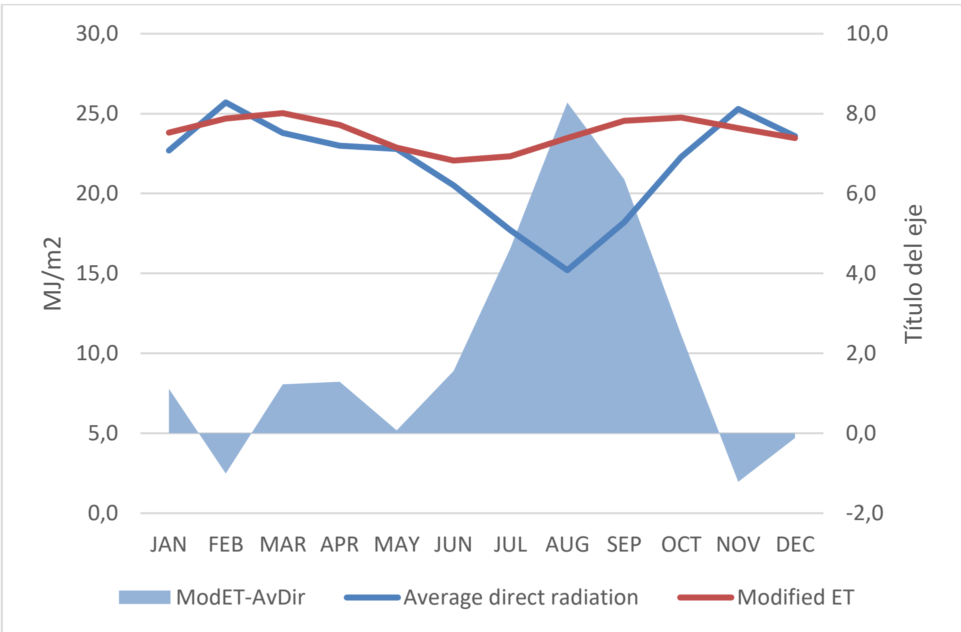

Figure 14. Experimental approach to relate precipitations with drop in solar direct radiation

This can be seen in the previous graph, where the average direct radiation is depicted alongside with of a modified extra-terrestrial one. This modified is the result of obtaining the average radiation for the months with almost no precipitations (January, February, March, November and December) in both types, and then escalating the extra-terrestrial radiation to equate the direct average. Then, the average direct is subtracted to the modified extra-terrestrial, obtaining the greened area curve. The previous intuition is confirmed, as both this new curve obtained, and the precipitation data are very close in shape.

These results are however not surprising, since rain comes with clouds, and clouds block the direct solar radiation. Therefore, the more rain, the less direct solar radiation, which can help to explain the passive self-regulating concept attributed to PVWP systems.

3.2 Calculation of the crops watering needs

3.2.1 Evapotranspiration of the crop field

The evapotranspiration is a concept to obtain the need of water for plants, and it is explained in the theory section 2.1.1. Following the calculations explained there (and with the climatic values of the previous chapter), Figure 15 is obtained. There, the values of ET_0 for both the equations and the range of mean values estimated by different sources in subsection 2.1.1.1 (between 4 and 9 mm/day) are depicted.

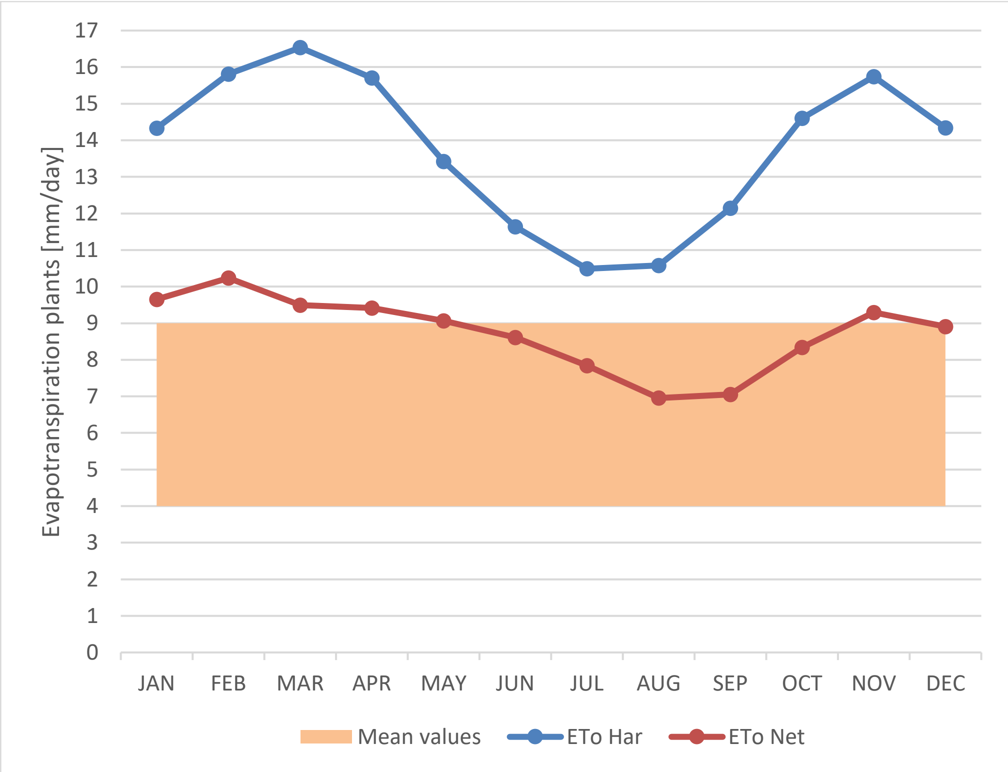

Figure 15. Estimated monthly value for the reference evapotranspiration in Fada N'Gourma for different methods

The values for the Net Radiation Method Equation (Equation 2) are close to the range estimated; they therefore are accepted as so.

However, the values obtained for the Hargreaves equation (Equation 3) are well above the range estimated. Since the latter is considered more comprehensive, we would therefore escalate them to have the same average as the one obtained with the net radiation method. These new values are ET_0 Hargreaves modified (Table 31) and are still on the upper limit of the range found in the references, and therefore still conservative.

3.2.1.1 Estimated reference evapotranspiration

The average for both the reference evapotranspiration obtained by the net radiation method and the one obtained by the Hargreaves equation modified is calculated. This value of ET_0 (ET_0 work) is the one to be used from now on in this work, and is depicted in the following graph:

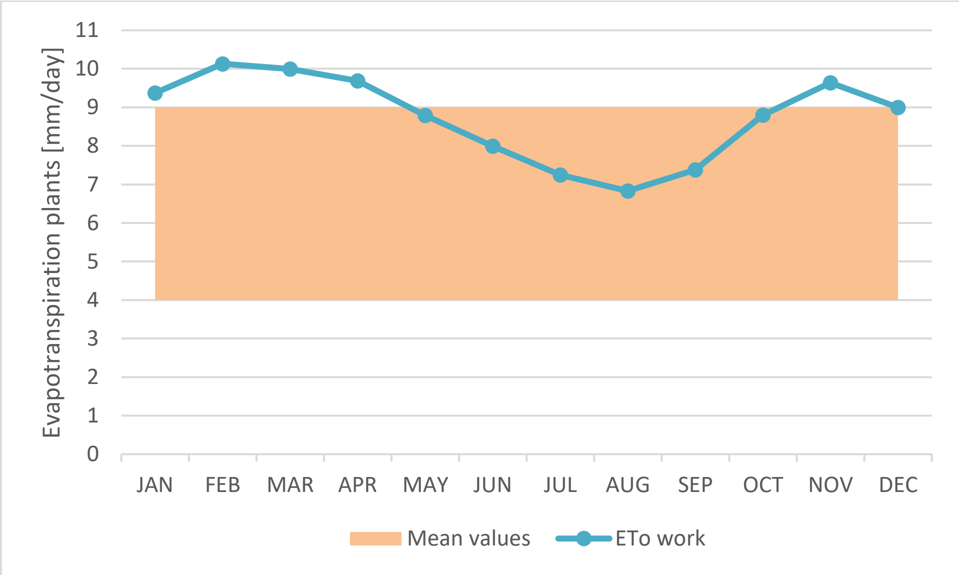

Figure 16. Estimated monthly value for the reference evapotranspiration in Fada N'Gourma

As can be seen in the figure, this value calculated is conservative if compared to the range found in the references.

Furthermore, the shape of the resultant reference evapotranspiration is very similar to the one presented by the direct solar radiation. This again helps to sustain the arguments behind the concept of passive self-regulation of PVWP for irrigation.

3.2.1.2 Maximum evapotranspiration

The values of single crop coefficient for different crops (Kc, concept explained in section 2.1.2) are shown in Allen *et al.* (1998), with the highest peaks of Kc being for some trees and rice (1,2). But it would be recommended to use trees adapted to the local climate, such as the Pomme du Sahel, and rice is not a type of crop worth to plant for smallholder farmers (subsection 1.3.6.2). Therefore, the highest value of Kc for a crop that could be convenient is for example with tomato, which has a still high peak of 1,15.

Using tomato as a reference crop in this work is subsequently a conservative assumption. Furthermore, since the planting date can vary from year to year in the climate studied if irrigation is available, to simplify the calculations only the value of Kcmax to calculate ETcmax is used.

$$ET_{cmax} = ET_0 \cdot K_{cmax} = ET_0 \cdot 1{,}15 \ \{mm \cdot day^{-1}\}$$

3.2.2 Watering necessities for the plants

To obtain the final value of the watering needs, the steps of section 2.1.3 of the theory are to be followed, as presented in Equation 4:

$$Watering = ET_c - Prec_{ef}$$

To be more conservative, the precipitation used will be the minimal, and ETc the maximal value.

As the value of the monthly precipitation used is never over 250 mm, only Equation 5 will be used. With this, the value of $Prec_{ef}$ is obtained, and will be subtracted to the evapotranspiration of the crop field in order to obtain the watering necessity (Figure 17).

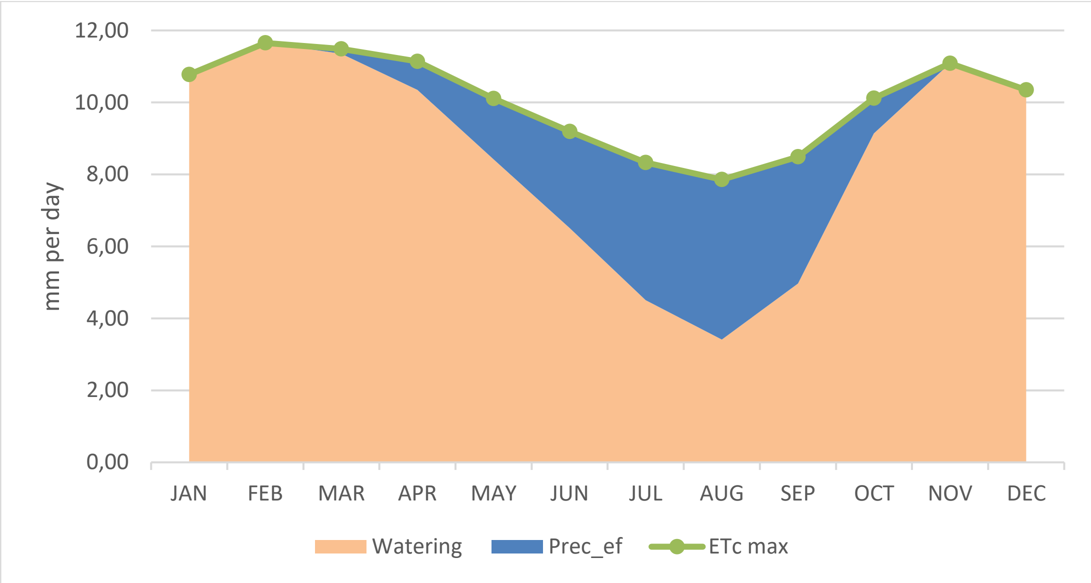

Figure 17. Maximum evapotranspiration for a field in Fada N'Gourma (ETcmax), divided between the watering need and the water obtained from the rain ($Prec_{ef}$), in a monthly distribution.

As can be seen, the water supplied by the rain is strongly related with the monthly rain. Looking into the artificial watering need, the valley present in ETc in summer (wet season) is increased due to the rain input, whereas the amount in winter remains constant.

3.2.3 Real evapotranspiration, ETc

It is interesting to remember that, even if these are the values to be used for further calculations, they are not the real ones. Indeed, a more comprehensive study should consider the variation of Kc over the year.

To have an idea of this effect, a rough estimation of ETc real and the watering needs will be calculated here for tomato in Fada N'Gourma. With the climatic conditions of the location, tomato can be cultivated up to three times, or cycles, per year (Balana *et al.*, 2017). Adapting data from Allen *et al.* (1998), the following graph with the evolution of Kc over the year is obtained, given that the first cycle is started in January.

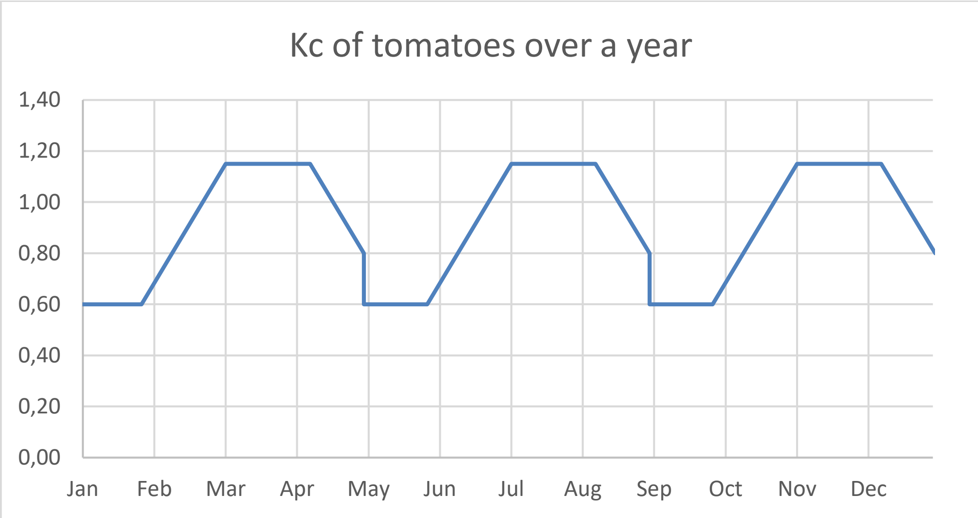

Figure 18. Evolution of Kc over the year for tomato.

Following the steps previously done, we obtain:

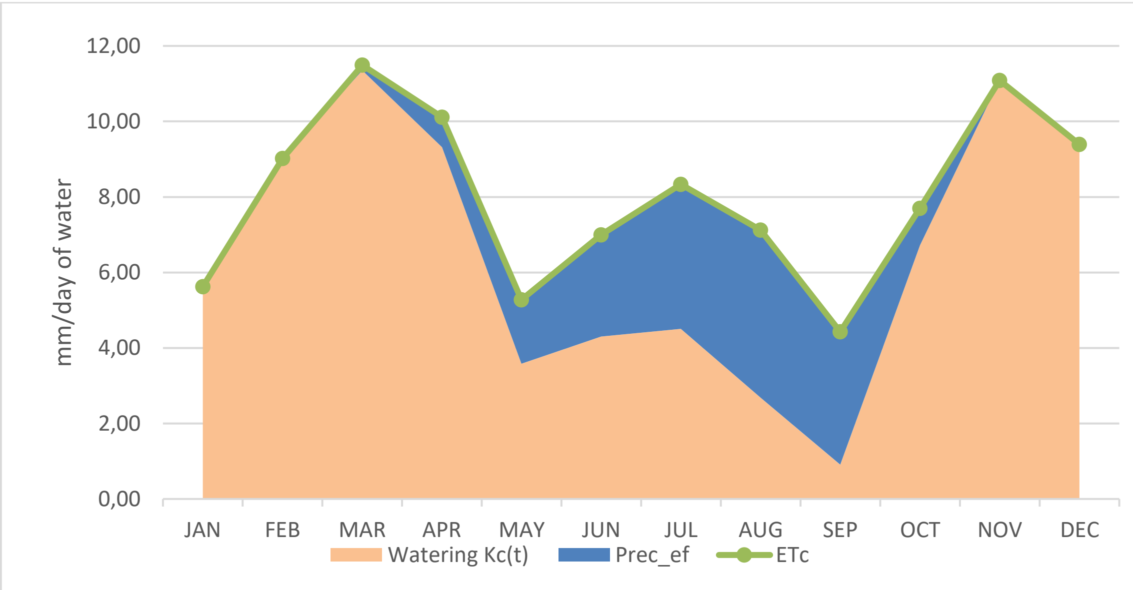

Figure 19. Evapotranspiration for a field in Fada N'Gourma (ETcmax), divided between the watering need and the water obtained from the rain ($Prec_{ef}$), in a monthly distribution for three cycle tomato crop field started in January.

We can see how the phase of development of the crop, and therefore the moment chosen to plant, has great influence in certain months. A more detailed study could consider optimising the match between the watering needs Kc(t) and the solar PV system output or increasing the resilience of the system (see section 3.6.1).

Indeed, the difference between the watering needs used and the real one will make the system more resilient to changes in weather conditions (like a security coefficient). If an electrical system was to be installed to take advantage of the excess electricity production, these valleys will also help greatly with the production.

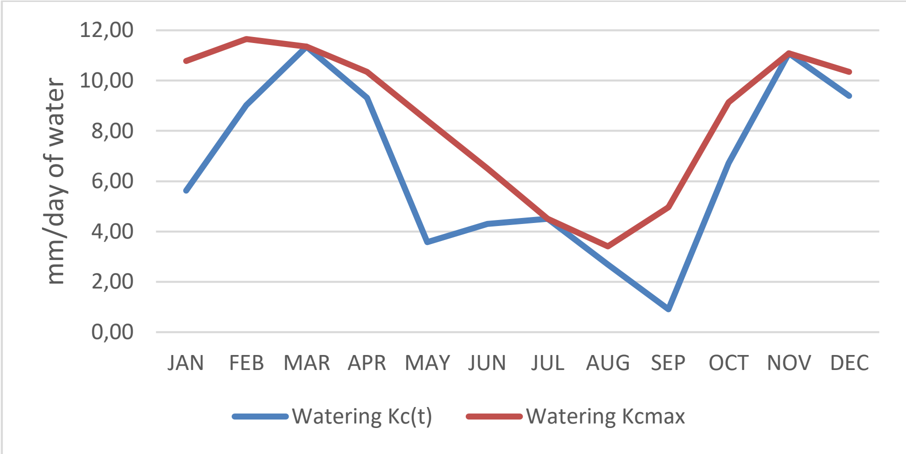

Figure 20. Watering needs for a tomato crop field when using Kcmax and when using Kc variable with crop development, planting in January

3.2.4 Water volume scenarios

Finally, it is now possible to estimate the total volume to be extracted for each scenario. The water needs of a person in a day have been estimated to be 100 L (subsection 1.3.7.1). If we consider a household with 6 members, this would be 0,6 m^3 per day, every day. The water for irrigation must be added to this value, obtaining the next equation.

EQUATION 18

$$V\left\{{m^3}/{day}\right\} = 0{,}1 \cdot people\ \{m^3\} + \frac{Watering\left\{{mm}/{day}\right\} \cdot Surface\ \{m^2\}}{1000}$$

The results are shown in Figure 21. The smaller the orchard, the more constant the monthly volume needed. This is because the 0,6 m^3 for domestic use must always be kept, and the smaller the orchard, the smaller the proportion on the water used is for irrigation.

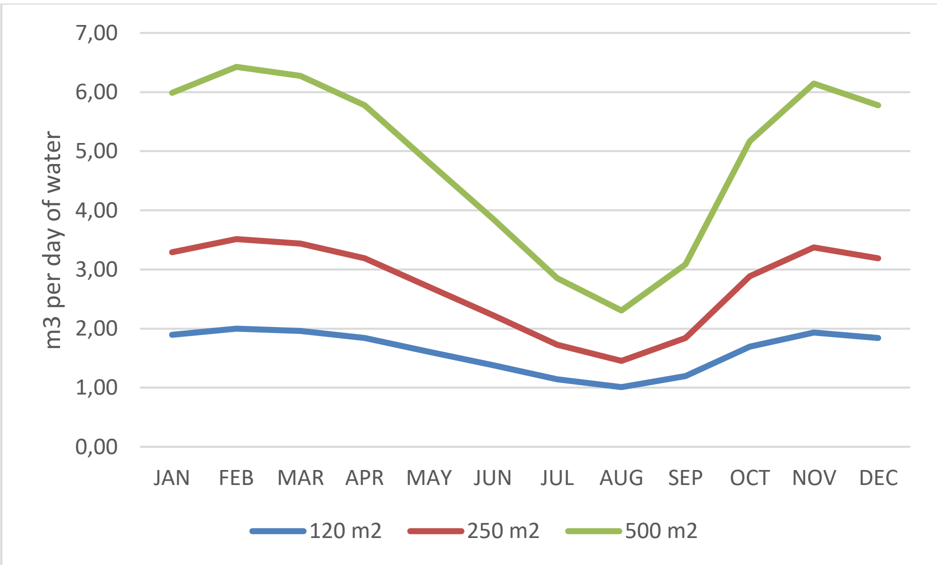

Figure 21. Daily volume needed per month for each orchard

3.3 Evaluation of range of operation

Once the climatic conditions of the location studied, and the values of the water needed calculated, the next step is to study the different parameters of design. However, two different goals are pursued. On the one hand, to show how to estimate the values for these parameters using the example of Fada N'Gourma. On the other hand, to obtain general conclusions (aiming to go beyond this example) on how to perfect the modelling of PVWP systems for irrigation are explored.

3.3.1 Water flow rates

The first value analysed is the water flow. To obtain the flow rate, two things are needed: first, the total volume to be extracted in a day; second, the profile of extraction of the pump (instant power of extraction). In this case, to reduce the storage capacity (tank volume or battery size), we would design a pump working directly with the energy generated by the sun. The objective of this section is to obtain the range of the average water flows of operation for each type of orchard.

3.3.1.1 Monthly optimal angles

Since the consumption is variable due to the changes in the watering needs of the field, it is not immediate to determine the month that needs to be prioritised while determining the angle of inclination. Thus, until one is chosen, all the monthly optimal angles will be considered. These angles only depend on the latitude and the month of the year and can therefore be easily obtained. For this case, (Http://solarelectricityhandbook.com, 2009) was used, obtaining the values of inclination shown in the next table.

Table 1. Optimal monthly angle of inclination

	opt ang	DEC	36
JAN	28	NOV	28
FEB	20	OCT	20
MAR	12	SEP	12
APR	4	AUG	4
MAY	-4	JUL	-4
JUN	-12		**opt ang**

The angles are presented in the table. As can be seen, they can be sorted by couples, plus the values corresponding to the limits in June and December. This way, it can be observed that there are only seven monthly optimum angles of inclination. The negative angles of inclination correspond to solar panels headed north with an equivalent but positive angle of inclination.

3.3.1.2 Electricity generation and Peak Extraction Hours

Once these angles determined, they are to be put in the PVGIS software, which will be run for each one of them. Thus, the data of the daily energy generation for a 1 kWp is obtained and depicted in the following figure.

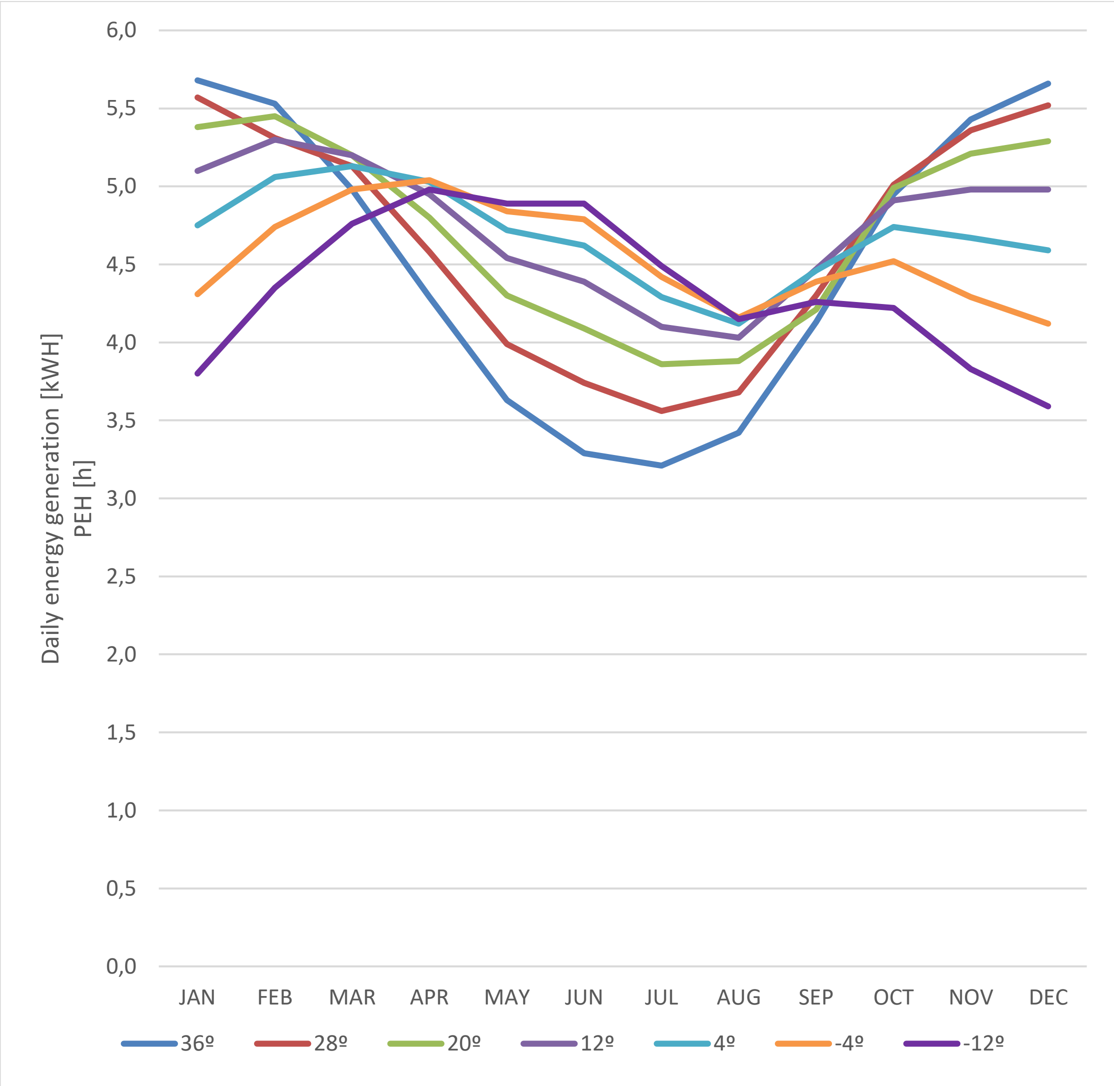

Figure 22. Daily electricity generation for a 1 kWp solar PV system (or peak extraction hours) per month.

It can be observed that the shape and values of the generation vary with the angle, but all of them are between 3 and 6 kWh.

These results are the same as for the Peak Extraction Hours, to be used from now on as stated in Section 2.1.4 of the Theory. The concept of PEH is a simplification of the reality to make the calculations manageable, and its precision for the results obtained is explored later in Section 3.5.2.

3.3.1.3 Water flow values

Once all this done, the daily volume of water needed (by month, for the three different fields, section 3.2.4) is to be divided by all the possible combinations of angles in the corresponding month. This way, all the possible water flows is obtained for each of the three field sizes. This evolution of water flow rates over the year for different angles and fields is shown in the next graphs.

$$Q = f(Month, Tilt); \{Surface\}$$

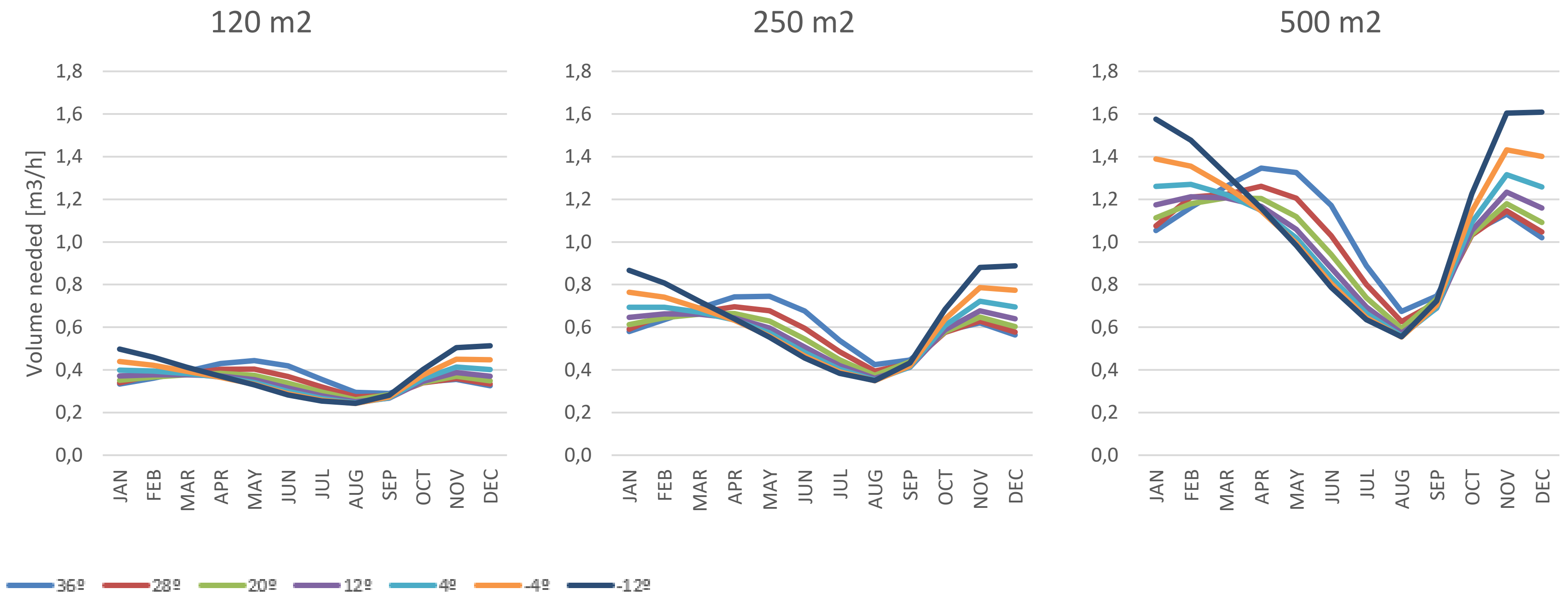

Figure 23. Water flow for different angles of inclination and field size, per month

But since it is too complex to use all this data variation (per month, per angle, per field, and later per diameter and per depth), the range of water flow for each field size is estimated, and depicted in the next page.

First, the annual range of water flow for each field and angle of inclination is depicted in the next graph. It is relevant to notice the average value for each field remains very similar despite big changes in the angle of inclination.

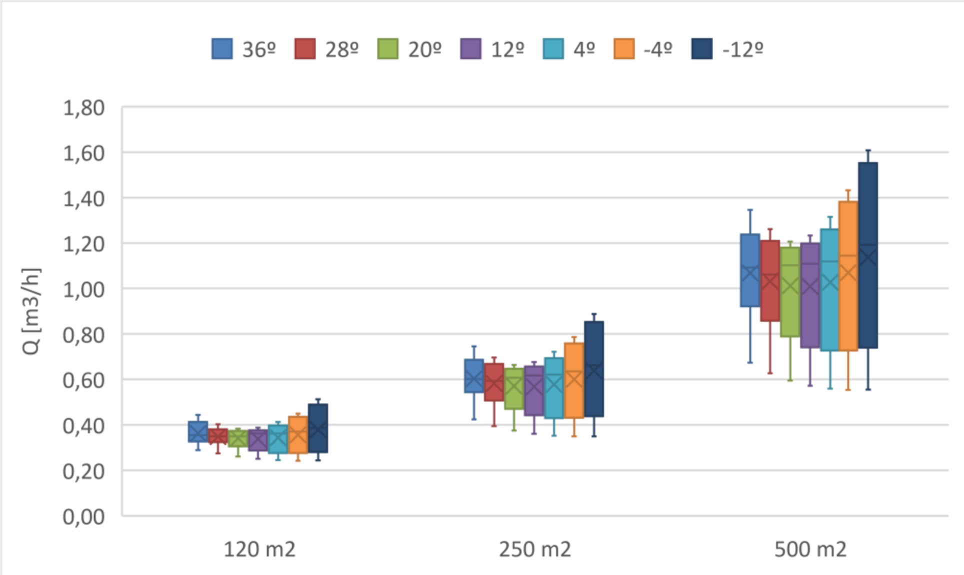

Figure 24. Annual water flow range, for different angles of inclination and field size

The only noticeable difference is in the spread of the range, but they remain comparable. It will therefore not be very unprecise to estimate a unique range of water flow for each orchard area, obtaining the following graphic.

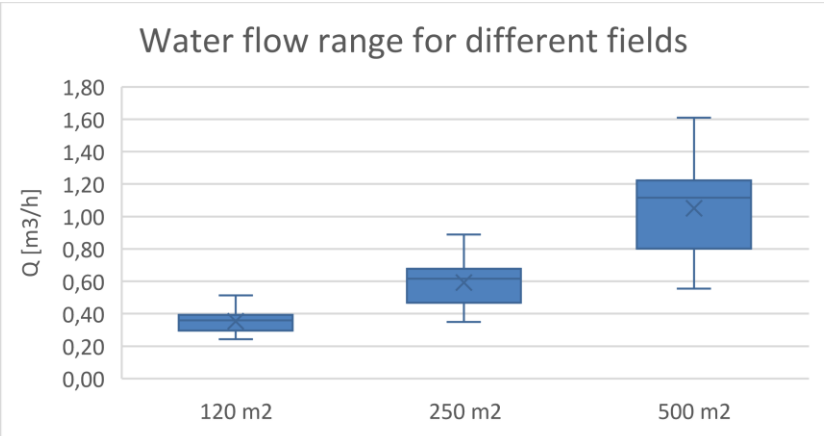

Figure 25. Total range of annual water flow for all the studied inclinations, for each field size

We can see that for 120 m^2 it goes from 0,24 to 0,51 m^3/h, for 250 m^2 from 0,35 until 0,89 m^3/h, and for 500 m^2 from 0,55 to 1,61 m^3/h. As for the average values, they are 0,35; 0,59 and 1,05 m^3/h respectively.

These ranges are to be used in the next section to evaluate the impact of the losses for different system configurations in a simpler way. This allows to consider the effects of the monthly variation and the angle of inclination in a single variable, the water flow rate, and reducing its spread to the range obtained.

3.3.2 Dynamic head

Once the range of water flow determined, it is important to calculate the losses (or the dynamic head) according to it. This initial calculation is done to estimate if a variation of the diameter of the pipes is relevant enough to take it into account in the next sections. Consequently, the variation of the dynamic head will be calculated as a function of the diameter and water flow (with the depth as a parameter), as shown in Equation 15 in Section 2.1.5 of the theory.

$$H_{dyn} = f(Q, D); \{Depth\}$$

The water flow itself can be divided into different ranges for each size of the orchard (Surface) to make the approach more precise. Therefore, it would be calculated using the water flow ranges shown in Figure 25 as:

$$H_{dyn} = f(Q, D); \{Depth; Surface\}$$

As for the values of the diameter, the options studied would go from ½” pipes (12,7 mm of diameter) to 2” pipes (50,8 mm), increasing the diameter by ¼” each (7 pipes in total). These have been chosen for being the most common pipes for this type of project.

All this is to be done for the three different values of the two parameters, or nine different scenarios. The results of the calculation are shown in Figure 26.

However, the values of Hdyn are influenced by the depth of the well in a linear way (once Q and D fixed), as can be seen from the development of Equation 15, and is simplified here:

$$H_{dyn} = \big[0{,}2345 + f_1(Q, D) \cdot [Depth + 5]\big] \cdot f_2(Q, D)$$

$$H_{dyn} = f_3(Q, D) + f_b(Q, D) \cdot [Depth + 5]$$

$$H_{dyn} = f_a(Q, D) + f_b(Q, D) \cdot Depth$$

Where:

$$f_b(Q, D) = f_1(Q, D) \cdot f_2(Q, D)$$

$$f_a(Q, D) = f_2(Q, D) \cdot [0{,}2345 + 5 \cdot f_1(Q, D)]$$

Since the point of interest really is to study the influence of the friction relative to the energy expenditure, it looks possible and better to present the data of Hdyn as a percentage of the total head (which is linearly related to the power expenditure). This will allow to better compare each scenario, since the linear correlation would be turned into an inverse one (which fades with the depth).

Thus, Figure 27 depicts the percentage of the effective energy expenditure that goes to cover the losses due to the friction. We can see that in the worst case it can go up to 65% of the total head (for 7 m and 500 m2) for the scenarios studied. This is a very high value, that will obviously have a big impact in all the other parameters. Therefore, the effect of the dynamic head must be studied to calculate the system, regardless of its complexity.

As for the influence of the different parameters, it can be seen that when decresing the diameter, Hdyn increases for all the combinations. Likewise, augmenting the water flow increases the value of Hdyn. It can also be observed that the values of Hdyn can be as high as the depth of the well in the biggest field, which would mean loosing half the energy only because of the friction in the pipe.

These values, especially for the ½" pipe for 500 m^2, look a priori excessive, but a more detailed cost analysis need to be held to determine it definitely. It is nonetheless evident the essential role the diameter of the pipe plays in the energy needs of the syste. Hence, the determination of the optimal diameter can be vital for the viability of any project.

Figure 26. Evolution of Hdyn for different diameters and flows, for each depth and field size studied

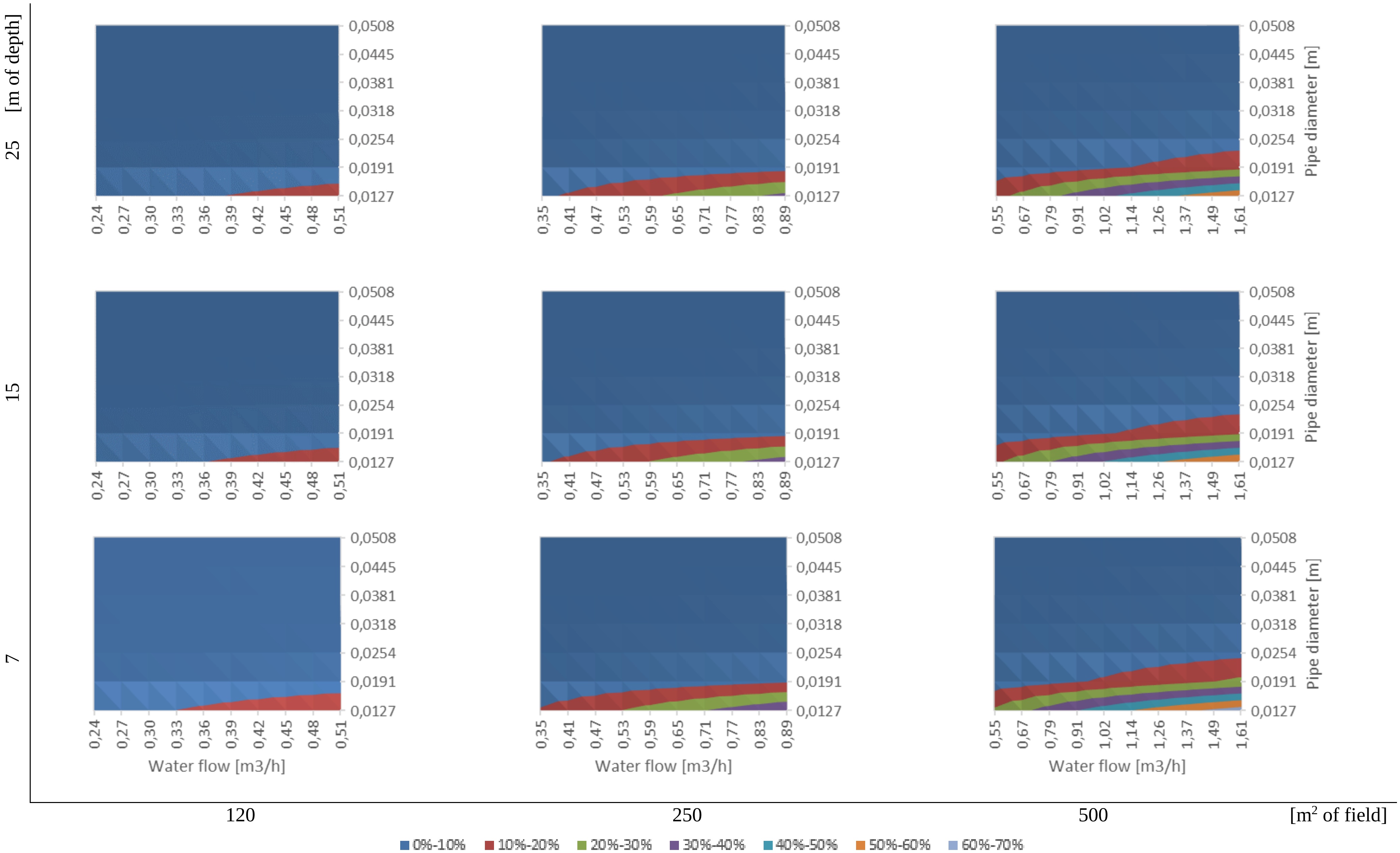

Figure 27. Evolution of Hdyn/Htot [%] for different diameters and flows, for each depth and field size studied

3.3.3 Values for the pump efficiency

The efficiency of the pump depends on the characteristics of the pump bought. Since it is beyond the scope to select a pump, a reference value of the efficiency will be used. In (Tomillo Gutiérrez, 2005), a reasonable review over handpumps is done; and with these values, Figure 28 is depicted. It shows all the efficiencies of the pumps ranged by static head (depth) of the system. The important conclusion to extract from this figure is that the average efficiency of a water pump of the categories considered in this thesis is around 65%. This is going to be the value used by default when the pump efficiency is not considered as variable.

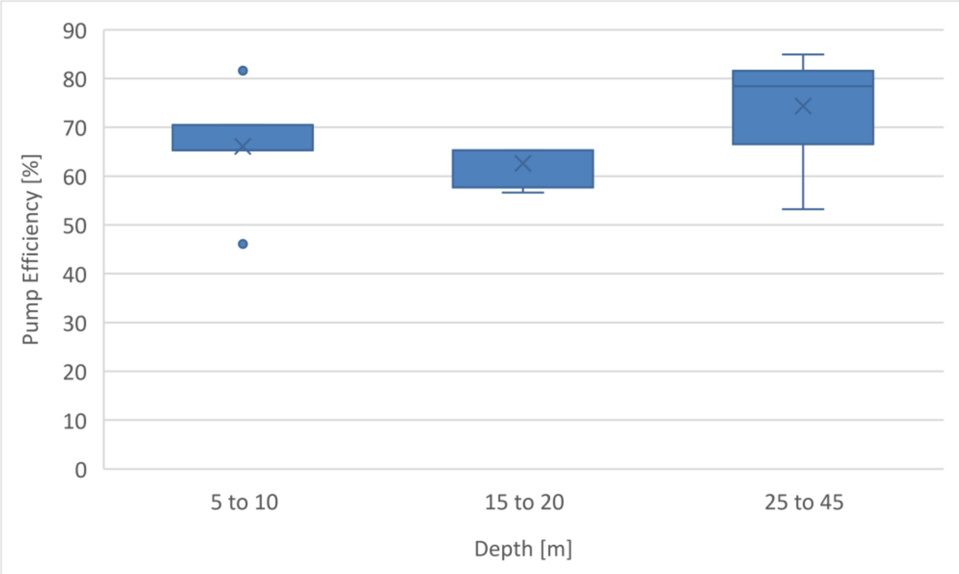

Figure 28. Range of efficiencies for the pump (Tomillo Gutiérrez, 2005)

3.3.4 Estimated values for the cost

For the calculations where the cost is to be minimised, it is necessary to know how expensive the project is going to be. Since it would be too complicated to do a budget for every possible scenario and then check the most suitable, simplifications over the cost will be done.

Therefore, the costs will be divided into two main components. The first one will be the relative to the solar system (PV panel, inverter, cables, etc) and to the pump. These costs depend directly on the power needed, and therefore would be one sole coefficient multiplying the PV panel dimension. It would be presented in USD/Wp. The second component will be the relative to the drilling and piping and is therefore independent from the size of the PV system. It is linearly dependent to the depth of the water and would be presented in USD/m.

For the cost of the solar system, we would take into account the data from (IRENA, 2016). According to the study, the cost of solar systems varies widely depending on the location and the type of system, being generally more expensive in Africa than other regions. The type of system used in this project is a little bit peculiar, in between mini-grid without battery (still not considered) and utility on-and-off grid. For this type of systems, the range goes between 2 USD/W and 8 USD/W as for 2015 prices. For this study, we would choose 5 USD/W, which is in the middle, even though the model should allow to change the value easily.

As for the drilling cost, it is 21 USD/m (Carter, 2009) for a pipe of 1/2" of diameter. To estimate the corresponding cost for other diameters, an assumption is made that the cost of the drilling is directly related to the volume of earth drilled. Therefore, the cost of drilling when changing the diameter will be:

EQUATION 19

$$Drill\ Cost_D = Drill\ Cost_{1/2"} \cdot \left(\frac{A_D}{A_{1/2"}}\right)^2 = Drill\ Cost_{1/2"} \cdot \left(\frac{D}{0{,}0127}\right)^2 \ \left\{{}^{\$}/_{m}\right\}$$

It is important to remind that these are assumptions and simplifications for the matter of this thesis. Therefore, not only these values need to be properly assessed for a more detailed study, but the model resulting of this thesis needs to be designed in order to easily modify the way both parameters evolve.

3.4 Preliminary design of the system

3.4.1 Selection of the tilt

As seen in section 3.3.1, the tilt of the solar panel has effects in the water flow, but also on the daily electricity generation (Figure 22). It is therefore crucial to obtain the angle that optimizes the system, along with the critical month. To obtain these values, parameters like the size of the field, the depth of the well, the diameter of the pipe or the efficiency of the pump must be considered. Consequently, a great number of calculations must be done. To simplify them, several assumptions would be done in each case.

3.4.1.1 Example of case

First, an example for a certain scenario is done. This example is intended to show how all the calculations are held in the following parts of this section. The parameters affecting the system are given a value:

Table 2. Parameters selected for the example

Surface of the field (Sf)	250 m2
Groundwater depth (Depth)	15 m
Pipe diameter (D)	0,0127 m
Pump efficiency (ηpump)	65%

First, the value of the daily electricity generation (Figure 22) is obtained for a 1 kWp size PV system. These values only depend on the month and tilt selected and are therefore not affected by the parameters of Table 2.

$$E_{gen} = f(month, tilt)$$

Second, the value of the flow rate for each month and tilt is obtained like in section 3.3.1. These values still do not depend on any of the parameters of Table 2 . The value of the total daily volume needed is also used, which only depends on the orchard size.

$$Q = f\left(month, tilt, S_f\right)$$

$$V = f\left(S_f\right)$$

Third, the value of Hdyn is obtained for the water flow corresponding to each month and tilt, taking into consideration now the orchard area, depth and pipe diameter. It is obtained with Equation 15, here simplified. The values are shown in Table 3.

$$H_{dyn} = f\left(S_f, Depth, D, \eta_{pump}, Q\right) = f\left(S_f, Depth, D, \eta_{pump}, month, tilt\right)$$

$$H_{dyn} = f\left(S_f, Depth, D, \eta_{pump}, month, tilt\right)$$

Table 3. Monthly average dynamic head for different solar panel tilts. System with 250 m2 orchard, 15 m deep groundwater and pipe diameter of 0,0127 m

	Solar panel tilt [º]						
	36º	28º	20º	12º	4º	-4º	-12º
JAN	4,2	4,3	4,6	5,1	5,8	6,8	8,6
FEB	4,9	5,3	5,1	5,3	5,8	6,5	7,5
MAR	5,7	5,4	5,3	5,3	5,4	5,7	6,2
APR	6,5	5,8	5,3	5,1	4,9	4,9	5,0
MAY	6,5	5,5	4,9	4,4	4,1	3,9	3,9
JUN	5,5	4,4	3,8	3,3	3,0	2,8	2,7
JUL	3,7	3,1	2,7	2,4	2,2	2,1	2,0
AUG	2,4	2,1	2,0	1,8	1,8	1,7	1,7
SEP	2,7	2,5	2,6	2,3	2,3	2,4	2,5
OCT	4,2	4,2	4,2	4,3	4,6	5,0	5,6
NOV	4,7	4,9	5,1	5,5	6,2	7,2	8,8
DEC	4,0	4,2	4,5	5,0	5,8	7,0	8,9

Fourth, with all these data, we are ready to calculate the daily energy needed, measured in size of the solar panel (in Wp) that would be required to meet the needs. This is obtained thanks to Equation 17 (estimated energy consumption), that considers indirectly all the variables here in question. The results are shown Figure 29.

$$E = f\left(H_{dyn}, Depth, \eta_{pump}, V\right) = f\left(S_f, Depth, D, \eta_{pump}, month, tilt\right)$$

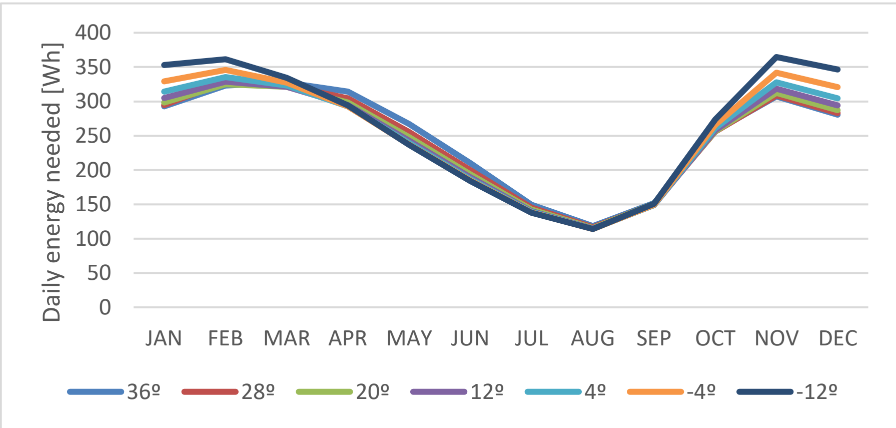

Figure 29. Evolution of the daily energy need for each slope

Fifth, the value of the energy needed (in Wh per month and angle) must be divided by the energy generated by the 1 kWp solar panel (in Wh) for these same months and angles. This same number is to be multiplied by 1000, obtaining then the peak power size of the PV panel to comply with the monthly needs at this angle in W. These results change month by month for a certain angle, but logically, the PV panel is not going to be changed month after month. Therefore, the relevant value would be the yearly maximum for each tilt with these parameters. This would give the minimum size that can meet the energy requirements throughout the year. These are shown in the next table.

Table 4. Monthly PV system size needed (in Wp) for the parameters chosen, and maximum size needed per tilt.

	Solar panel tilt [º]						
	36º	28º	20º	12º	4º	-4º	-12º
JAN	52	53	55	60	66	76	93
FEB	58	62	60	62	66	73	83
MAR	66	63	62	62	63	66	70
APR	73	67	62	60	58	58	59
MAY	74	64	58	53	51	49	48
JUN	64	53	47	43	40	39	38
JUL	47	41	37	34	32	31	31
AUG	35	32	30	28	28	27	27
SEP	37	35	36	33	33	34	35
OCT	52	51	51	52	55	59	65
NOV	57	58	60	64	70	80	95
DEC	50	51	54	59	66	78	97
	Max PV peak power needed [Wp]						
	74	67	62	64	70	80	97

The month in which the maximum value is obtained would hence be the critical month, and therefore the one with the highest risk of not being able to meet the requirements.

Now, the minimum size for the PV panel to install is to be determined, and therefore, the optimal angle. With the values already calculated, it is 20° for this case, being April and March the critical months.

But to be more precise, the exact optimal angle can be obtained with two methods. First, with the help of Figure 30 depicting the size of PV to install for each angle. The optimal angle corresponds to the minimum in the solar PV size and can now be obtained with the graph directly (18,5º).

The value can also be obtained with the help of the tendency curves (polynomial, 2º degree, since they match well the distribution). The main advantage of it is that it allows to automate the process with the help of the LINEST command in excel. For an equation of the type:

EQUATION 20

$$f(x) = a \cdot x^2 + b \cdot x + c$$

The value of the maximum/minimum (in this case, minimum) is:

EQUATION 21

$$x_{min} = \frac{-b}{2a}$$

As so, it can be calculated:

$$x_{min} = -\frac{-1{,}3435}{2 \cdot 0{,}0368} = 18{,}3º$$

Both the angle obtained visually, and the one obtained mathematically are very close to each other. This is because the polynomial approximation is very close to the reality. The mathematical value would be nonetheless the one used.

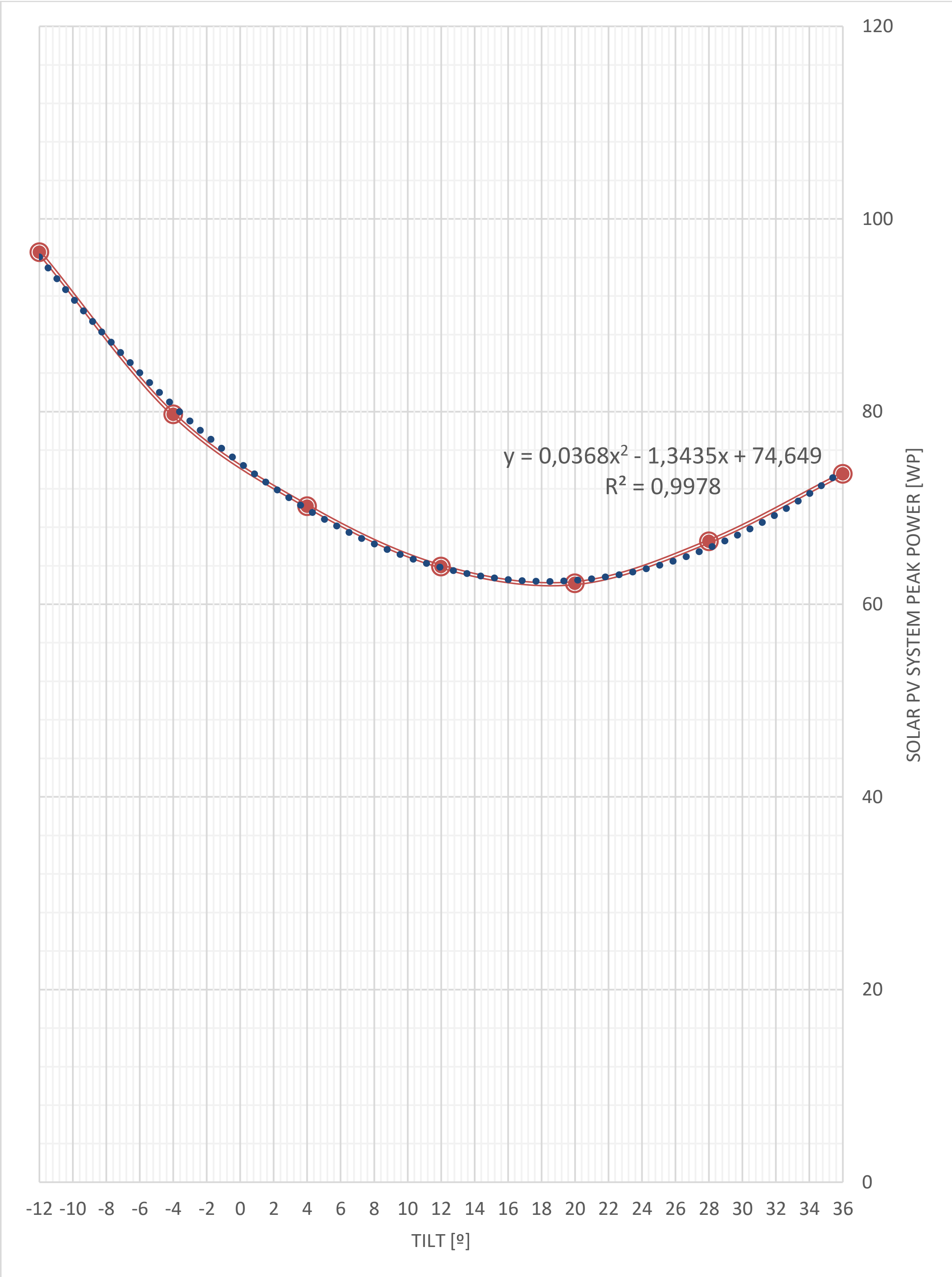

Figure 30. Variation of the PV system peak power with the angle.

3.4.1.2 Influence of the diameter

Once the method to calculate the optimum angle has been exposed, this procedure is now to be repeated with variations in the different parameters affecting the optimum angle. The first one studied will be the influence of the diameter of the pipes (D). In order to correctly assess the influence, not only D is going to be a variable, but the Depth and the Surface to irrigate would be considered as parameters, obtaining nine scenarios. The efficiency of the pump will remain constant at 65%, as there are too many parameters now.

The data are presented in Figure 31, and the optimal angles summarised in Table 5. A few interesting facts can be concluded. The first one, which was the point of this subsection, is that the diameter of the pipe does not have a noticeable effect in the optimal angle. This can be better seen in the following table, displaying the optimal angles for each diameter, each depth and each surface. The second one is that it also seems that the depth does not have an influence over the optimal angle. This is confirmed in subsection 3.4.1.3.

Table 5. Optimal angle for different depths, orchards and diameters

		Diameter						
	Depth [m]	0,0127	0,01905	0,0254	0,03175	0,0381	0,0445	0,0508
120 m2	7	16,8	16,7	16,7	16,7	16,7	16,7	16,7
	15	16,8	16,7	16,7	16,7	16,7	16,7	16,7
	25	16,8	16,7	16,7	16,7	16,7	16,7	16,7
250 m2	7	18,3	18,2	18,2	18,2	18,2	18,2	18,2
	15	18,3	18,2	18,2	18,2	18,2	18,2	18,2
	25	18,3	18,2	18,2	18,2	18,2	18,2	18,2
500 m2	7	18,7	18,6	18,6	18,5	18,5	18,5	18,5
	15	18,7	18,6	18,6	18,5	18,5	18,5	18,5
	25	18,7	18,6	18,6	18,5	18,5	18,5	18,5

Only the surface of the field, and in a mild way, has therefore an influence. This makes sense because the change in the surface to irrigate does not change the configuration of the water distribution over the months for irrigation, since it will only multiply it by a constant. But, since the needs for WSS are independent of the orchard, they are not affected by the same coefficient. Thus, the monthly distribution varies relatively, especially for smaller surfaces, since at a certain point the water needs for irrigation are so high they make the water for WSS not noticeable. This can be observed even with the three data calculated: the angle varies much more from 120 to 250 m^2 than from 250 to 500 m^2. Thus, it looks that for bigger fields than 500 m^2, the optimal angle will be around 19º.

Last, but probably the most important to notice in the graphs, is that for all the scenarios, there is nearly no gain in any pipe bigger than 0,0254 m. Indeed, the gain between this one and the one of diameter 0,01905 m is very small. Consequently, only the three smallest pipes will be tested from now on (½ “, ¾”, 1”).

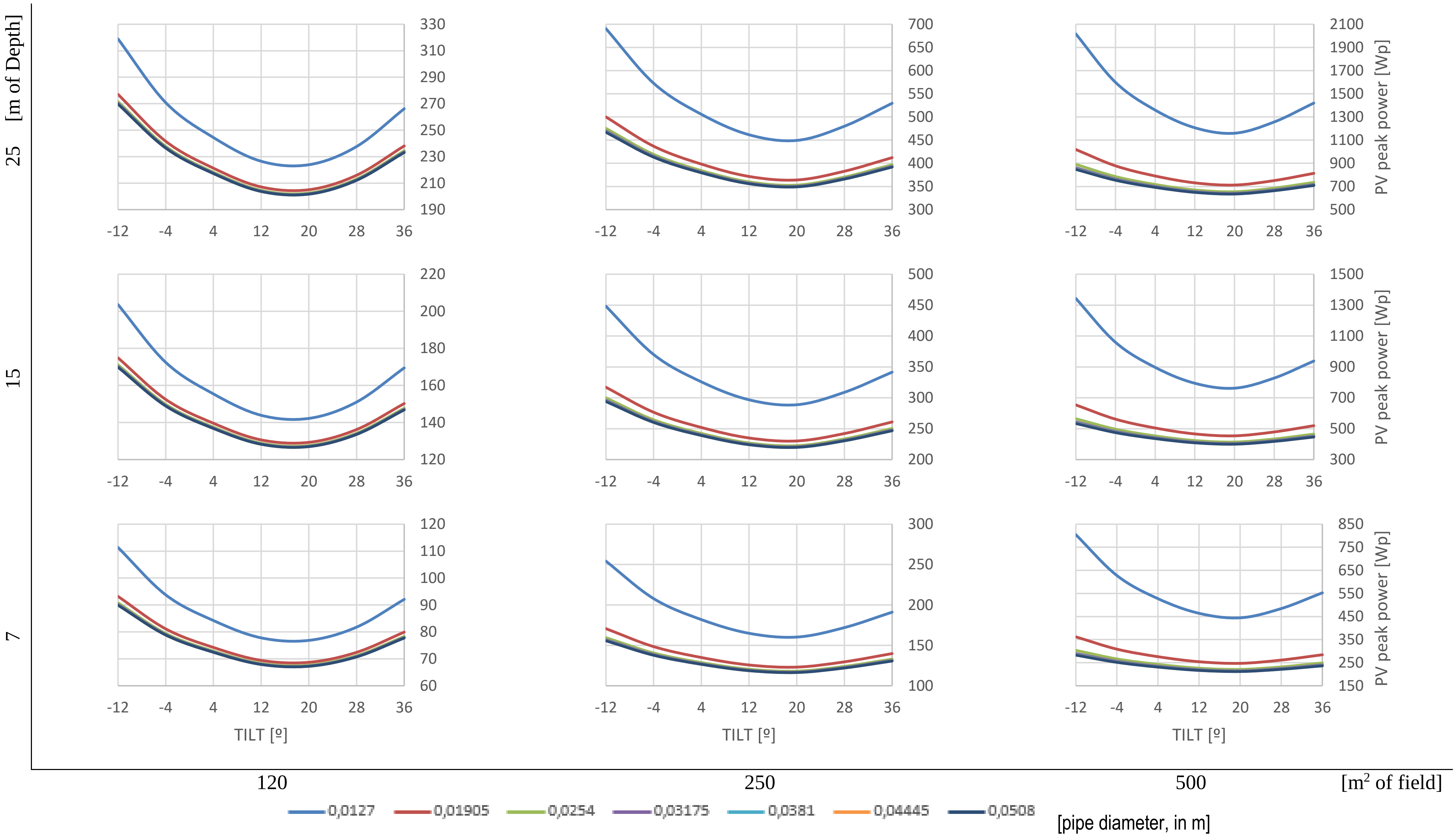

Figure 31. Evolution of the PV system peak power for different tilts and pipe diameters, per value of depth and orchard surface

3.4.1.3 Verifying the influence of the depth

Even if the influence of the depth was already deemed minimal, in the next graph this point is proven to clear all doubts. It can be clearly seen how the optimal angle remains constant while changing the depth, even beyond the range of this work. Thus, the first estimation was correct.

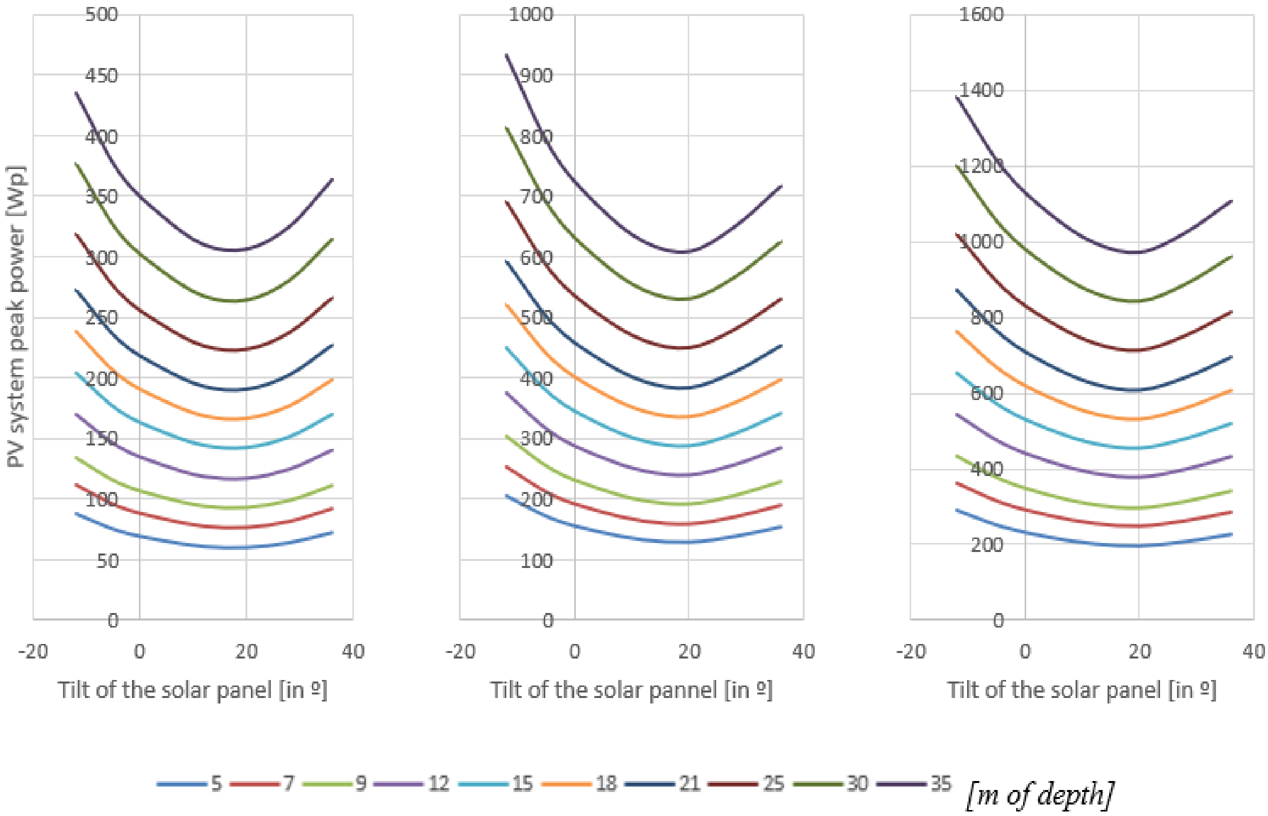

Figure 32. Variation of the PV system peak power with the angle for different depths and for each field size.

3.4.1.4 Influence of the efficiency

The interest in this subsection is now to evaluate how the efficiency influence the optimal angle to choose.

It has already been discarded to use any pipe bigger than the PVC 1" for the orchard and depths of this work. Therefore, aside from the efficiency and the tilt, the nine scenarios can have each three pipe diameters, but this would mean doing 27 different graphs (3^3).

However, since the irrelevance of the depth and the pipe diameter over the optimal angle has already been stated, we choose to set a fixed depth of 15 m (the intermediate). This let nine scenarios for each combination of orchard size and pipe diameter where the influence of the efficiency over the optimal angle is studied. For this, the efficiency is selected as a variable, ranging from a very low efficiency (14%) to a very good one (90%).The results are shown in the next page.

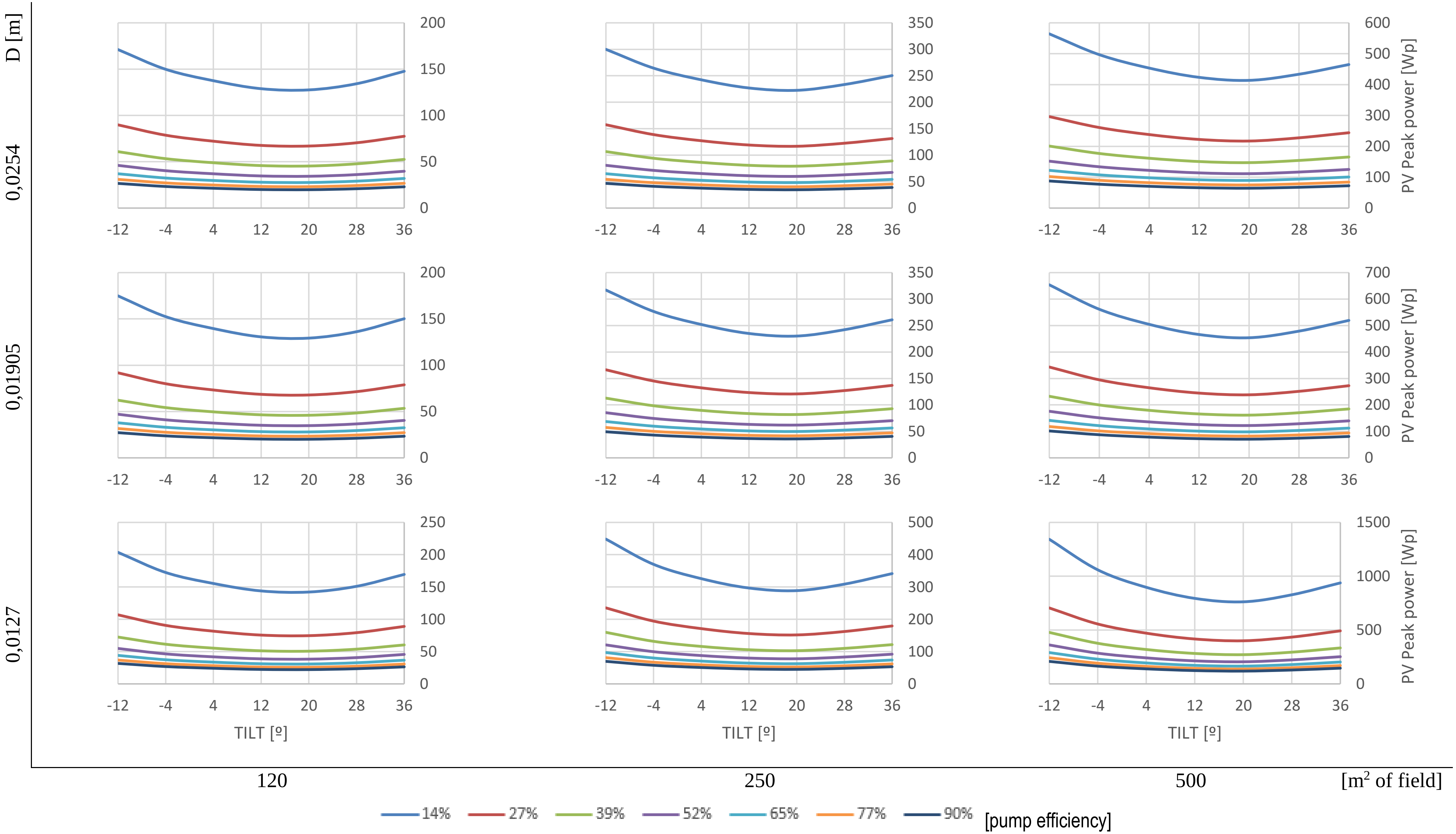

Figure 33. Evolution of the PV system peak power for different tilts and pump efficiencies, per each diameter and orchard surface

As it seems logical, the value of the peak power for the PV system needed increases when the efficiency of the pump diminishes. Furthermore, this increase is the biggest the closest to zero the efficiency gets. But, at least visually, it seems that the efficiency of the pump has no influence over the optimal angle. This makes sense since the efficiency is dividing all the value of the effective energy needed, and thus a change in it do not influence the relative evolution of the water needs. Thus, the critical month and the optimal angle will remain the same independently on the efficiency. This can be confirmed with the next table, showing the exact value of the optimal angle.

Table 6. Optimal angle for different pump efficiencies, diameters and orchards.

		Efficiency of the pump						
	Diameter	14%	27%	39%	52%	65%	77%	90%
500 m2	0,025	16,72	16,72	16,72	16,72	16,72	16,72	16,72
	0,019	16,73	16,73	16,73	16,73	16,73	16,73	16,73
	0,013	16,79	16,79	16,79	16,79	16,79	16,79	16,79
250 m2	0,025	18,16	18,16	18,16	18,16	18,16	18,16	18,16
	0,019	18,18	18,18	18,18	18,18	18,18	18,18	18,18
	0,013	18,27	18,27	18,27	18,27	18,27	18,27	18,27
120 m2	0,025	18,56	18,56	18,56	18,56	18,56	18,56	18,56
	0,019	18,60	18,60	18,60	18,60	18,60	18,60	18,60
	0,013	18,69	18,69	18,69	18,69	18,69	18,69	18,69

3.4.1.5 Optimal angle, critical month and critical water flow

The diameter, efficiency of the pump and height have all of them no (or almost) influence over the value of the optimal angle, and therefore neither over the critical month and the critical flow. In the next table (Table 7), a calculation for an orchard of 120 m2 (tilt 16,8º), a diameter of 0,0127 m, a depth of 15 m and a pump efficiency of 65% is presented as an example. With this it is possible to calculate the minimum viable power peak of the solar system and obtain the critical month and the critical water flow (which is the average water flow in the critical month), as shown in subsection 3.4.1.1.

Table 7. Example of general calculation

Diameter	0,0127	Depth	15

	En. gen. [kWh/day]	Daily volume (m3/day)	Q [m3/h]	Hdyn [m]	Daily energy needed [Wh]	Solar PV system size [Wp]
JAN	5,28	1,89	0,36	1,8	149	28
FEB	5,4	2,00	0,37	1,9	158	29
MAR	5,21	1,96	0,38	2,0	156	30
APR	4,87	1,84	0,38	2,0	147	30
MAY	4,41	1,61	0,37	1,9	127	29
JUN	4,22	1,38	0,33	1,5	107	25
JUL	3,97	1,14	0,29	1,2	87	22
AUG	3,94	1,01	0,26	1,0	76	19
SEP	4,45	1,20	0,27	1,1	91	20
OCT	4,95	1,70	0,34	1,7	133	27
NOV	5,13	1,93	0,38	2,0	154	30
DEC	5,18	1,84	0,36	1,8	145	28
					MAX	Max PV peak
					158	30

It has been proven in this section that the critical month and the critical water flow remain constant with changes of the diameter, depth and efficiency. Therefore, this table only needs to be replicated for the different orchard sizes, obtaining the results summarised in Table 8.

Table 8. Critical flow and critical month for each orchard

Area [m^2]	Critical flow [m^3/h]	Critical month	Optimal angle
120	0,38	APR	16,7º
250	0,66	MAR	18,2º
500	1,20	MAR	18,6º

3.4.2 Optimal pipe diameter

Now the last parameter to optimise in the system for this work is the pipe diameter. Depending on the diameter chosen and the flow, the value of the frictional forces acting over the fluid varies, resulting in a change on the pressure drop. The bigger the diameter of the pipe, the closer would be the power needed to the theoretical, and thus the smaller the solar system can be. But on the other hand, the bigger the diameter of the pipe, the more expensive the drilling and piping cost will be. An economical compromise is therefore to be obtained in this section, using the values set in Section 3.3.4.

The size of the solar panel will be calculated as in section 3.3.3, and the depth of the water is a parameter that depends on the conditions. The water flow used is the critical one, calculated earlier. The total cost will thus be:

EQUATION 22

$$Total\ cost = Drill\ Cost_D \cdot Depth + Solar\ system\ cost \cdot Size\ panel$$

The calculations are done for different values of the pump efficiency in order to assess its influence over the cost, and for the scenarios wih different depths and orchards. The results are presented below (Figure 34).

As can be seen, the optimal diameter is clearly 0,0127 m for all the efficiencies and depths in the orchards of 120 and 250 m^2.

For the orchard of 500 m^2, it looks like both the options of 0,0127 and 0,01905 m of diameter can be suitable depending on the depths and efficiencies. However, the pipe of 0,0254 is never the most suitable with these values. In the specific case of our assumption of 65% efficiency, the preferred diameter is 0,01905 for the scenario with 7 m of depth, and 0,0127 for the other two.

It can be noted that the cost of the system drops drastically when the efficiency of the pump increases from low values, but starts to stagnate around 40% of efficiency. This is coherent with the inverse function tendency, since the effciency is dividing the part corresponding to the solar system costs. Therefore, it looks important that the efficiency of the pump never stands on the low range (below 50%), while not much is gained for the sizes assumed with an expensive and very efficient pump.

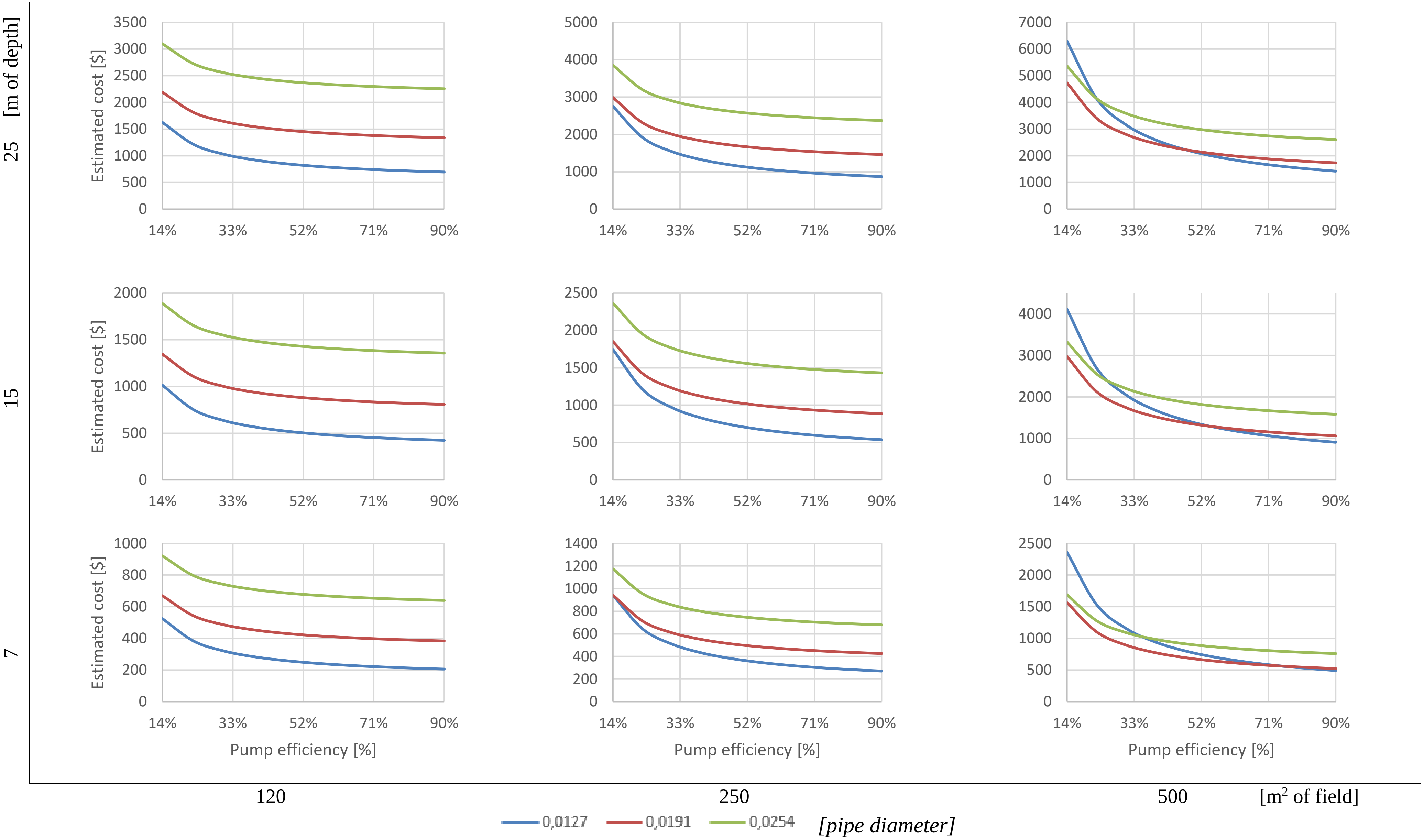

Figure 34. Estimated cost for different diameters, depths and orchards

3.5 Summary and validation

3.5.1 Summary

All the previous calculus can be summarised in the following table, that shows all the relevant data for the system design with a pump efficiency of 65%.

Table 9. Summary of the parameters calculated

		SURFACE OF THE ORCHARD					
		120 m^2		250 m^2		500 m^2	
DEPTH	25 m	Diameter [mm]	12,7	Diameter [mm]	12,7	Diameter [mm]	12,7
		Panel tilt [º]	16,8º	Panel tilt [º]	18,3º	Panel tilt [º]	18,6º
		Critical month	APRIL	Critical month	MARCH	Critical month	MARCH
		PV size [Wp]	47,4	PV size [Wp]	95,9	PV size [Wp]	248,9
		Estim. cost [$]	762,08	Estim. cost [$]	1004,54	Estim. cost [$]	1769,42
	15 m	Diameter [mm]	12,7	Diameter [mm]	12,7	Diameter [mm]	12,7
		Panel tilt [º]	16,8º	Panel tilt [º]	18,3º	Panel tilt [º]	18,6º
		Critical month	APRIL	Critical month	MARCH	Critical month	MARCH
		PV size [Wp]	30,1	PV size [Wp]	61,6	PV size [Wp]	163,6
		Estim. cost [$]	465,54	Estim. cost [$]	623,10	Estim. cost [$]	1132,98
	7 m	Diameter[mm]	12,7	Diameter [mm]	12,7	Diameter [mm]	19,05
		Panel tilt [º]	16,8º	Panel tilt [º]	18,3º	Panel tilt [º]	18,6º
		Critical month	APRIL	Critical month	MARCH	Critical month	MARCH
		PV size [Wp]	16,3	PV size [Wp]	34,2	PV size [Wp]	53,1
		Estim. cost [$]	228,32	Estim. cost [$]	317,95	Estim. cost [$]	596,25

The values for the solar PV system size are depicted below in Figure 35. The effect of the change of pipe diameter over the PV panel size can be observed. Indeed, it can be seen how for the depths close to 7 meters, the size of the solar system to be installed increases only mildly when going from a 250 m^2 orchard to a 500 m^2 one (bottom-right quarter of the graph). This because the increase in the power needed for watering (caused by the higher water demand while having a bigger orchard) is compensated by the reduction over the power lost (due to the decreases in the losses of the piping system due to wider pipes).

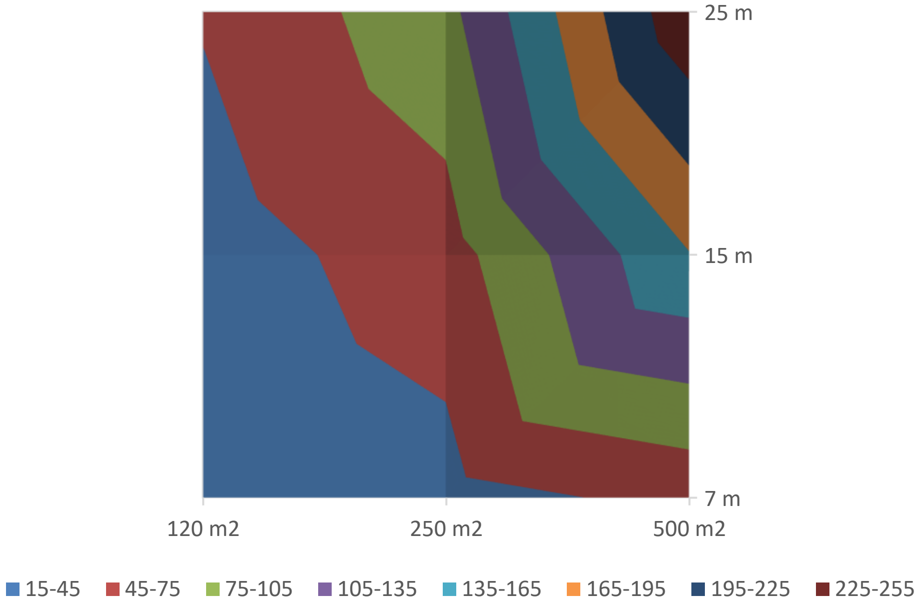

Figure 35. Solar PV system size, in Wp, for different orchard sizes and water depths (pump efficiency of 65%)

However, this effect is not perceived on the evolution of the total cost as can be seen in Figure 36. This is because the high reduction in the solar system cost (due to the high reduction in PV need explained before) is compensated by the high increase in drilling cost (due to the steep increase in volume to be drilled while augmenting the pipe size). In this case, the transition is smooth because of the mere conception of the problem, that tried to optimise the cost. Indeed, this makes that the a change in the pipe diameter is only selected from the very moment where the "fall" in the solar system cost exceeds the "jump" in the drilling cost.

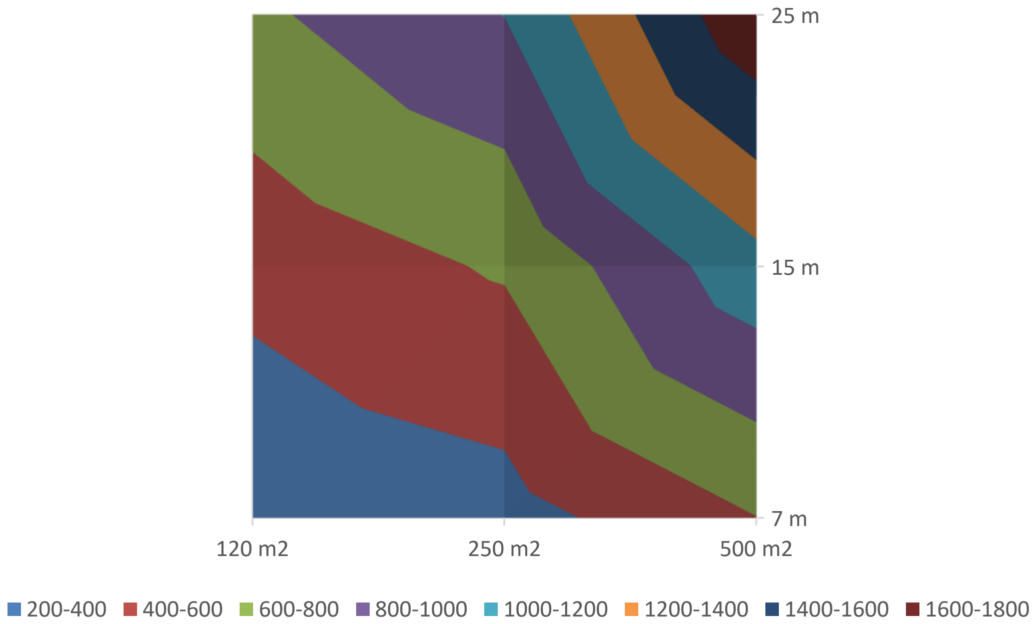

Figure 36. Estimated cost, in USD, for different orchard sizes and water depths (pump efficiency of 65%)

3.5.2 Validation of the water flow assumption

Until now and as explained in section 3.3.1, the water flow extraction was estimated to be at a constant rate. In this section, the validity of this simplification to design the system for the nine scenarios is proven.

3.5.2.1 Hourly power distribution

First of all, the hourly electricity production profile must be obtained. Since the monthly average is not directly given by PVGIS, the assumption that the relative hourly distributions are similar for the generation and for the radiation is used. This is done after analysing some sources (Ghitas, 2012) and because PVGIS does offer the monthly average hourly distribution for the direct radiation.

Since what is interesting from the Global direct irradiance is the relative hourly distribution, this is to be calculated for each month. However, before that an angle must be chosen, as it has an influence over the shape of the profile: higher angles have indeed more flattened profiles. Since this is simply a quick verification, and the angle variation was very small in for all the scenarios, an inclination of 17,5° is chosen as a compromise. The values obtained as such are presented below (Table 10).

Table 10. Relative distribution of the Global Direct Irradiance for 17,5° of inclination in Fada N'Gourma

	JAN	FEB	MAR	APR	MAY	JUN	JUL	AUG	SEP	OCT	NOV	DEC
6:45	0,9%	0,7%	0,9%	1,1%	1,3%	1,2%	1,0%	0,9%	1,3%	1,7%	1,8%	1,6%
7:45	4,0%	3,9%	3,9%	4,1%	4,6%	4,3%	4,3%	3,9%	4,6%	5,4%	5,7%	5,1%
8:45	8,1%	8,0%	8,0%	8,2%	8,3%	8,0%	7,9%	7,9%	8,5%	9,4%	9,8%	9,1%
9:45	11,5%	11,3%	11,8%	12,2%	12,2%	11,6%	11,1%	11,4%	12,2%	12,9%	12,8%	12,4%
10:45	14,2%	14,3%	14,7%	15,1%	15,2%	14,4%	14,1%	14,1%	15,0%	15,4%	15,0%	14,8%
11:45	15,5%	15,3%	16,0%	16,5%	16,6%	16,2%	15,4%	16,5%	15,8%	15,8%	15,4%	15,2%
12:45	15,0%	14,9%	15,0%	15,3%	15,5%	15,1%	15,8%	16,0%	14,3%	14,6%	14,5%	14,6%
13:45	13,0%	12,9%	13,0%	12,6%	12,3%	12,6%	13,3%	12,6%	12,4%	11,8%	11,7%	12,1%
14:45	9,8%	10,0%	9,1%	8,5%	8,1%	9,1%	9,1%	9,0%	8,9%	8,0%	8,1%	8,8%
15:45	5,9%	6,2%	5,5%	4,8%	4,5%	5,5%	5,9%	5,8%	5,3%	3,9%	4,0%	4,9%
16:45	2,1%	2,5%	2,1%	1,7%	1,4%	2,1%	2,2%	2,0%	1,6%	0,9%	1,2%	1,5%

This distribution is going to be the same one followed by the power generated. Since the section's aim is only to assess the validity of the simplification, only the values over the critical month are analysed. This is because the critical month is the one where a wrong assumption could provoke to design an undersized system that will lead to water scarcity.

With this, the PV system size, the pipe diameter, the critical month and the critical flow calculated for each scenario; the comparison of the volume extracted with the simplification and the real volume extracted is done.

3.5.2.2 Hourly water flow distribution

From now on the values for the scenario with 250 m^2 and 15 m depth will be presented as an example. Table 11 presents the values of design, as well as the daily volume and energy generated (for 1 kWp and then for the size of the module designed) for the critical month (CM).

Table 11. Design parameters and relevant values on the critical month for a 250 m^2 orchard and 15 m depth

Area&Depth 250 m2	15 m
Diametre [m]	0,0127
PV Size [Wp]	62
Critical month	MAR
Crit. Flow [m3/h]	0,66
En.gen. by 1 kW CM [kWh]	5,21
Volume needed CM	3,44
En. Gen. PV syst CM [kWh]	0,321

Once the energy generated by the system in an average day of the critical month obtained (0,321 kWh), the value is multiplied for each time of the day by the percentage of energy generated in the critical month. Then, the water flow corresponding to this power is obtained for each hour. This is shown in Table 12.

Table 12. Hourly power and water flow for a 250 m^2 orchard and 15 m depth

Time	% En. Gen. CM	Hourly Power [W]	Q [m3/h]
6:45	1,1%	1,63	0,023
7:45	4,1%	5,96	0,083
8:45	8,2%	12,04	0,164
9:45	12,2%	17,89	0,239
10:45	15,1%	22,09	0,289
11:45	16,5%	24,22	0,313
12:45	15,3%	22,45	0,293
13:45	12,6%	18,44	0,245
14:45	8,5%	12,40	0,169
15:45	4,8%	6,98	0,097
16:45	1,7%	2,53	0,035

These values are also depicted in their relative values in Figure 37. This allows to see how the distribution of the water flow and the power generated may differ.

It can be seen how the water flow is flatter than the energy generated, even though in this scenario the difference is mild. This difference is because of the losses. Indeed, since the losses increase when the water flow does so, more proportion of the power is wasted in the central hours. This effect can be better seen in the scenario with an orchard of 500 m^2 and 15 and 25 m of depth (Figure 39), as they are close to need a change of pipe size (and thus the most affected by the losses).

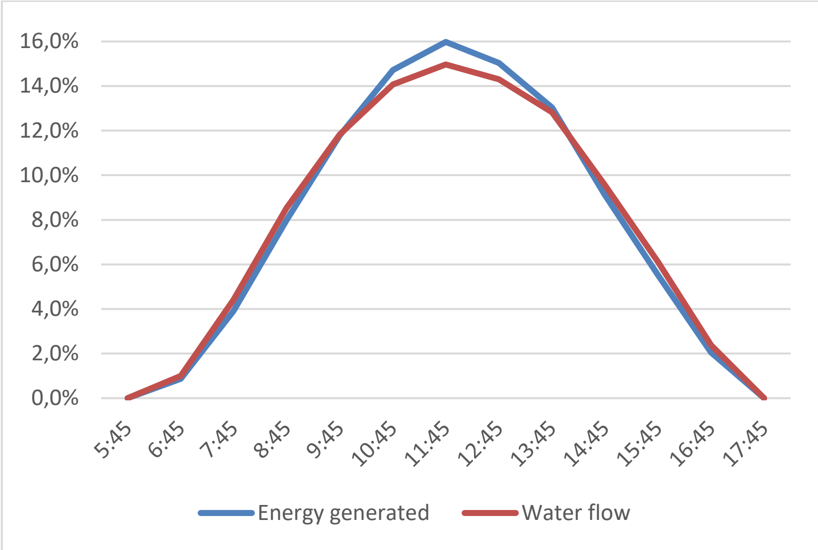

Figure 37. Relative distribution of energy generated and water flow in the critical month (250 m² ; 15 m)

3.5.2.3 Total volume extracted

After this, the total average volume extracted in the critical month can be calculated. For this, two methods are introduced. The first one considers the water flow constant hour by hour (called discrete approach here). The second one considers it continuously variable.

Both the continuous and discreet water flow distribution are presented in the following Figure 38. It can be observed that both cases are going to have similar values for the total volume.

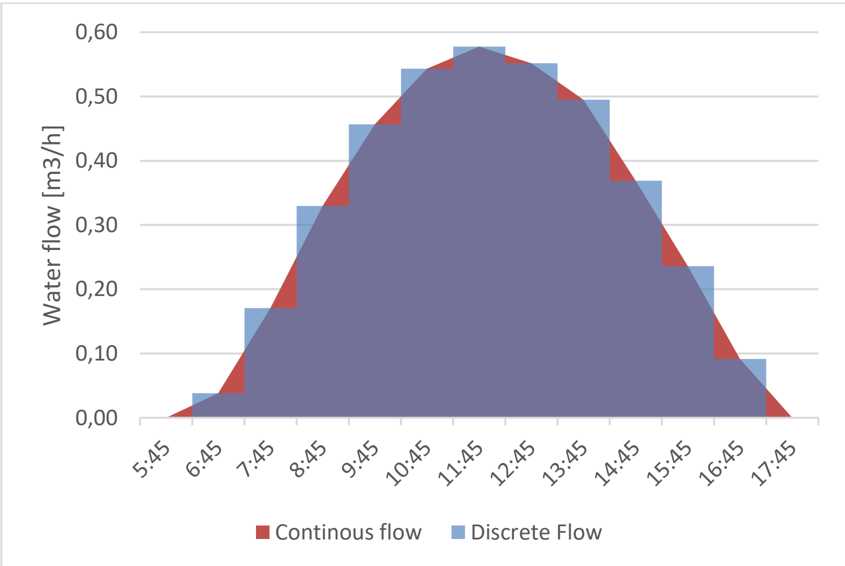

Figure 38. Average hourly water flow distribution in the critical month for a 250 m² orchard and 15 m depth

To obtain the volume from the first approach, all the hourly values of water values need simply to be added. On the other hand, for the second approach the water flow distribution is approximated by a polynomial of degree 6 (Equation 23), that is integrated (Equation 24), to obtain the volume (Equation 25).

Equation 23. Hourly water flow distribution

$$Q(t) = a_6 \cdot x^6 + a_5 \cdot x^5 + a_4 \cdot x^4 + a_3 \cdot x^3 + a_2 \cdot x^2 + a_1 \cdot x^1 + a_0$$

Equation 24. Integral of the water flow distribution

$$V_Q(t) = \frac{a_6}{7} \cdot x^7 + \frac{a_5}{6} \cdot x^6 + \frac{a_4}{5} \cdot x^5 + \frac{a_3}{4} \cdot x^4 + \frac{a_2}{3} \cdot x^3 + \frac{a_1}{2} \cdot x^2 + \frac{a_0}{1} \cdot x^1 + c$$

Equation 25. Water volume calculation

$$V = V_Q(t_{end}) - V_Q(t_{ini}) = V_Q(5{:}45) - V_Q(17{:}45)$$

The coefficients of the approximation are obtained through the LINEST command and are shown in Table 13.

Table 13. Coefficients of the continuous hourly water flow distribution for a 250 m² orchard and 15 m depth

a6	a5	a4	a3	a2	a1	a0
4,44E-06	-1,72E-04	2,90E-03	-2,66E-02	1,11E-01	-4,96E-02	1,43E-04

With this, the volumes from both methods can be obtained, and the smallest of the two would be the one considered in each case to make it more conservative (even though the difference is minimal. The results of this are shown in Table 14.

Table 14. Resultant volumes for each method for a 250 m² orchard and 15 m depth

Vol Continous	3,86
Vol Discreet	3,86
Vol simplification	3,44
Error	10,9%

As can be seen, in this case the real value of volume extracted with a PV system dimensioned as calculated is 11% higher than the volume needed. This means that the simplification over the water volume was a conservative one in this scenario, and therefore, valid.

3.5.2.4 General results for each scenario

This procedure is now repeated for each scenario, obtaining Table 15 and Figure 39. Table 15 presents the errors induced by the water flow simplification. As stated before, if positive, this mean that the simplification is conservative and thus valid. Therefore, the simplification is valid for all scenarios, meaning that the size of the PV system calculated will deliver the water need. Furthermore, the error is never higher than 20%, which makes this approximation a reasonable one.

Table 15. Resultant error for each scenario

	120 m2	250 m2	500 m2
25 m	5,1%	10,2%	18,9%
15 m	5,5%	10,9%	19,8%
7 m	6,4%	12,4%	7,0%

Figure 39 on the other hand presents the relative distribution of the water flow and the energy generated, as explained at the end of subsection 3.5.2.2. it can be easily observed the effect induced by the change in the pipe width for 7 m depth and 500 m² orchard.

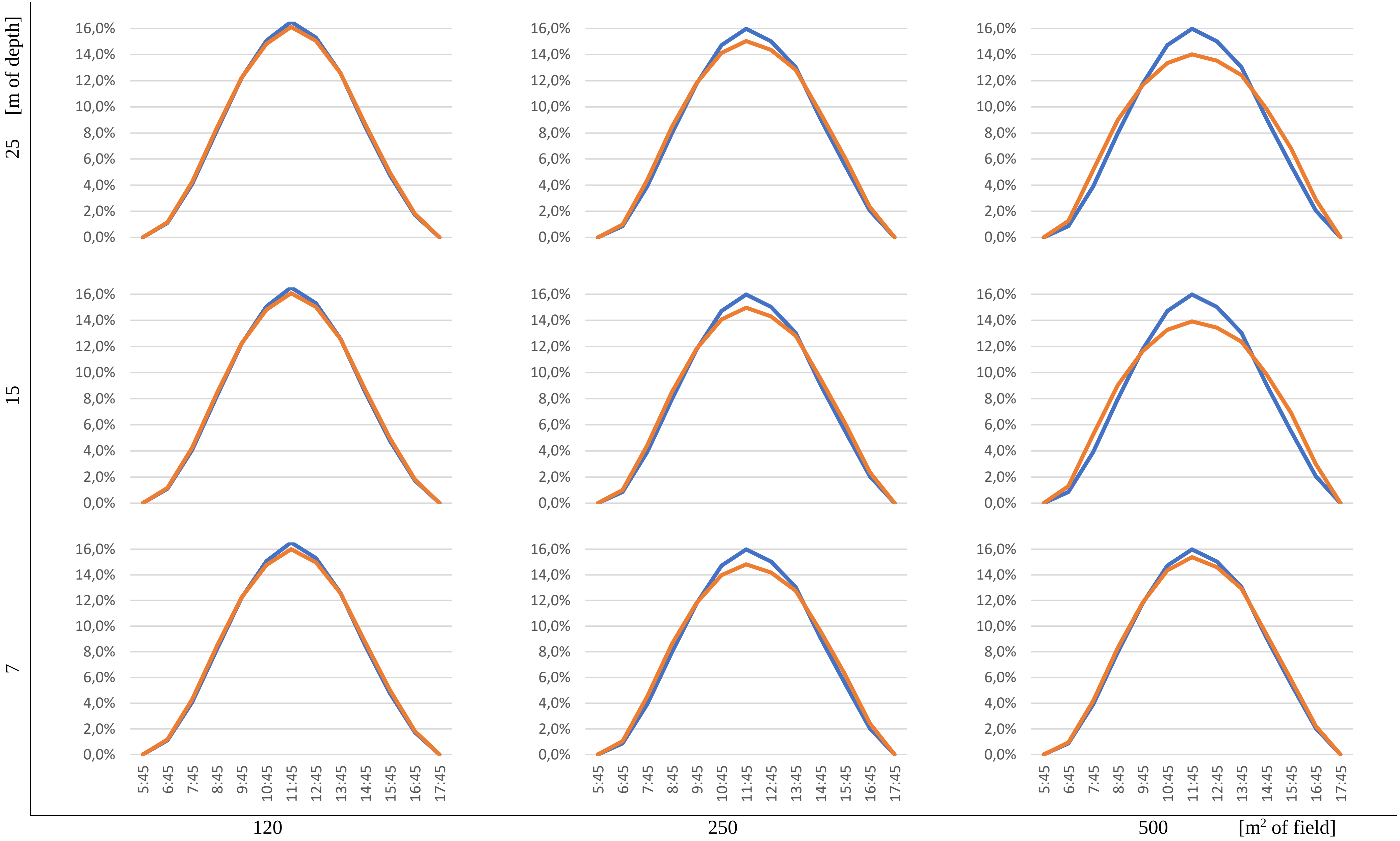

Figure 39. Relative distribution of energy generated (blue) and water flow (orange) for each scenario.

3.6 Example of final calculation

Now some details are going to be studied in this chapter for a specific scenario (orchard size and depth): 250 m^2 and 15 m depth, chosen because of being in the middle. The other parameters are the ones presented in section 3.5.1: Angle 18,3º; PV size 61,6 Wp, efficiency 65%, diameter 0,0127 m.

The data calculated until now to optimise was with Kc max (obtaining Figure 40). This not only simplifies the process, but also allows to design a system that makes possible to start the crop cycle in every month of the year. However, it is still relevant to choose the best pattern for crop planting to make the system even more resilient to changes.

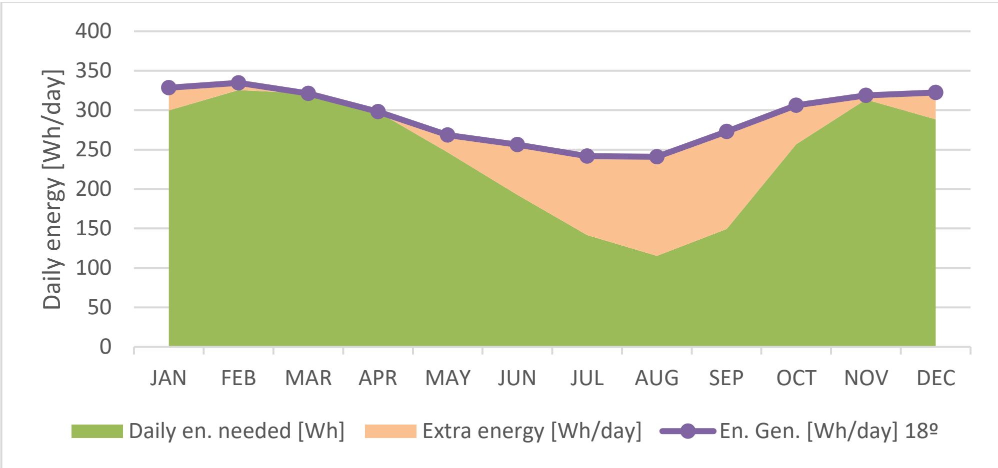

Figure 40. Daily energy distribution by category with Kc max

3.6.1 Initial planting date selection

Introducing now Kc as a new variable not only changes the evolution of water needs over the year but adds the variable of the starting date for the cycle. Being the case studied the tomato, that can be planted in three cycles a year, we have then that there could be 4 different months to start planting (January, February, March, April).

The variation in these water needs as a function of the planting date are presented in the next table.

Table 16. Evolution of Kc/Kcmax and volume needed for a 250 m2 orchard and different planting months

	PLANT IN JANUARY		PLANT IN FEBRUARY		PLANT IN MARCH		PLANT IN APRIL	
	Kc/Kcmax [-]	V [m^3/day]	Kc/Kcmax [-]	V [m^3/day]	Kc/Kcmax [-]	V [m^3/day]	Kc/Kcmax [-]	V [m^3/day]
JAN	52%	2,01	91%	3,04	100%	3,29	77%	2,69
FEB	77%	2,86	52%	2,12	91%	3,24	100%	3,51
MAR	100%	3,44	76%	2,75	52%	2,06	91%	3,17
APR	91%	2,93	100%	3,19	76%	2,52	52%	1,86
MAY	52%	1,50	91%	2,47	100%	2,70	76%	2,10
JUN	76%	1,68	52%	1,13	91%	2,01	100%	2,23
JUL	100%	1,73	76%	1,23	52%	0,73	91%	1,53
AUG	91%	1,27	100%	1,45	76%	0,98	52%	0,51
SEP	52%	0,83	91%	1,65	100%	1,84	76%	1,33
OCT	76%	2,28	52%	1,68	91%	2,65	100%	2,89
NOV	100%	3,37	77%	2,75	52%	2,05	91%	3,11
DEC	91%	2,95	100%	3,19	77%	2,60	52%	1,95

With this new volume and the PEH obtained for a panel with 18,3º of tilt, the monthly water flow can be estimated. This will enable to calculate Hdyn, and therefore calculate the new (and more precise) energy needs for each planting date. Meanwhile, the energy generated remains the same for each case, as it is not influenced by the demand (once the PV system dimensioned). The extra daily energy generated can therefore be estimated for each month; these data are shown below.

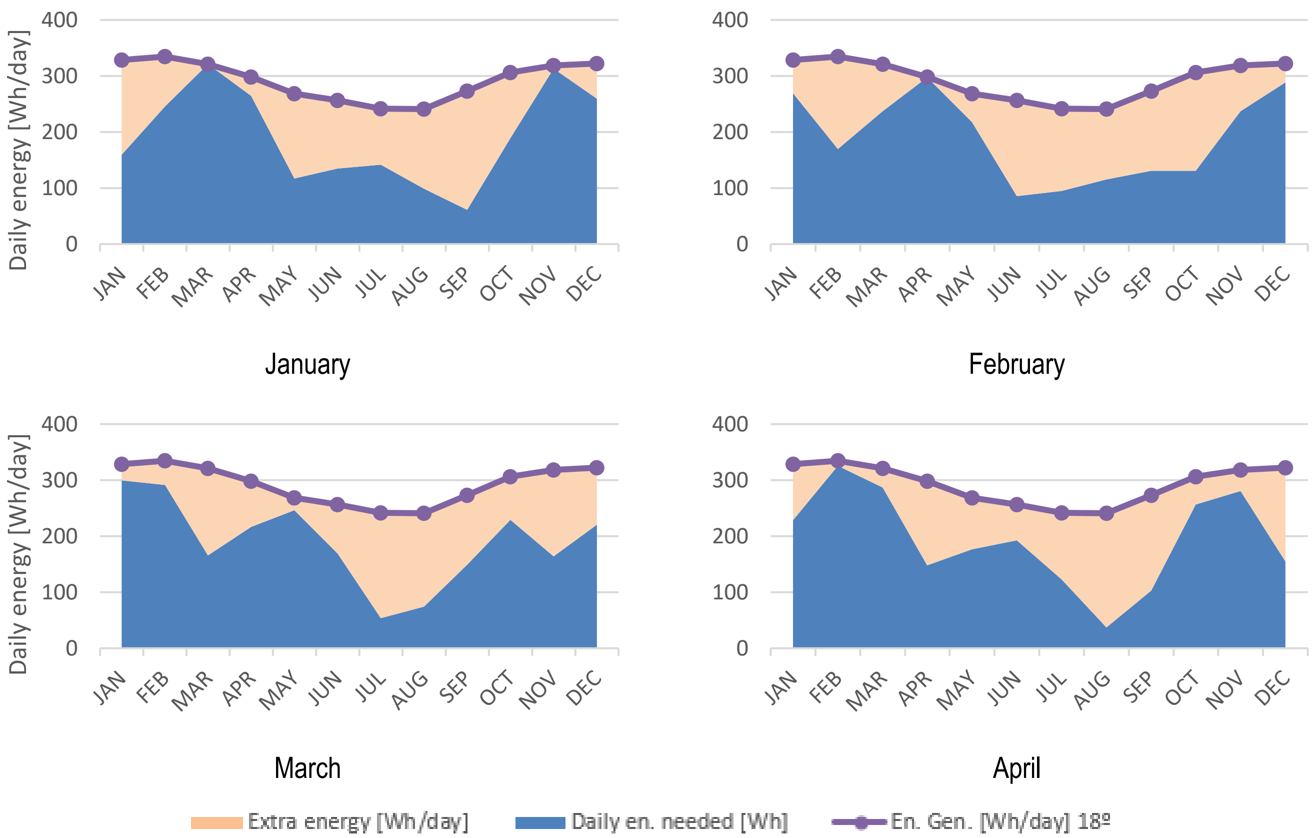

Figure 41. Daily energy needed, daily energy generated and daily extra energy generated for each case

First, we can see that introducing the variability of Kc augments noticeably the extra energy generated by the system, however its distribution depends on the planting day greatly. Since the system is not intended to have a big energy storage capacity, the key parameter to check is not the total energy saved, but rather a more qualitative result. Indeed, it is more important to select the date that makes the system more resilient to possible inconvenients. These could be changes in the weather (most likely), but also temporary drawbacks in the system efficiency (for example due to dust in the panel, or to a lower efficiency in the pump).

Thus, it would be interesting to assure that the system does not fail to accomplish its duties in any month. Therefore, the planting date that makes it harder not to comply with the water needs in every month is to be chosen. Looking at Figure 41, it might look that a priori January and February should be dismissed, since in both cases there are some critical months. But to estimate this better, the following table with the relative weight of the extra energy generated over the energy consumption is made.

Table 17. Extra energy generated/Consumption for different starting months

	January	February	March	April
JAN	106%	22%	10%	44%
FEB	36%	97%	15%	3%
MAR	0%	35%	94%	12%
APR	13%	0%	38%	101%
MAY	129%	23%	9%	52%
JUN	90%	200%	51%	33%
JUL	70%	155%	349%	97%
AUG	144%	109%	225%	546%
SEP	348%	109%	83%	166%
OCT	62%	134%	34%	19%
NOV	2%	34%	94%	14%
DEC	24%	12%	46%	108%

Some conclusions can be extracted. If the tomatoes are to be planted in January, March would have no buffer for any possible unexpected event, and November will be also close to not meeting the requirements. If it were to start in February, April would be the month without capacity to overthrow an unexpected event. Hence, starting to plant in March would be the more convenient thing to do, since the most critical month would be May, but still with 9% of extra energy as a security.

But this first estimation, as interesting as it is, would be more relevant if the variables affecting the proper work of the system were uniformly distributed over the year. This could be true for the case of failures in the pumping or solar system; however, the rain is one the variables with a higher impact and is not uniformly distributed. Therefore, a year drier than the average would have a big effect in the system during the wet season, but none during the dry season. This is because an important part of the water needs is covered by the rain during the wet season.

Consequently, all the data of water flow, dynamic head, daily energy need, daily energy generated, and daily extra energy generated will be calculated for each initial planting date, and for different rain predictions. An example of this table is presented next.

Table 18. Example of table with daily volume, flow rate, Hdyn, energy needed extra energy generated and energy generated ***for a year with 50% of the average rain*** *and with January as initial planting date.*

	Daily volume [m3/day]	Q [m3/h]	Hdin [m]	Daily en. needed [Wh]	Extra energy [Wh/day]	En. Gen. [Wh/day] 18º	Extra En. /Cons. En.
JAN	2,01	0,38	2,0	159	169	328	106%
FEB	2,86	0,53	3,5	246	89	335	36%
MAR	3,46	0,66	5,3	323	-2	321	-1%
APR	3,03	0,63	4,8	276	22	298	8%
MAY	1,68	0,39	2,1	134	134	269	100%
JUN	1,96	0,47	2,9	163	93	256	57%
JUL	2,10	0,54	3,7	182	60	242	33%
AUG	1,66	0,42	2,4	135	106	241	79%
SEP	1,11	0,25	1,0	84	189	273	225%
OCT	2,40	0,48	3,0	201	105	306	52%
NOV	3,37	0,65	5,2	313	5	319	2%
DEC	2,95	0,56	4,0	259	63	322	24%

These rain predictions range from a year with the same rain as the average (100%) until a year with no rain at all. The relevant data in this case is the minimum monthly value of the daily extra energy generated on each scenario, as it is the margin the system will have for unexpected events with these rain conditions. These data are presented in the next table.

Table 19. Percentage of the Minimum daily extra energy generated over the energy consumption in that month, for different planting dates and different values of rain

% of rain over the average year		JANUARY	FEBRUARY	MARCH	APRIL
	100%	0%	0%	9%	3%
	90%	0%	-1%	7%	3%
	80%	0%	-1%	5%	3%
	70%	0%	-2%	3%	3%
	60%	-1%	-3%	1%	3%
	50%	-1%	-4%	-1%	3%
	40%	-1%	-5%	-3%	3%
	30%	-1%	-6%	-5%	3%
	20%	-1%	-6%	-7%	1%
	10%	-1%	-7%	-9%	-3%
	0%	-5%	-8%	-11%	-8%

The previous hypothesis is confirmed also in this case, which is that January and February are not suitable months to start planting. As for choosing between March and April, the decision would be subjective. In this study, the steadiness of April has been preferred over the better results of March for years with similar rain as the average.

3.6.2 Storage capacity

This work has been calculated until now without considering any kind of storage capacity. However, it is always convenient to have such storage capacities, even if reduced, to mitigate non-modelled variations or breakdowns of the system. Since in this work the energy generated is used to extract water, the storage capacity could easily be either a water tank, either a battery array.

To choose between a battery or a water tank is in fact a decision subjected to the priorities of the project and the advantages and disadvantages of each storing method. The batteries have as advantage that they allow the storage of electricity for other purposes than water pumping. The tank has the advantage that it is a basic technology and that it has very low risk of breakdown. As for the price of each, it will vary with each project.

Therefore, for isolated communities with difficult access to technological advances or spare parts, a tank is the best solution. If the project is going to be done in a well-connected area (close to a big city), the cost of both systems is to be considered, but the batteries are probably going to be more convenient.

As said prior, since the system is designed to be able to work without a storage, the storage capacity will be small. It has been decided to determine this capacity as the one ensuring all the water necessities of one day in the most critical month, for the configuration selected and for an average rainy year. Since we have chosen to start planting in April, this month will be February.

In these conditions, if a tank is installed, the water needs are 3,51 m^3/day, and consequently the tank will be of 3,51 m^3. The cost of the tank may vary widely depending on many factors (technology, labour costs, etc.).

It is recommended to ensure in the tank that water is never used for irrigation when a certain threshold is trespassed (the daily need of water for WSS, or 600 L). An easy way to achieve this would be to have the outlet of the irrigation pipe placed higher in the tank so the volume below it is 600L.

If a battery system is installed, the energy needed in one day in February is 325 Wh, and therefore its storage capacity should be 325 Wh. For a standard 12 V battery, that would be a 27 Ah battery, which is a fairly small battery. For example, one commercial truck battery of 12V / 180 Ah (2160 Wh), which is enough capacity for almost a week in February, costs 174,55 $ on the internet (Voltabatería as for 05/08/2018). Even in the worst scenario (500 m^2 and 25 m depth), the energy needed is 814 Wh, and therefore the aforementioned battery will still be suitable.

3.6.3 Economic study

3.6.3.1 Initial investment

The cost of the solar system and pump and the drilling were already calculated in previous chapter (see table Table 9 with the summary), but some additional costs are going to be added. However, we remind the reader that these values are very rough approximations that deserve a further study.

First, the cost of the battery. The size of the battery will be escalated to the size of the other solar systems to make it the same proportion as the studied prior. We obtain therefore the following price (which corresponds to roughly one week of storage).

Table 20. Battery cost

	Battery cost (USD)		
	120 m2	250 m2	500 m2
7 m	46,07	96,85	150,41
15 m	85,29	174,55	463,41
25 m	134,31	271,68	705,00

Second, the cost of the dripping system needs to be considered; this cost varies depending on the sources. It starts as low as 0,1 USD/m2 in India and 0,4 USD/m2 in South Africa, but for large and industrialised fields (Dobbs *et al.*, 2011). For projects similar to this one, the cost is higher: 1,65 USD/m^2 in a 500 m^2 field (Woltering, Pasternak and Ndjeunga, 2011) or 3,96 USD/m^2 in a 120 m2 field (Burney *et al.*, 2010).

These values are presented below with a tendency curve, that would be used to estimate the unitary cost for a 250 m^2 field.

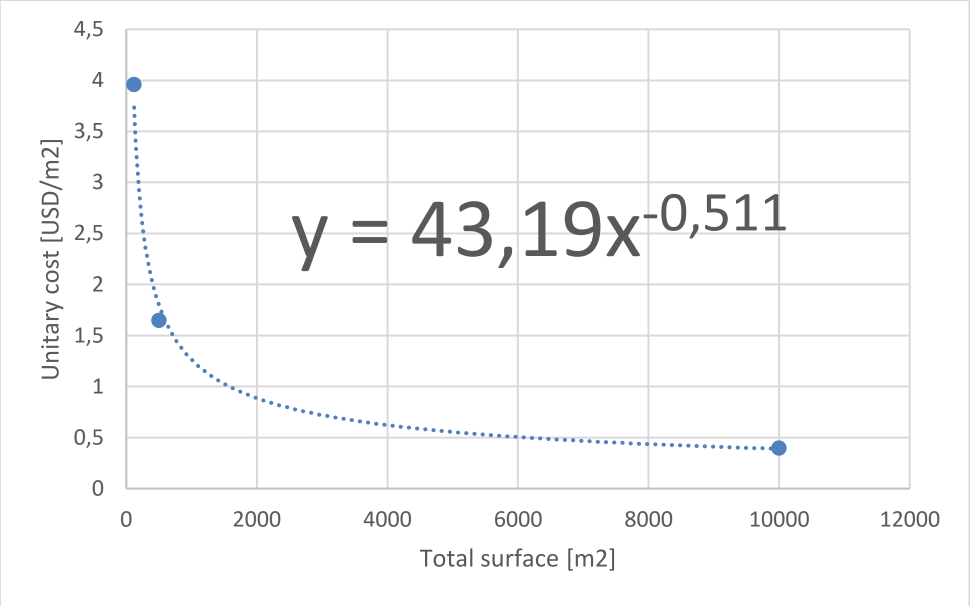

Figure 42. Unitary cost of a drip irrigation system, for different sizes of field.

With this, we can calculate the total cost of the drip system, that does not depend on the depth of the water.

Table 21.Drip system cost

	Drip system cost		
Surface [m2]	120 m2	250 m2	500 m2
Unitary [USD/m3]	3,96	2,57	1,65
Total	475,20	642,65	825,00

Now, the initial investment can be estimated for each scenario, as the sum of the cost for the PV system and pump, the drilling, the battery and the drip system.

Table 22. Estimated total investment for each scenario

	Total investment		
	120 m2	250 m2	500 m2
7 m	749,59 USD	1.057,30 USD	1.387,91 USD
15 m	1.026,03 USD	1.440,15 USD	2.421,39 USD
25 m	1.371,59 USD	1.918,72 USD	3.299,42 USD

Finally, in the next page the cost distribution for the different parts here presented is depicted for each scenario.

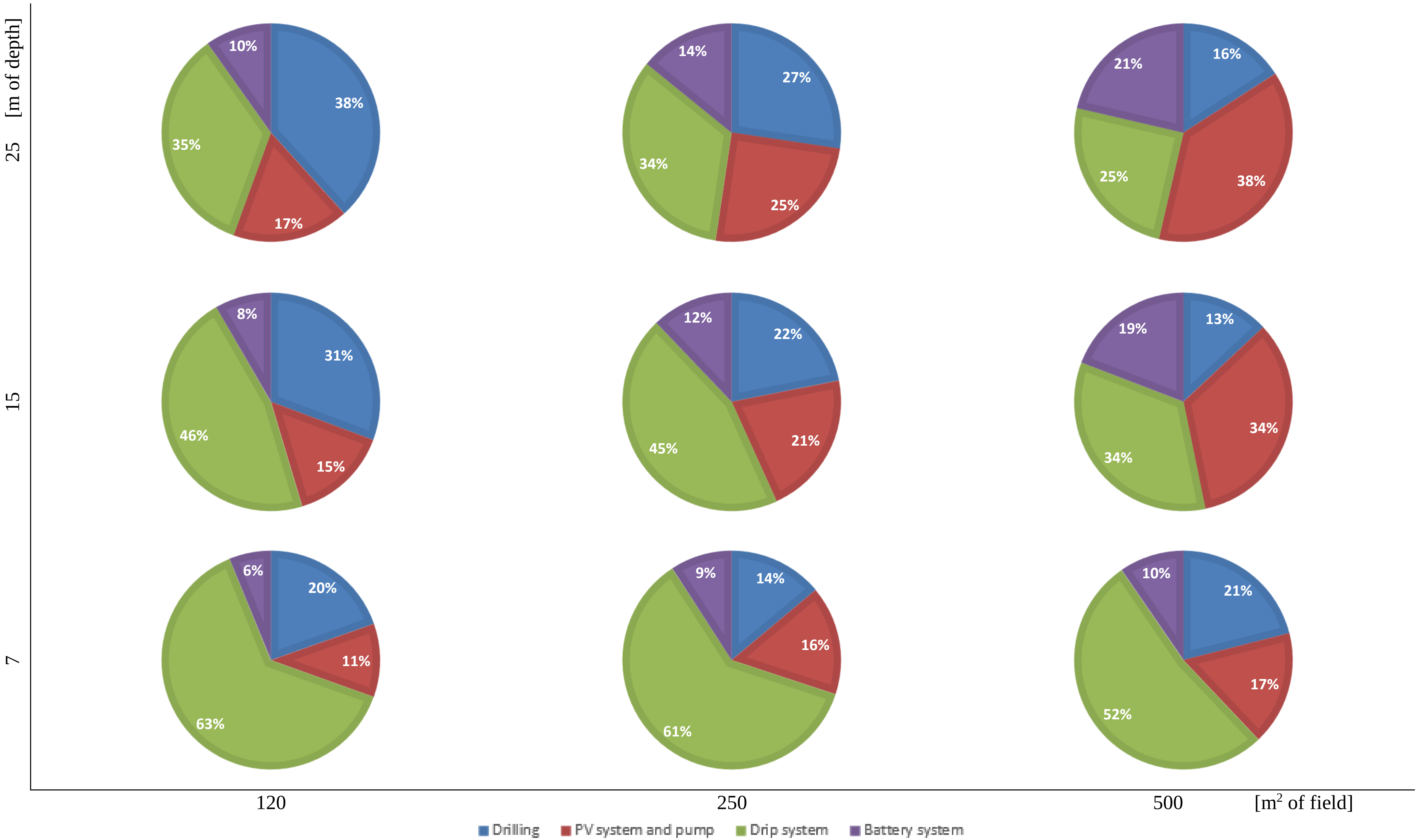

Figure 43. Relative distribution of energy generated (blue) and water flow (orange) for each scenario.

3.6.3.2 Yearly benefits

After the data obtained in section 1.3.8 (economic befits), the annual gross income per square meter can be of 9,72 USD if pepper is planted, of 10,32 for lettuce and of 17,5 USD for tomato (Balana *et al.*, 2017). For Burney *et al.* (2010), the annual income can be of 3,2 USD/m^2. In conclusion, a big variability in the incomes is presented depending on the source, and for the moment all of them are going to be considered.

On the other hand, the annual expenses required for inputs, labour, support of technicians and extension services are 1,20 USD/m^2 (Burney *et al.*, 2010). However, according to Houessionon *et al.* (2017) this cost is as low as 0,30 USD/m^2 in Burkina Faso. The first value will be the one used to be conservative.

We obtain the following annual net income for the different values of gross income.

Table 23. Net income for different values of gross income

	Net income		
Gross income [USD/m2]	120 m2	250 m2	500 m2
17,5	1956,00	4075,00	8150,00
10,32	1094,40	2280,00	4560,00
9,72	1022,40	2130,00	4260,00
3,2	240,00	500,00	1000,00

With these values, the return on investment is calculated for different values of the gross income.

Table 24. Return on Investment for different scenarios and values of the gross income

	Gross income 3,2 USD/m2				Gross income 9,72 USD/m2				Gross income 17,5 USD/m2		
	120 m2	250 m2	500 m2		120 m2	250 m2	500 m2		120 m2	250 m2	500 m2
7 m	3,12	2,11	1,39	7 m	0,73	0,50	0,33	7 m	0,38	0,26	0,17
15 m	4,28	2,88	2,42	15 m	1,00	0,68	0,57	15 m	0,52	0,35	0,30
25 m	5,71	3,84	3,30	25 m	1,34	0,90	0,77	25 m	0,70	0,47	0,40

We see that in all the cases, it looks like it could be a viable project. For the next calculations, only the scenarios with 25 m of depth will be calculated, as they are the more expensive, and thus more conservative. Three different hypotheses are studied: that the system lasts 5 years, that the system lasts 10 years, and that the system lasts 20 years. This last assumption is very realistic, at least for the solar components that tend to last long. Additionally, it is estimated that every 4 years (starting in the 6th) there need to be an extra expenditure of 20% of the initial cost as maintenance cost. This expenditure needs to be considered if the system is intended to last long.

The project is to be done in a developing country, therefore the inflation is high. The discount rate we are going to use is 12%, as it is the same one stated by the World Bank for similar projects (You, 2008).

With this data, the Net Present Value (VPN) and Investment Return Rate (IRR) are obtained for 5, 10 and 20 years of duration, and for the projects with 25 m of depth.

The values obtained are shown in the following tables.

Table 25. VPN and IRR for the 3,2 USD/m² income, 25 m

3,20 USD	120 m2	250 m2	500 m2
IRR 5	-4%	10%	16%
VPN 5	-506,44 USD	-116,33 USD	305,35 USD
IRR 10	7%	20%	25%
VPN 10	-242,83 USD	588,42 USD	1.804,02 USD
IRR 20	13%	23%	28%
VPN 20	101,98 USD	1.369,61 USD	3.402,40 USD

Table 26. VPN and IRR for the 9,72 USD/m² income, 25 m

9,72 USD	120 m2	250 m2	500 m2
IRR 5	69%	108%	127%
VPN 5	2.313,94 USD	5.759,45 USD	12.056,92 USD
IRR 10	74%	111%	129%
VPN 10	4.177,90 USD	9.798,28 USD	20.223,74 USD
IRR 20	74%	111%	129%
VPN 20	5.946,07 USD	13.544,80 USD	27.752,79 USD

Table 27. VPN and IRR for the 17,5 USD/m² income, 25 m

17,50 USD	120 m2	250 m2	500 m2
IRR 5	141%	212%	247%
VPN 5	5.679,36 USD	12.770,74 USD	26.079,50 USD
IRR 10	142%	212%	247%
VPN 10	9.452,95 USD	20.787,97 USD	42.203,11 USD
IRR 20	142%	212%	247%
VPN 20	12.919,54 USD	28.072,87 USD	56.808,92 USD

It can be seen how the profitability of the project increases with the incomes generated by the crops. It would depend on the value of all the variables that were determined whether the project is suitable (if IRR is bigger than the discount rate). However, we can already conclude that bigger fields have more chances to be profitable, and that in general it seems likely that a system such as the one deigned is profitable.

Table 28. IRR for a 5-year project for a gross income of 3,2 USD/m²

3,2	120 m2	250 m2	500 m2
7 m	18%	38%	66%
15 m	5%	22%	30%
25 m	-4%	10%	16%

This can be seen from the previous tables: even in the worst case (5-year duration of the system, lowest gross income, and in general all the conservative assumptions made along the work), the value of the IRR is very high in many of the scenarios (painted green). Indeed, only by augmenting the gross income to 5 USD/m^2, the value of IRR becomes very high in all the scenarios, which means the project is profitable.

Table 29. IRR for a 5-year project for a gross income of 5 USD/m²

5	120 m2	250 m2	500 m2
7 m	54%	86%	135%
15 m	34%	60%	73%
25 m	20%	40%	50%

4 Conclusions

4.1 Ethical conclusions

The work has shown the vital importance of water supply for drinking, sanitation and hygiene, but also agriculture. The benefits are numerous, from the most important, the ethical one, which is to save lives and reduce suffering, to the economical one. Indeed, helping developing countries in their pursuit to gain access to a reliable improved source of water is not only the right thing to do, but also the smart. Most of the economic studies state that improving access to water is a good investment, as the returns exceed the expenses, and the economic boost could help the world economy greatly.

But it is also important to address this problem from a perspective that considers the effects of climate change. Undeniably, any solution not having in mind the need of a sustainable solution is risking harming more than helping. This is true because Africa is the most exposed continent to the devastating effects of climate change. Therefore, every solution spreading the access of renewable energy in the continent is welcomed.

It is also important to always take into consideration the local needs, wants and beliefs when addressing a project like this. What might seem a good solution in one case cannot be good in another. It is paramount to design a project sustainable, that aims to last more than "the time of the picture" because such projects are usually more harmful. Thus, the use of technology should be restricted to levels that are accessible to the technical abilities of the locals. Any other approach reinforces the dominant roles of colonialism.

4.2 Theoretical conclusions

4.2.1 Suitability of PVWP

The first conclusion of this work is that solar PV systems are the most suitable ones for water pumping for irrigation. Certainly, PV systems have great advantages always, such as the reduction of carbon emissions if compared to diesel systems, the facility in the maintenance (almost inexistent) and the long duration of the components. All this makes PV systems the paradigm of a technology in concordance with the sustainable development principles. Furthermore, the dramatic drop in cost of PV panels and batteries over the last years has improved its perspectives, since now this is even the cheapest solution many times.

But in the case of PVWP for irrigation, the benefits are even more. First, since there is no real need of watering the plants at a specific moment of the day (especially with drip technology), there is no problem in not having an on-demand technology. Therefore, the need of batteries is reduced. This is especially true because solar, even if not an on-demand source, is much more predictable than for example wind power: the sun rises every day.

It is true that clouds can reduce drastically the power generated (even though PV panels are increasingly able to use the diffuse energy, mitigating these drops). But since the watering needs depend on the evapotranspiration, and this value is directly related to the irradiance, a cloudy day means less energy generated, but also less energy needed (more so if the clouds bring rain). In conclusion, even if not perfect, this passive self-regulation is very advantageous to these systems.

4.2.2 Optimum slope and critical month

The second conclusion is that the optimum panel slopes for each month must be modelled to evaluate the optimum tilt. This is so because the energy consumption is variable, and thus it is not easy to determine without calculations the optimum tilt.

However, the diameter of the pipes, the efficiency of the pump and the depth of the groundwater do not have a noticeable effect on the determination of the optimum angle. The optimum tilt is obtained along with the critical month and the critical flow, which is the flow in the month with more risk of not complying with the demands.

Indeed, once a location selected (thus the weather fixed), the watering needs per square meter are fixed, and the tilt will only vary slightly because of variations in the area. But this is only true in cases where there is some part of the water needs that don’t grow linearly with the area of the orchard (like the volume for WSS). If all the water were for irrigation, or once the water for irrigation exceeds greatly the water independent from the area, the optimum angle and critical month would not depend on the parameters of the system, and only on the location (and climate).

4.2.3 Efficiency of the pump

The average efficiency of a pump in a project of these characteristics has been calculated, and its value has been estimated to be around 65%. This is far from the efficiencies of big pumps, but it is reasonable for this type of projects.

4.2.4 Effect of the diameter

Another conclusion is that in these systems, the dynamic head can grow to big proportions, and therefore it is important to take it into account. In some cases, it would be more convenient to increase the diameter of the pipes in the system. This decision would be the first one considering costs, so the result is subject to the relative cost of each component studied. Two independent variables, the cost due to the solar system and the cost due to the drilling are presented (Equation 22):

$$Total\ cost = Drill\ Cost_D \cdot Depth + Solar\ system\ cost \cdot Size\ panel$$

The drill cost increases when the diameter increases to the power two, whereas the size of the panel decreases when D augments. A compromise must be reached, obtaining the optimum diameter, that will depend on the efficiency of the pump, the drilling cost, the solar system cost, the area of the orchard and the depth of the groundwater.

However, for the values of volume and depth here studied (no more than 7 m^3 per day nor more than 25 m depth), the diameter would be ½" or ¾", being bigger diameters too expensive due to the drilling costs.

4.2.5 Water flow simplification

It has also been proven that for the purposes of a preliminary design, the estimation of the water flow profile as constant over the period of time that we have named PEH is valid. The PEH is a concept like the Sun Peak Hours but regarding the electric generation. It is the number of hours needed to obtain the real electricity generation of a certain day if the power generated was constant and equal to the peak power of the panel.

4.2.6 Planting schedule

Once the optimal diameter determined, and with a value for the pump efficiency, one last parameter can be adjusted to the benefit of the project. This is the planting date of the crops. Indeed, since the watering needs depend on the stage of development, it would be wise to match the valleys of production with the valleys of the single crop coefficient Kc.

It would be interesting also to consider the effect of variations in the rain (since it is not evenly distributed over one season). Therefore, the planting date could also be changed in order to make the system more resilient to specially dry years.

4.2.7 Rentability

Finally, it seems confirmed that these types of projects can nowadays be very profitable. Indeed, even if throughout all the thesis, conservative approaches as to the way of selecting the values to use have been made, and even taking the highest operational costs and lowest incomes of the ones found in the literature review and considering a short use period (5 years), the system is still profitable for certain scenarios. If the incomes generated were to be considered higher than the minimum (but still much lower than others in the literature review), the system would be very profitable.

Logically, the bigger the depth of the groundwater is, the less profitable the system is. On the contrary, the biggest the size of the orchard, the cheapest the system (because of scale economy, less drilling per m^2, etc). This raises the question of the preferability of PVWP with drip systems for a single household or for a community that would later divide the field into orchards as desired.

4.3 Future work

A series of considerations should be taken for future works. First, it would be to perfect the model used, and make it able to calculate more variables in an easier way.

Second, another work should study the best pump to use in these kinds of projects, as well as the best PV system. Third, the effect of a variable efficiency of the pump with the water flow should be explored. Fourth, a more detailed study of the drilling and PV system cost should be done.

It would be also interesting to study, as stated in 4.2.7, the influence on making these projects for an entire community or for different households. Indeed, it could happen that the sense of entitlement makes the individual projects work better even if they are more expensive. But it could also happen that when designing the system with the group in mind, the synergies generated make these projects work better.

Another interesting work would be to study the best crop selection to plant throughout the year. Indeed, there is no need of planting the same thing over the year, nor there is of planting only one type of crop in each cycle. It is interesting in fact to evaluate the impact of what is called FCV methods (Fruit, Cereals, Vegetables), or permaculture, in the long-term crop production.

Finally, a further assessment of the specific needs of the locals would be essential before thinking about investing a reasonable amount of money.

References

Allen G., R. *et al.* (2006) 'Evapotranspiración del cultivo: Guias para la determinación de los requerimientos de agua de los cultivos.', *FAO :Estudios FAO Riego y Drenaje 56*. Organización de las Naciones Unidas para la Agricultura y la Alimentación, p. 297. doi: 10.1590/1983-40632015v4529143.

Allen, R. G., Pereira, L. S., Raes, D. and Smith, M. (1998) *Chapter 1 - Introduction to evapotranspiration*, *Crop evapotranspiration - Guidelines for computing crop water requirements - FAO Irrigation and drainage paper 56*. Available at: http://www.fao.org/docrep/X0490E/x0490e04.htm (Accessed: 26 July 2018).

Allen, R. G., Pereira, L. S., Raes, D., Smith, M., *et al.* (1998) *Crop evapotranspiration : guidelines for computing crop water requirements*. Food and Agriculture Organization of the United Nations. Available at: http://www.fao.org/docrep/X0490E/x0490e00.htm (Accessed: 18 July 2018).

Andrić, I. *et al.* (2018) 'Solar Driven Irrigation Systems for Remote Rural Farms', *Energy Procedia*, 142, pp. 184–191. doi: 10.1016/j.egypro.2017.12.030.

Bain, L. E. *et al.* (2013) 'Malnutrition in Sub - Saharan Africa: Burden, causes and prospects', *Pan African Medical Journal*. African Field Epidemiology Network. doi: 10.11604/pamj.2013.15.120.2535.

Balana, B. B. *et al.* (2017) 'Can drip irrigation help farmers to adapt to climate change and increase their incomes?', *WLE Briefing series no. 15*. Available at: https://cgspace.cgiar.org/bitstream/handle/10568/83175/WLE Briefing 15_English_Final_Web.pdf?sequence=1 (Accessed: 16 July 2018).

Banerjee, A. V and Duflo, E. (2007) 'The Economic Lives of the Poor', *Journal of Economic Perspectives*, 21(1), pp. 141–167. doi: 10.1257/jep.21.1.141.

Bartram, J. and Cairncross, S. (2010) 'Hygiene, sanitation, and water: Forgotten foundations of health', *PLoS Medicine*. Public Library of Science, 7(11), p. e1000367. doi: 10.1371/journal.pmed.1000367.

Bell, F. and Millward, R. (2018) 'Public health expenditures and mortality in England and Wales, 1870–1914', *Continuity and Change*. Cambridge Uniersity Press, 13(2), pp. 221–249. Available at: https://www-cambridge-org.webproxy.student.hig.se/core/services/aop-cambridge-core/content/view/EBC4340A310F097AC0D019CB226EB761/S0268416098003142a.pdf/public_health_expenditures_and_mortality_in_england_and_wales_18701914.pdf (Accessed: 7 May 2018).

Burney, J. *et al.* (2010) 'Solar-powered drip irrigation enhances food security in the Sudano-Sahel', *Proceedings of the National Academy of Sciences*. National Academy of Sciences, 107(5), pp. 1848–1853. doi: 10.1073/pnas.0909678107.

Campana, P. E. (2015) 'PV Water Pumping Systems for Agricultural Applications', *Malardalen University Sweden*, p. 85. Available at: http://www.divaportal.org/smash/get/diva2:792682/FULLTEXT02.pdf (Accessed: 6 May 2018).

Campana, P. E., Li, H. and Yan, J. (2015) ‘Techno-economic feasibility of the irrigation system for the grassland and farmland conservation in China: Photovoltaic vs. wind power water pumping’, *Energy Conversion and Management*, 103, pp. 311–320. doi: 10.1016/j.enconman.2015.06.034.

Carter, K. (2009) ‘Guidelines for Community Supply and Protection in Africa. Cost-Effective Boreholes in sub-Saharan Africa’. Available at: http://nora.nerc.ac.uk/id/eprint/9185/1/CEB Danert Draft 4 UNESCO 22 April09.pdf (Accessed: 25 July 2018).

CLIMATE-DATA.ORG (2018) *Climate Fada N’Gourma: Temperature, Climograph, Climate table*. Available at: https://en.climate-data.org/location/766890/ (Accessed: 26 July 2018).

Dastane, N. G. (1978) *Chapter II. Measurement of effective rainfall*, *FAO IRRIGATION AND DRAINAGE PAPER*. Available at: http://www.fao.org/docrep/x5560e/x5560e03.htm (Accessed: 26 July 2018).

Dobbs, R. *et al.* (2011) ‘Resource Revolution: Meeting the world’s energy, materials, food, and water needs’. Available at: https://www.mckinsey.com/~/media/McKinsey/Business Functions/Sustainability and Resource Productivity/Our Insights/Resource revolution/MGI_Resource_revolution_full_report.ashx (Accessed: 6 May 2018).

FAO *et al.* (2017) *The State of Food Security and Nutrition in the World*, *Food and Agriculture Organization of the United Nations*. Available at: http://www.fao.org/3/a-I7695e.pdf (Accessed: 17 July 2018).

George H. Hargreaves and Zohrab A. Samani (1985) ‘Reference Crop Evapotranspiration from Temperature’, *Applied Engineering in Agriculture*. American Society of Agricultural and Biological Engineers, 1(2), pp. 96–99. doi: 10.13031/2013.26773.

Ghitas, A. E. (2012) ‘Studying the effect of spectral variations intensity of the incident solar radiation on the Si solar cells performance’, *NRIAG Journal of Astronomy and Geophysics*, 1, pp. 165–171. doi: 10.1016/j.nrjag.2012.12.013.

Houessionon, P. *et al.* (2017) ‘Economic Valuation of Ecosystem Services from Small-Scale Agricultural Management Interventions in Burkina Faso: A Discrete Choice Experiment Approach’, *Sustainability*. Multidisciplinary Digital Publishing Institute, 9(9), p. 1672. doi: 10.3390/su9091672.

Howard, G. and Bartram, J. (2003) ‘Domestic Water Quantity , Service Level and Health’, *World Health Organization*, p. 39. doi: 10.1128/JB.187.23.8156.

Http://solarelectricityhandbook.com (2009) *Solar Angle Calculator*. Available at: http://solarelectricityhandbook.com/solar-angle-calculator.html (Accessed: 30 July 2018).

Hutton, G., Haller, L. and Bartram, J. (2007) ‘Global cost-benefit analysis of water supply and sanitation interventions', *Journal of Water and Health*. IWA Publishing, 5(4), pp. 481–501. doi: 10.2166/wh.2007.009.

IRENA (2016) *Solar PV in Africa: Costs and Markets*, *Irena*. Available at: www.irena.org (Accessed: 23 July 2018).

Irmak, S. *et al.* (2003) 'Solar and Net Radiation-Based Equations to Estimate Reference Evapotranspiration in Humid Climates', *Journal of Irrigation and Drainage Engineering*, 129(5), pp. 336–347. doi: 10.1061/(ASCE)0733-9437(2003)129:5(336).

Leimbach, M. *et al.* (2018) 'Long-Term Development Perspectives of Sub-Saharan Africa under Climate Policies', *Ecological Economics*. Elsevier, 144, pp. 148–159. doi: 10.1016/j.ecolecon.2017.07.033.

MacDonald, A. M. *et al.* (2011) 'Groundwater resilience to climate change in Arica', *British Geological Survey Open Report*, (OR/11/031), p. 25. Available at: www.geologyshop.com (Accessed: 18 July 2018).

MacDonald, A. M. and Bonsor, H. C. (2011) 'An initial estimate of depth to groundwater across Africa', *Groundwater Science Programme. Open Report OR/11/067*, p. 26. Available at: www.bgs.ac.uk/gsni/ (Accessed: 18 July 2018).

Marsh, B. *et al.* (2007) 'Low-pressure drip system in reduced tillage cotton', *WIT Transactions on Ecology and the Environment*, 103, pp. 73–80. doi: 10.2495/WRM070081.

Milnes, M. (2000) 'The mathematics of pumping water', *The Royal Academy of Engineering*. Available at: https://www.raeng.org.uk/publications/other/17-pumping-water (Accessed: 25 July 2018).

Onda, K., Lobuglio, J. and Bartram, J. (2012) 'Global access to safe water: Accounting for water quality and the resulting impact on MDG progress', *International Journal of Environmental Research and Public Health*. Molecular Diversity Preservation International, 9(3), pp. 880–894. doi: 10.3390/ijerph9030880.

Prüss-Üstün, A. *et al.* (2008) 'Safer water, better health', *World Health Organization*, p. 53. doi: ISBN 9789241596435.

Ruiz Baena, N. (2017) *El SISTEMA DE ASISTENCIA AL REGANTE DEL IFAPA*. Available at: http://multimedia.dipusevilla.es/cantillana/Ponencias_Feria_Agraria/PONENCIA_10.pdf (Accessed: 26 July 2018).

Salami, A. *et al.* (2011) 'Development Aid and Access to Water and Sanitation in sub-Saharan Africa', *Water International*, 39:3, pp. 294–314. Available at: https://www.afdb.org/fileadmin/uploads/afdb/Documents/Publications/WPS 140 Development Aid and Access to Water NV1 22.pdf (Accessed: 15 March 2018).

Serdeczny, O. *et al.* (2017) 'Climate change impacts in Sub-Saharan Africa: from physical changes to their social repercussions', *Regional Environmental Change*.

Springer Berlin Heidelberg, 17(6), pp. 1585–1600. doi: 10.1007/s10113-015-0910-2.

Singandhupe, R. B. *et al.* (2003) 'Fertigation studies and irrigation scheduling in drip irrigation system in tomato crop (Lycopersicon esculentum L.)', *European Journal of Agronomy*, 19(2), pp. 327–340. Available at: www.elsevier.com/locate/eja (Accessed: 14 July 2018).

Testa, G., Gresta, F. and Cosentino, S. L. (2011) 'Dry matter and qualitative characteristics of alfalfa as affected by harvest times and soil water content', *European Journal of Agronomy*. Food and Agriculture Organization of the United Nations, 34(3), pp. 144–152. doi: 10.1016/j.eja.2010.12.001.

The World Bank Group (2015) *Country Historical Climate - Burkina Faso*. Available at: http://sdwebx.worldbank.org/climateportal/index.cfm?page=country_historical_climate&ThisCCode=BFA (Accessed: 26 July 2018).

Tomillo Gutiérrez, U. (2005) 'Estudio acerca del empleo de la bomba manual de agua en el ámbito rural en países en vías de desarrollo'. Available at: https://e-archivo.uc3m.es/handle/10016/7232 (Accessed: 5 May 2018).

UN-Water (2015) 'A Post-2015 Global Goal for Water: Synthesis of key findings and recommendations from UN-Water'. Available at: http://www.un.org/waterforlifedecade/pdf/27_01_2014_un-water_paper_on_a_post2015_global_goal_for_water.pdf (Accessed: 6 May 2018).

Voltabatería (2018) *Batería de camión 180Ah 1250A + DCHA - Volta Baterías*. Available at: https://voltabaterias.com/baterias-de-camion/31-bateria-professional-180ah-d.html?gclid=CjwKCAjwhqXbBRAREiwAucoo-_zxPOabZcIxchSYKML4oFUDVXd9dnyco1kar0GAfGAqMfx6MW_38xoCp3oQAvD_BwE (Accessed: 8 August 2018).

Weatherbase (2018) *Fada N'gourma, Burkina Faso Travel Weather Averages*. Available at: https://www.weatherbase.com/weather/weatherall.php3?s=592485&cityname=Fada+N%27gourma%2C+Est%2C+Burkina+Faso&units= (Accessed: 26 July 2018).

WHO (2012) 'Global costs and benefits of drinking-water supply and sanitation interventions to reach the MDG target and universal coverage'. Available at: http://www.who.int/about/licensing/copyright_form/en/index.html (Accessed: 6 May 2018).

Who and Unicef (2014) 'Progress on sanitation and drinking-water - 2014 update', *… Monitoring Programme for water supply and sanitation …*, pp. 1–78. doi: 978 92 4 150724 0.

Woltering, L., Pasternak, D. and Ndjeunga, J. (2011) 'The African market garden: The development of a low-pressure drip irrigation system for smallholders in the Sudano Sahel', *Irrigation and Drainage*. Wiley-Blackwell, 60(5), pp. 613–621. doi: 10.1002/ird.610.

www.saecanet.com (2010) *Calculation of monthly average extraterrestrial daily solar radiation on a horizontal surface.* Available at: https://www.saecanet.com/calculation_page/000436_000565_extraterrestrial_radiation.php (Accessed: 26 July 2018).

You, L. Z. (2008) 'AFRICA INFRASTRUCTURE Irrigation Investment Needs in Sub-Saharan Africa', (June). Available at: www.infrastructureafrica.org. (Accessed: 8 August 2018).

Zhang, J. *et al.* (2014) 'Model of evapotranspiration and groundwater level based on photovoltaic water pumping system', *Applied Energy*, 136, pp. 1132–1137. doi: 10.1016/j.apenergy.2014.05.045.

Appendix A

Table 30. Weather data

	TEMPERATURE			PRECIPITATION			Radiation daily [MJ/m2]: 22 years			ET Radiation
	Max High	Average	Min low	Max Av. prec	Av. Av. Prec	Mín Av. Prec	Max Direct	Av Direct	Min Direct	
JAN	33,5	25,1	16,6	0,0	0,0	0,0	29,7	22,7	19,1	35,3
FEB	36,4	27,9	19,5	0,3	0,1	0,0	31,5	25,7	23,0	36,6
MAR	38,8	31,1	23,1	10,8	7,7	4,4	28,7	23,8	20,2	37,1
APR	39,6	32,5	25,4	28,4	26,4	24,7	28,3	23,0	18,8	36,0
MAY	37,3	31,3	25,0	85,8	71,2	57,8	27,2	22,8	18,1	33,9
JUN	34,2	28,9	23,2	115,0	107,1	95,3	25,8	20,5	16,7	32,7
JUL	31,6	26,9	22,1	186,0	174,8	159,4	23,3	17,7	14,6	33,1
AUG	30,5	26,0	21,4	243,7	225,2	205,0	20,3	15,2	10,8	34,8
SEP	31,9	26,6	21,2	156,0	143,2	134,5	20,6	18,2	13,0	36,4
OCT	35,2	28,4	21,2	45,0	38,7	32,0	24,9	22,3	19,1	36,7
NOV	36,2	27,3	18,1	1,0	0,5	0,0	28,3	25,3	22,1	35,7
DEC	33,9	25,4	16,7	1,4	0,8	0,0	27,1	23,6	20,4	34,8
ANNUAL	34,9	28,1	21,1	873,4	795,8	713,1	26,3	21,7	18,0	35,3

Table 31. Calculated values for the reference evapotranspiration in Fada N'Gourma

	ETo Hargreaves	ETo Net	ETo Harg. modified
JAN	14,33	9,65	9,09
FEB	15,81	10,23	10,03
MAR	16,53	9,50	10,49
APR	15,70	9,42	9,96
MAY	13,43	9,07	8,52
JUN	11,64	8,61	7,38
JUL	10,49	7,84	6,65
AUG	10,58	6,95	6,71
SEP	12,15	7,05	7,71
OCT	14,60	8,34	9,26
NOV	15,74	9,29	9,98
DEC	14,34	8,91	9,09
	13,78	8,74	8,74

Table 32. Irrigation with Kcmax

	Days month	ETo mine	ETc max	Rain (min av.)	Precef	Prec_ef	Watering
JAN	31	9,37	10,77	0,0	0,00	0,00	10,77
FEB	28	10,13	11,65	0,0	0,00	0,00	11,65
MAR	31	9,99	11,49	4,4	4,37	0,14	11,35
APR	30	9,69	11,14	24,7	23,72	0,79	10,35
MAY	31	8,79	10,11	57,8	52,45	1,69	8,42
JUN	30	8,00	9,20	95,3	80,77	2,69	6,50
JUL	31	7,25	8,33	159,4	118,75	3,83	4,50
AUG	31	6,83	7,85	205,0	137,76	4,44	3,41
SEP	30	7,38	8,49	134,5	105,56	3,52	4,97
OCT	31	8,80	10,12	32,0	30,36	0,98	9,14
NOV	30	9,64	11,09	0,0	0,00	0,00	11,09
DEC	31	9,00	10,35	0,0	0,00	0,00	10,35
ANNUAL	365	8,74	10,05	59,43	46,15	1,51	8,54

Table 33. Irrigation with Kc variable

	Días/mes	Día medic.	Kc/Kc max	ETo mine	ETc	Prec_ef	Watering Kc(t)	Watering Kcmax
JAN	31	15	0,52	9,37	5,62	0,00	5,62	10,77
FEB	29	46	0,77	10,13	9,02	0,00	9,02	11,65
MAR	31	75	1,00	9,99	11,49	0,14	11,35	11,35
APR	30	106	0,91	9,69	10,11	0,79	9,32	10,35
MAY	31	136	0,52	8,79	5,28	1,69	3,58	8,42
JUN	30	167	0,76	8,00	7,00	2,69	4,30	6,50
JUL	31	197	1,00	7,25	8,33	3,83	4,50	4,50
AUG	31	228	0,91	6,83	7,13	4,44	2,68	3,41
SEP	30	259	0,52	7,38	4,43	3,52	0,91	4,97
OCT	31	289	0,76	8,80	7,70	0,98	6,72	9,14
NOV	30	320	1,00	9,64	11,09	0,00	11,09	11,09
DEC	31	350	0,91	9,00	9,39	0,00	9,39	10,35

APPENDIX B

Table 34. Daily water flow for each month and tilt

	Q [m3/h] for 120 m2						
	36º	**28º**	**20º**	**12º**	**4º**	**-4º**	**-12º**
JAN	0,33	0,34	0,35	0,37	0,40	0,44	0,50
FEB	0,36	0,38	0,37	0,38	0,39	0,42	0,46
MAR	0,39	0,38	0,38	0,38	0,38	0,39	0,41
APR	0,43	0,40	0,38	0,37	0,37	0,37	0,37
MAY	0,44	0,40	0,37	0,35	0,34	0,33	0,33
JUN	0,42	0,37	0,34	0,31	0,30	0,29	0,28
JUL	0,36	0,32	0,30	0,28	0,27	0,26	0,25
AUG	0,30	0,27	0,26	0,25	0,24	0,24	0,24
SEP	0,29	0,28	0,28	0,27	0,27	0,27	0,28
OCT	0,34	0,34	0,34	0,35	0,36	0,38	0,40
NOV	0,36	0,36	0,37	0,39	0,41	0,45	0,50
DEC	0,33	0,33	0,35	0,37	0,40	0,45	0,51

	Q [m3/h] for 250 m2						
	36º	**28º**	**20º**	**12º**	**4º**	**-4º**	**-12º**
JAN	0,58	0,59	0,61	0,65	0,69	0,76	0,87
FEB	0,64	0,66	0,64	0,66	0,69	0,74	0,81
MAR	0,69	0,67	0,66	0,66	0,67	0,69	0,72
APR	0,74	0,70	0,66	0,64	0,63	0,63	0,64
MAY	0,75	0,68	0,63	0,60	0,57	0,56	0,55
JUN	0,68	0,60	0,54	0,51	0,48	0,46	0,46
JUL	0,54	0,48	0,45	0,42	0,40	0,39	0,38
AUG	0,42	0,39	0,37	0,36	0,35	0,35	0,35
SEP	0,45	0,43	0,44	0,41	0,41	0,42	0,43
OCT	0,58	0,58	0,58	0,59	0,61	0,64	0,68
NOV	0,62	0,63	0,65	0,68	0,72	0,79	0,88
DEC	0,56	0,58	0,60	0,64	0,69	0,77	0,89

	Q [m3/h] for 500 m2						
	36º	**28º**	**20º**	**12º**	**4º**	**-4º**	**-12º**
JAN	1,05	1,07	1,11	1,17	1,26	1,39	1,58
FEB	1,16	1,21	1,18	1,21	1,27	1,36	1,48
MAR	1,26	1,22	1,21	1,21	1,22	1,26	1,32
APR	1,35	1,26	1,20	1,17	1,15	1,15	1,16
MAY	1,32	1,21	1,12	1,06	1,02	0,99	0,98
JUN	1,17	1,03	0,94	0,88	0,83	0,80	0,79
JUL	0,89	0,80	0,74	0,70	0,66	0,65	0,64
AUG	0,67	0,63	0,59	0,57	0,56	0,55	0,56
SEP	0,75	0,72	0,73	0,69	0,69	0,70	0,72
OCT	1,04	1,03	1,04	1,05	1,09	1,14	1,23
NOV	1,13	1,15	1,18	1,23	1,32	1,43	1,60
DEC	1,02	1,05	1,09	1,16	1,26	1,40	1,61

APPENDIX C

Table 35. Solar PV system size for pump efficiency = 65% and Depth 15 m

PV Size [W] when 120 m2 and 15 m					Diam		0,0127
	Solar panel tilt [º]						
	36º	28º	20º	12º	4º	-4º	-12º
JAN	26	27	28	29	32	36	42
FEB	29	30	29	30	32	34	38
MAR	32	31	30	30	31	32	33
APR	35	32	31	30	29	29	29
MAY	36	33	30	28	27	26	26
JUN	34	29	26	24	23	22	22
JUL	28	25	23	21	20	19	19
AUG	23	21	20	19	18	18	18
SEP	22	21	22	20	20	21	21
OCT	27	26	27	27	28	30	32
NOV	28	28	29	31	33	37	43
DEC	25	26	27	29	32	37	44
	Max PV peak power needed [Wp]						
	36	33	31	31	33	37	44

PV Size [W] when 250 m2 and 15 m					Diam		0,0127
	Solar panel tilt [º]						
	36º	28º	20º	12º	4º	-4º	-12º
JAN	52	53	55	60	66	76	93
FEB	58	62	60	62	66	73	83
MAR	66	63	62	62	63	66	70
APR	73	67	62	60	58	58	59
MAY	74	64	58	53	51	49	48
JUN	64	53	47	43	40	39	38
JUL	47	41	37	34	32	31	31
AUG	35	32	30	28	28	27	27
SEP	37	35	36	33	33	34	35
OCT	52	51	51	52	55	59	65
NOV	57	58	60	64	70	80	95
DEC	50	51	54	59	66	78	97
	Max PV peak power needed [Wp]						
	74	67	62	64	70	80	97

PV Size [W] when 500 m2 and 15 m					Diam		0,0127
	Solar panel tilt [º]						
	36º	28º	20º	12º	4º	-4º	-12º
JAN	129	133	142	156	178	215	277
FEB	153	165	157	166	181	205	243
MAR	178	168	164	164	168	178	194
APR	202	178	163	154	150	149	153
MAY	196	164	143	130	121	116	114
JUN	155	124	106	95	87	83	80
JUL	97	82	73	66	62	60	58
AUG	64	57	53	51	49	49	49
SEP	74	70	72	66	66	67	70
OCT	127	124	125	129	137	149	169
NOV	146	149	157	171	193	228	288
DEC	122	127	137	153	178	219	289
	Max PV peak power needed [Wp]						
	202	178	164	171	193	228	289

APPENDIX D

Table 36. Summary table for A=120 m2

120 m2 ; 16,8º								
	Diameter	0,01905	Depth	25				
	Energy generated [kWh/day]	Daily volume (m3/day)	**Q [m3/h]**	Hdyn [m]	Daily energy needed [Wh]	Solar PV system size [Wp]		
JAN	5,28	1,89	0,36	0,4	217	41		
FEB	5,4	2,00	0,37	0,4	230	43		
MAR	5,21	1,96	0,38	0,4	226	43		
APR	4,87	1,84	0,38	0,4	212	44	0,38	APR
MAY	4,41	1,61	0,37	0,4	185	42		
JUN	4,22	1,38	0,33	0,3	158	37		
JUL	3,97	1,14	0,29	0,3	130	33		
AUG	3,94	1,01	0,26	0,2	115	29		
SEP	4,45	1,20	0,27	0,2	137	31		
OCT	4,95	1,70	0,34	0,4	195	39		
NOV	5,13	1,93	0,38	0,4	222	43		
DEC	5,18	1,84	0,36	0,4	212	41		
					MAX	Max PV peak		
					230	44	0,38	

Table 37. Summary table for A=250 m2

250 m2 ; 18,3º							
	Diameter	0,01905	Depth	25			
	Energy generated [kWh/day]	Daily volume (m3/day)	**Q [m3/h]**	Hdyn [m]	Daily energy needed [Wh]	Solar PV system size [Wp]	
JAN	5,33	3,29	0,62	1,0	387	73	
FEB	5,43	3,51	0,65	1,1	414	76	
MAR	5,21	3,44	0,66	1,1	406	78	0,65978545 MAR
APR	4,84	3,19	0,66	1,1	376	78	
MAY	4,36	2,70	0,62	1,0	318	73	
JUN	4,16	2,23	0,54	0,8	259	62	
JUL	3,91	1,73	0,44	0,6	199	51	
AUG	3,92	1,45	0,37	0,4	167	43	
SEP	4,43	1,84	0,42	0,5	212	48	
OCT	4,98	2,89	0,58	0,9	338	68	
NOV	5,17	3,37	0,65	1,1	398	77	
DEC	5,24	3,19	0,61	1,0	374	71	
					MAX	Max PV peak	
					414	78	0,66

Table 38. Summary table for A=500 m2

500 m2 ; 18,6º				
	Diameter	0,01905	Depth	25

	Energy generated [kWh/day]	Daily volume (m3/day)	**Q [m3/h]**	Hdyn [m]	Daily energy needed [Wh]	Solar PV system size [Wp]		
JAN	5,34	5,99	1,12	2,9	751	141		
FEB	5,43	6,43	1,18	3,2	814	150		
MAR	5,21	6,27	1,20	3,3	797	153	1,20440776	MAR
APR	4,83	5,78	1,20	3,3	733	152		
MAY	4,35	4,81	1,11	2,8	602	138		
JUN	4,15	3,85	0,93	2,1	470	113		
JUL	3,9	2,85	0,73	1,4	339	87		
AUG	3,91	2,31	0,59	0,9	270	69		
SEP	4,43	3,08	0,70	1,3	365	82		
OCT	4,98	5,17	1,04	2,5	640	129		
NOV	5,17	6,14	1,19	3,2	779	151		
DEC	5,25	5,77	1,10	2,8	722	138		
					MAX	Max PV peak		
					814	153	1,20	

APPENDIX E

Table 39. Global Direct Irradiance for 17,5º of inclination in Fada N'Gourma

	Global direct irradiance W/m² (17,5º, Fada N'Gourma)											
	JAN	FEB	MAR	APR	MAY	JUN	JUL	AUG	SEP	OCT	NOV	DEC
6:45	41	33	39	45	44	38	29	23	45	73	85	73
7:45	192	189	177	165	155	137	119	104	155	227	265	238
8:45	386	389	362	333	280	257	221	208	289	397	453	425
9:45	546	552	534	495	412	372	311	301	415	545	595	580
10:45	677	699	667	611	515	465	394	372	511	649	694	690
11:45	736	749	724	670	560	523	430	436	538	666	714	710
12:45	711	727	681	621	525	485	441	422	487	616	673	684
13:45	616	631	591	510	416	406	371	333	421	498	544	563
14:45	468	491	413	343	275	293	255	239	302	336	374	410
15:45	282	303	250	193	152	176	165	153	181	166	187	227
16:45	100	123	93	70	49	68	62	54	56	39	54	70